U.S. Department
of Commerce

Volume 121
Number 3
July 2023

Fishery Bulletin

Property of the
Pacific Islands Fisheries
Science Center
LIBRARY

U.S. Department of Commerce

Gina M. Raimondo
Secretary

National Oceanic and Atmospheric Administration

Richard W. Spinrad
Administrator

National Marine Fisheries Service

Janet Coit
Assistant Administrator
for Fisheries

Fishery Bulletin (ISSN 0090-0656) is published quarterly by the Scientific Publications Office, National Marine Fisheries Service, NOAA, 7600 Sand Point Way NE, Seattle, WA 98115-0070.

Although the contents of this publication have not been copyrighted and may be reprinted entirely, reference to source is appreciated.

The Secretary of Commerce has determined that the publication of this periodical is necessary according to law for the transaction of public business of this Department. Use of funds for printing of this periodical has been approved by the Director of the Office of Management and Budget.

For Sale by the Superintendent of Documents, U.S. Government Publishing Office, Washington, DC 20401. Subscription price per year: $32.00 domestic and $44.80 foreign. Cost per single issue: $19.00 domestic and $26.60 foreign. **See back for order form.**

Fishery Bulletin

Scientific Editor
José I. Castro
National Marine Fisheries Service, NOAA
263 13th Avenue South
Saint Petersburg, Florida 33701

Managing Editor
Kathryn Dennis
Scientific Publications Office
National Marine Fisheries Service, NOAA
1845 Wasp Boulevard, Building 176
Honolulu, Hawaii 96818

Associate Editor
Cara Mayo
Scientific Publications Office
National Marine Fisheries Service, NOAA
7600 Sand Point Way NE
Seattle, Washington 98115-0070

Editorial Board

Henry L. Bart Jr.	Tulane University, New Orleans, Louisiana
Katherine E. Bemis	National Systematics Laboratory, Washington, DC
Matthew D. Campbell	National Marine Fisheries Service, Pascagoula, Mississippi
William B. Driggers III	National Marine Fisheries Service, Pascagoula, Mississippi
Gretchen L. Grammer	South Australian Research and Development Institute, Adelaide, Australia
Richard Langton	National Marine Fisheries Service, Walpole, Maine (retired)
J. Fernando Márquez-Farías	Universidad Autónoma de Sinaloa, Mazatlán, México
Richard S. McBride	National Marine Fisheries Service, Woods Hole, Massachusetts
Richard L. Merrick	National Marine Fisheries Service, Falmouth, Massachusetts (retired)
Richard D. Methot	National Marine Fisheries Service, Seattle, Washington
Lisa J. Natanson	National Marine Fisheries Service, Narragansett, Rhode Island (retired)
Mark S. Peterson	University of Southern Mississippi, Ocean Springs, Mississippi
André E. Punt	University of Washington, Seattle, Washington
Joseph M. Quattro	University of South Carolina, Columbia, South Carolina
John F. Walter III	National Marine Fisheries Service, Miami, Florida

***Fishery Bulletin* website: https://spo.nmfs.noaa.gov/fb.htm**

Fishery Bulletin carries original research reports on investigations in fishery science, engineering, and economics. It began as the Bulletin of the United States Fish Commission in 1881; it became the Bulletin of the Bureau of Fisheries in 1904 and the *Fishery Bulletin* of the U.S. Fish and Wildlife Service in 1941. Separates were issued as documents through volume 46; the last document was no. 1103. Beginning with volume 47 in 1931 and continuing through volume 62 in 1963, each separate appeared as a numbered bulletin. A new system began in 1963, with volume 63, in which papers are bound together in a single issue. Beginning with volume 70, number 1, January 1972, *Fishery Bulletin* became a periodical, issued quarterly. In this form, it is available by subscription from the Superintendent of Documents, U.S. Government Publishing Office, Washington, DC 20401. It is also available free in limited numbers to libraries, research institutions, and state and federal agencies and in exchange for other scientific publications.

U.S. Department of Commerce
Seattle, Washington

Volume 121
Number 3
July 2023

Fishery Bulletin

Contents

Notes

73–77 **Takaya Kudoh, Anise Midooka, Satoshi Aida, and Takeshi Tomiyama**

Interspecific differences in the vertical distribution patterns of *Sebastes inermis* and *S. ventricosus*

78–83 **Julio Sánchez, Omar Santana Morales, Rebeca Zertuche, and Elisa Areano**

Elasmobranch bycatch of the shrimp trawl fishery along the Pacific coast of Guatemala

Articles

84–95 **Lisa J. Natanson, William B. Driggers III, Camilla T. McCandless, and Nancy E. Kohler**

Updated reproductive parameters for the tiger shark (*Galeocerdo cuvier*) in the western North Atlantic Ocean

96–111 **Henry D. Legett, Robert Aguilar, Keira Heggie, Kimberly D. Richie, and Matthew B. Ogburn**

Timing and environmental drivers of spawning migrations of alewife (*Alosa pseudoharengus*) and blueback herring (*A. aestivalis*) in rivers of Chesapeake Bay

112–123 **Cynthia Yeung, Stan Kotwicki, and Sean K. Rohan**

Effect of reduction in spatial survey effort on indices of bottom temperature for the eastern Bering Sea

Note

124–128 **Matthew S. Morris, Richard D. Ledgerwood, Alexander J. Borsky, Gabriel T. Brooks, and Paul J. Bentley**

Development and use of a large, flexible antenna to detect fish implanted with passive integrated transponder tags

The National Marine Fisheries Service (NMFS) does not approve, recommend, or endorse any proprietary product or proprietary material mentioned in this publication. No reference shall be made to NMFS, or to this publication furnished by NMFS, in any advertising or sales promotion that would indicate or imply that NMFS approves, recommends, or endorses any proprietary product or proprietary material mentioned herein or that has as its purpose an intent to cause directly or indirectly the advertised product to be used or purchased because of this NMFS publication.

The NMFS Scientific Publications Office is not responsible for the contents of the articles.

Article

129–140 **Adam G. Fox, Michael A. Baker, Alexander J. Cummins, Hudman S. Evans Jr., Katherine L. Cummins, Nathaniel Q. Hancock, and David L. Higginbotham**

Recruitment of juvenile Atlantic sturgeon (*Acipenser oxyrinchus oxyrinchus*) in the Savannah, Ogeechee, and Satilla Rivers in Georgia

141–144 **Guidelines for authors**

National Marine Fisheries Service
NOAA

Fishery Bulletin
established in 1881

Spencer F. Baird
First U.S. Commissioner of Fisheries and founder of *Fishery Bulletin*

Interspecific differences in the vertical distribution patterns of *Sebastes inermis* and *S. ventricosus*

Takaya Kudoh[1]
Anise Midooka[1]
Satoshi Aida[1]
Takeshi Tomiyama (contact author)[2]

Email address for contact author: tomiyama@hiroshima-u.ac.jp

[1] Fisheries and Ocean Technologies Center
Hiroshima Prefectural Technology Research Institute
6-21-1 Hatami, Ondo-cho
Kure, Hiroshima 737-1207, Japan

[2] Graduate School of Integrated Sciences for Life
Hiroshima University
1-4-4 Kagamiyama
Higashi-Hiroshima, Hiroshima 739-8528, Japan

Abstract—Information on behavioral variation among sympatric congeneric species is important for understanding the mechanisms that enable their coexistence. The aim of this study was to elucidate the characteristics of diurnal vertical distribution of congeneric *Sebastes inermis* and *S. ventricosus* through observations during laboratory experiments in 2011. When 25 individuals of each species were accommodated in a 1-kL tank, *S. inermis* stayed mainly at the bottom, whereas *S. ventricosus* actively swam 0–60 cm above the bottom. At various intraspecific densities, *S. inermis* were similarly distributed at the bottom, *S. ventricosus* were distributed more widely, and the frequency of individuals in the upper layers of water in the tank increased with density. These results indicate that the different behaviors of the 2 species make their coexistence possible without severe competition for microhabitats.

Manuscript submitted 12 January 2023.
Manuscript accepted 4 May 2023.
Fish. Bull. 121:73–77 (2023).
Online publication date: 17 May 2023.
doi: 10.7755/FB.121.3.1

The views and opinions expressed or implied in this article are those of the author (or authors) and do not necessarily reflect the position of the National Marine Fisheries Service, NOAA.

The genus *Sebastes* is widely distributed, mainly in temperate to Arctic waters throughout the North Pacific (Hyde and Vetter, 2007), and many *Sebastes* species are important in fisheries. *Sebastes* species are often segregated between habitats, possibly because of interspecific competition (Larson, 1980) or an interspecific difference in habitat preference (Richards, 1986). Nonetheless, some congeneric *Sebastes* species do coexist (Matthews, 1990; Benestan et al., 2021). Ecological differences would enable such closely related species to coexist (Love et al., 2002), but studies that focus on behavior between coexisting species have seldom been conducted (Tolimieri et al., 2009). Understanding of the mechanisms underlying species distribution is important for conservation and fisheries management (Williams and Ralston, 2002; Frid et al., 2018).

Three species, *Sebastes inermis*, *S. ventricosus*, and *S. cheni*, which are widely distributed in the coastal waters of Japan, had long been regarded as a single species owing to their morphological similarities (Kai and Nakabo, 2008; Mohri et al., 2013). They were classified into 3 species in 2008 on the basis of morphological and genetic differences (Kai and Nakabo, 2008). *Sebastes inermis* has a higher dependence on shrimp as food (Akeda et al., 2012) and a slower growth rate (Kamimura et al., 2014) than the other 2 species. These differences could possibly be attributed to interspecific behavioral differences. Local fishermen have suggested that the 3 species use different habitats, but so far the interspecific habitat variation has not been studied.

The aim of this study was to clarify the behavioral characteristics of *S. inermis* and *S. ventricosus* under laboratory conditions, by gaining insights into their habitat utilization and overlap. These 2 species are common in the Seto Inland Sea, in southwestern Japan, and the catch of these 2 species is usually much greater than that of *S. cheni*. We explored the following 2 hypotheses: 1) the behavioral patterns or layers of vertical distribution differ between species and 2) the behavioral characteristics of each species do not change under various intraspecific densities.

Materials and methods

Preparation and rearing methods

The individuals of both species, *S. inermis* and *S. ventricosus*, used in the experiments of this study were caught with a small set net (known as *Tsubo-ami*) in coastal areas from depths of approximately 5–8 m off Okino Island (34°09′13″N, 132°26′6″E) from March through May in 2010 and 2011. Approximately 500 fish, with total lengths of 130–160 mm, were captured. The fish were initially kept in a 5-kL tank in the laboratory and fed commercial dry pellets (Otohime EP4[1], Marubeni Nisshin Feed Co. Ltd., Tokyo, Japan) in the amount of 0.5% to 1% of the total mass of fish per day until December 2011.

Before the experiments, we identified the species of caught individuals on the basis of their external characteristics (e.g., pectoral fin length, differences in body color, and the presence or absence of reddish irregular stripes and dots in the interorbital region; see Suppl. Fig. 1 [online only]) (Kai and Nakabo, 2008; Nakabo and Kai, 2013). The species identification was validated on the basis of meristic characters that were counted for 50 individuals (25 individuals for each species) after the experiments were completed. The numbers of anal fin rays, pectoral fin rays, gill rakers, and pored lateral line scales are usually 7, 15, 35, and 40 in *S. inermis* and 7 or 8, 16, 37, and 46 in *S. ventricosus*, respectively (Kai and Nakabo, 2008).

Experiment on behavior during coexistence

To observe the distribution and behavior of *S. inermis* and *S. ventricosus* when they were allowed to coexist, we conducted an experiment in which individuals of the 2 species were accommodated in a 1-kL transparent tank and kept without feeding for 2 successive days (herein called the *coexistence experiment*). Twenty-five fish of each species (a total of 50 individuals) were accommodated in the tank. The experiment was carried out twice in 2011, on 28–29 July (first trial) and 23–24 August (second trial). The fish used in the first trial were replaced with other individuals for the second trial. The tank was filled with filtered seawater to a depth of 80 cm, and water was exchanged at a rate of 3.6 L/min. The water temperature ranged from 24.2°C to 25.6°C and from 25.2°C to 26.0°C in the first and second trials, respectively. The intensity of illumination above the water surface ranged from 37 to 40 lx, and the current velocity was <0.01 m/s in the tank during the period of the experiment. The depth of seawater in the tank was marked with white insulating tape every 20 cm from the bottom, and depth layers of seawater in the tank were defined, for the purposes of assessing vertical distribution, as surface (0–20 cm), subsurface (20–40 cm), medium (40–60 cm), and bottom (60–80 cm).

The behavior of the fish was recorded during the experiment by using a digital video camera (NV-GS70, Panasonic Holdings Corp., Kadoma, Japan, and DCR-PC350, Sony Group Corp., Tokyo, Japan). The recordings were made 9 times for a total of 90 min each day, with 10-min recordings from 3 viewing angles over the following 3 time periods: 0900–1000, 1300–1400, and 1700–1800 (Suppl. Fig. 2, Suppl. Video) (online only). A total of 18 video images per trial were used to count the number of individuals of each species distributed in each layer (Suppl. Fig. 1) (online only). The number of individuals of each species at each layer was counted 5 times at each angle. Additionally, individuals distributed in the bottom layer with part or several parts of their body (e.g., caudal, pelvic, or anal fin or other ventral regions) in contact with the bottom of the tank were regarded as demersal individuals.

Experiment on behavior at different densities

To test whether or not the distribution pattern of each species changed at different densities, an experiment was conducted by using individuals of each species after being kept without feeding for 3 d (herein called the *density experiment*). For each species, 10 individuals (low density), 25 individuals (medium density), and 50 individuals (high density) were accommodated in 3 circular 500-L tanks for observation. We used smaller tanks than those used in the coexistence experiment to make it easier to count the number of fish present. This strategy also accounted for the fact that none of the fish in the coexistence experiment appeared in the surface layer of their tanks. The tanks were filled with filtered seawater to a depth of 60 cm. The water conversion rate and illumination conditions were the same as those used in the coexistence experiment.

The experiment on *S. inermis* was carried out twice in 2011 for 2 consecutive days, on 21–22 November (first trial) and 24–25 November (second trial), with fish selected randomly for each trial. Similarly, the experiment on *S. ventricosus* was carried out in 2011 on 28–29 November (first trial) and 1–2 December (second trial). The water temperature ranged from 17.2°C to 18.7°C during the experiment. A line was drawn horizontally with a marker every 20 cm from the bottom of each tank to divide the tank into 3 depth layers: surface (0–20 cm), medium (20–40 cm), and bottom (40–60 cm). The layers where fish were distributed were observed visually, without the use of video recordings. These observations were recorded during 2 time periods: 1100–1200 and 1300–1400. In each of the 3 tanks, fish were counted for each layer 5 times at approximately 2-min intervals during each time period.

Data analyses

To compare the distribution patterns between species, nested multivariate analysis of variance (MANOVA) was performed by using the percentage of individuals at each depth layer. The data were arcsine square-root transformed. In the coexistence experiment, the initial explanatory variables were *species* and *time of day*, and *trial*

[1] Mention of trade names or commercial companies is for identification purposes only and does not imply endorsement by the National Marine Fisheries Service, NOAA.

and *date* were used as random variables. In the density experiment, the initial explanatory variables were *species* and *density*, and *trial* was used as a random variable. Additionally, in the coexistence experiment, the proportion of demersal individuals in contact with the bottom was compared between species for each time period of each day by using Fisher's exact test (Fisher, 1925). We conducted statistical analyses using R, vers. 4.1.0 (R Core Team, 2021).

Results

Coexistence experiment

Almost all the *S. inermis* were distributed in the bottom layer, whereas *S. ventricosus* were distributed not only in the bottom layer but also in the medium and subsurface layers (nested MANOVA: $F_{1,68}$=18.1, P<0.001) (Fig. 1). No individuals of either species were observed in the surface layer. Time of day did not have a significant effect on where the fish were distributed ($F_{2,68}$=2.0, P=0.07). The proportion of demersal individuals in the bottom layer was significantly greater for *S. inermis* (818 of 1080 individuals counted) than for *S. ventricosus* (61 of 1300 individuals counted) (Fisher's exact test: P<0.001, for all cases). *Sebastes ventricosus* swam actively, and a few individuals exhibited aggressive behavior toward other conspecific individuals. In contrast, *S. inermis* mostly lay on the bottom without moving and did not have aggressive behavior. Aggressive behavior of *S. ventricosus* toward *S. inermis* was rarely observed.

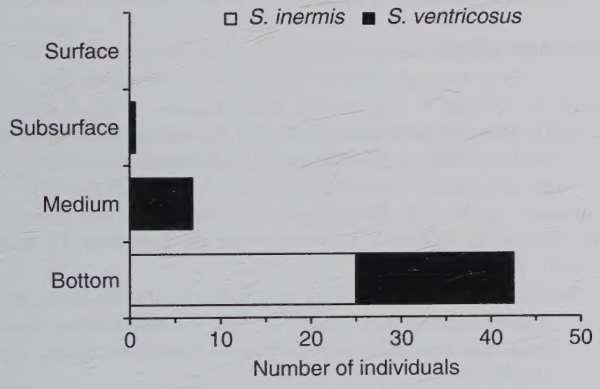

Figure 1

Average number of individuals of *Sebastes inermis* and *S. ventricosus* observed in each layer of seawater in a 1-kL tank during 2 trials of an experiment conducted at the Fisheries and Ocean Technologies Center of the Hiroshima Prefectural Technology Research Institute in 2011: 28–29 July (first trial) and 23–24 August (second trial). In this coexistence experiment, 25 individuals of each species were placed in the same tank. To assess vertical distribution of fish, 4 depth layers of seawater in the tank were defined as follows: surface (0–20 cm), subsurface (20–40 cm), medium (40–60 cm), and bottom (60–80 cm). The data presented are the averages from both trials.

Density experiment

Regardless of the density of fish in their tank, *S. inermis* were distributed almost exclusively in the bottom layer, and few individuals were found at the medium and surface layers (Fig. 2). In contrast, *S. ventricosus* were distributed more widely in the medium and surface layers, with a significant difference observed between species (nested MANOVA: $F_{1,236}$=578.7, P<0.001). The proportion of *S. ventricosus* distributed at the medium and surface layers was higher under greater densities, and the effect of density was also significant ($F_{2,236}$=13.3, P<0.001).

Discussion

This study is the first to clarify the behavioral difference between *S. inermis* and *S. ventricosus*. When these 2 species were accommodated in the same tank, *S. ventricosus* clustered farther from the bottom and swam more actively than *S. inermis*. This tendency was commonly observed in the intraspecific density experiment, although the proportion of individuals of *S. ventricosus* at the medium and

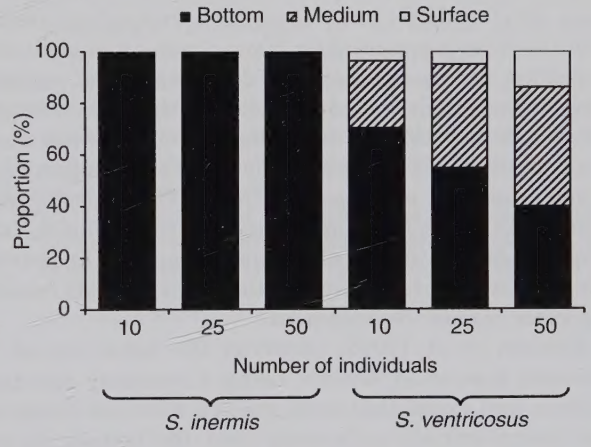

Figure 2

Proportions of fish observed in layers of seawater in three 500-L tanks, each with 10, 25, or 50 individuals of *Sebastes inermis* or *S. ventricosus*, during an experiment conducted at the Fisheries and Ocean Technologies Center of the Hiroshima Prefectural Technology Research Institute in 2011. The density experiment was carried out in 2 trials for each species: *S. inermis* on 21–22 November and 24–25 November and *S. ventricosus* on 28–29 November and 1–2 December. To assess vertical distribution of fish, 3 depth layers of seawater in the tanks were defined as follows: surface (0–20 cm), medium (20–40 cm), and bottom (40–60 cm), The data presented are the average proportions from both trials.

surface layers increased with increasing density. These results indicate that both species have species-specific behavioral patterns, regardless of the presence of the other species or the density of the same species. Therefore, the results support the 2 hypotheses.

The difference in behaviors of *S. inermis* and *S. ventricosus*, with *S. inermis* being bottom dwelling and far less active in comparison to the constantly swimming *S. ventricosus*, may be related to their feeding habits. Both *S. inermis* and *S. ventricosus* are highly selective for shrimp; however, high selectivity for amphipods and mysids has been reported for *S. ventricosus* (Akeda et al., 2012). Such prey may be more available for off-bottom individuals because the prey often appears in the water column (Sudo and Azeta, 1992). On the west coast of North America, *Sebastes* species that are distributed near the bottom of the seafloor mainly feed on benthic animals, whereas those distributed in the water column mainly feed on zooplankton (Brodeur and Pearcy, 1984; Hallacher and Roberts, 1985).

Notably, *S. inermis* were less active and consumed less energy than *S. ventricosus* in our study. The amount of food intake may largely differ between the 2 species because *S. inermis* grow slower than *S. ventricosus* (Kamimura et al., 2014). Faster growth in *S. ventricosus* would require greater food consumption than that of *S. inermis*, and shoaling behavior, which has been observed only in *S. ventricosus*, may be advantageous for foraging efficiency (Pitcher et al., 1982). Additionally, it has been hypothesized that the swim bladder is more developed in *S. ventricosus* for hovering because the swim bladder is essential for buoyancy maintenance and, therefore, reduces the energy consumption of actively swimming fish (Schwebel et al., 2018). However, we could not detect any differences in the size of the swim bladder between the 2 species, on the basis of photographs of 5 individuals for each species (Suppl. Fig. 3) (online only) taken with a soft X-ray apparatus (MI100F, Haitex, Inc., Nagoya, Japan). As a result, we are unable to provide support for the previously mentioned hypothesis regarding swim bladder development.

Johnson et al. (2003) observed the behaviors of 14 *Sebastes* species in Alaska, using a remotely operated vehicle, and found that most species were not demersal and swam actively or hovered near the bottom. In our study, *S. inermis* exhibited demersal behavior, chiefly resting at the bottom. It should be noted that many species of the genus *Sebastes* have different distribution or swimming patterns during the day and night (Green and Starr, 2011; Hannah and Rankin, 2011). For example, *S. cheni* exhibit active swimming and vertical movement to the bottom and surface of the water column only at night (Sakurai et al., 2013). *Sebastes inermis* move to eelgrass beds at night and exhibit active feeding behavior (Shoji et al., 2017). Moreover, habitat use may change ontogenetically (Rooper et al., 2007). Future studies are expected to reveal the diel changes in habitat use, feeding activity, and behavioral patterns of *S. inermis* and *S. ventricosus*.

Resumen

La información sobre las variaciones en el comportamiento entre especies congéneres y simpátricas es importante para comprender los mecanismos que permiten su coexistencia. El objetivo de este estudio fue elucidar las características de la distribución vertical diurna de las especies congéneres *Sebastes inermis* y *S. ventricosus* mediante observaciones realizadas durante experimentos de laboratorio en 2011. Cuando se alojaron 25 individuos de cada especie en un tanque de 1 kL, *S. inermis* permaneció principalmente en el fondo, mientras que *S. ventricosus* nadó activamente a 0–60 cm por encima del fondo. A distintas densidades intraespecíficas, *S. inermis* se distribuyó de forma similar en el fondo, *S. ventricosus* se distribuyó más ampliamente, y la frecuencia de individuos en las capas superiores del agua del tanque aumentó con la densidad. Estos resultados indican que los diferentes comportamientos de las 2 especies hacen posible su coexistencia sin una competencia severa por los microhábitats.

Acknowledgments

We thank T. Okazaki and S. Akashige, the former directors of the Fisheries and Ocean Technologies Center, Hiroshima Prefectural Technology Research Institute, for their constant encouragement throughout our study. We also thank the center's staff, especially Y. Yamane, K. Yoshimura, M. Nishimura, and M. Iwamoto, for their valuable assistance. The comments from the anonymous reviewers are gratefully acknowledged.

Literature cited

Akeda, K., T. Yodo, Y. Kai, and M. Yoshioka.
2012. Feeding habit of the *Sebastes inermis* species complex in western Wakasa Bay, central Japan. Aquac. Sci. 60:207–214. [In Japanese.]

Benestan, L. M., Q. Rougemon, C. Senay, E. Normandeau, E. Parent, E. Rideout, L. Bernatchez, Y. Lambert, C. Audet, and G. J. Parent.
2021. Population genomics and history of speciation reveal fishery management gaps in two related redfish species (*Sebastes mentella* and *Sebastes fasciatus*). Evol. Appl. 14:588–606.

Brodeur, R. D., and W. G. Pearcy.
1984. Food habits and dietary overlap of some shelf rockfishes (genus *Sebastes*) from the northeastern Pacific Ocean. Fish. Bull. 82:269–293.

Fisher, R. A.
1925. Statistical methods for research workers, 239 p. Oliver and Boyd, Edinburgh, UK.

Frid, A., M. McGreer, K. S. P. Gale, E. Rubidge, T. Blaine, M. Reid, A. Olson, S. Hankewich, E. Mason, D. Rolston, et al.
2018. The area–heterogeneity tradeoff applied to spatial protection of rockfish (*Sebastes* spp.) species richness. Conserv. Lett. 11:e12589.

Green, K. M., and R. M. Starr.
2011. Movements of small adult black rockfish: implications for the design of MPAs. Mar. Ecol. Prog. Ser. 436:219–230.

Hallacher, L. E., and D. A. Roberts.
1985. Differential utilization of space and food by the inshore rockfishes (Scorpaenidae: *Sebastes*) of Carmel Bay, California. Environ. Biol. Fishes 12:91–110.

Hannah, R. W., and P. S. Rankin.
2011. Site fidelity and movement of eight species of Pacific rockfish at a high-relief rocky reef on the Oregon coast. North Am. J. Fish. Manag. 31:483–494.

Hyde, J. R., and R. D. Vetter.
2007. The origin, evolution, and diversification of rockfishes of the genus *Sebastes* (Cuvier). Mol. Phylogenet. Evol. 44:790–811.

Johnson, S. W., M. L. Murphy, and D. J. Csepp.
2003. Distribution, habitat, and behavior of rockfishes, *Sebastes* spp., in nearshore waters of southeastern Alaska: observations from a remotely operated vehicle. Environ. Biol. Fishes 66:259–270.

Kai, Y., and T. Nakabo.
2008. Taxonomic review of the *Sebastes inermis* species complex (Scopaeniformes: Scorpaenidae). Ichthyol. Res. 55:238–259.

Kamimura, Y., M. Kawane, M. Hamaguchi, and J. Shoji.
2014. Age and growth of three rockfish species, *Sebastes inermis*, *S. ventricosus* and *S. cheni*, in the central Seto inland Sea, Japan. Ichthyol. Res. 61:108–114.

Larson, R. J.
1980. Competition, habitat selection, and the bathymetric segregation of two rockfish (*Sebastes*) species. Ecol. Monogr. 50:221–239.

Love, M. S., M. Yoklavich, and L. Thorsteinson.
2002. The rockfishes of the northeast Pacific, 405 p. Univ. Calif. Press, Berkeley, CA.

Matthews, K. R.
1990. An experimental study of the habitat preferences and movement patterns of copper, quillback, and brown rockfishes (*Sebastes* spp.). Environ. Biol. Fishes 29:161–178.

Mohri, K., Y. Kamimura, K. Mizuno, H. Kinoshita, S. Toshito, and J. Shoji.
2013. Seasonal changes in the fish assemblage in a seagrass bed in the central Seto Inland Sea. Aquac. Sci. 61:215–220.

Nakabo, T., and Y. Kai.
2013. Sebastidae. *In* Fishes of Japan with pictorial keys to the species, 3rd ed. (T. Nakabo, ed.), p. 668–681. Tokai Univ. Press, Hadano, Japan. [In Japanese.]

Pitcher, T. J., A. E. Magurran, and I. J. Winfield.
1982. Fish in larger shoals find food faster. Behav. Ecol. Sociobiol. 10:149–151.

R Core Team.
2021. R: a language and environment for statistical computing. R Foundation for Statistical Computing, Vienna, Austria. [Available from website, accessed May 2021.]

Richards, L. J.
1986. Depth and habitat distributions of three species of rockfish (*Sebastes*) in British Columbia: observations from the submersible PISCES IV. Environ. Biol. Fishes 17:13–21.

Rooper, C. N., J. L. Boldt, and M. Zimmermann.
2007. An assessment of juvenile Pacific Ocean perch (*Sebastes alutus*) habitat use in a deepwater nursery. Estuar. Coastal Shelf Sci. 75:371–380.

Sakurai, Y., K. Uchida, H. Mitamura, Y. Miyamoto, T. Kakihara, and N. Arai.
2013. Monitoring behavioral characteristics of the rockfish Sebastescheni [*sic*] inhabitinga [*sic*] seawall using LBL acoustic positioning system. *In* Proceedings of the Design Symposium on Conservation of Ecosystem (12th SEASTAR2000 workshop); Bangkok, 20–21 February 2012, p. 103–108. Kyoto Univ. Design School, Kyoto, Japan. [Available from website.]

Schwebel, L. N., K. Stuart, M. S. Lowery, and N. C. Wegner.
2018. Swim bladder inflation failure affects energy allocation, growth, and feed conversion of California Yellowtail (*Seriola dorsalis*) in aquaculture. Aquaculture 497:117–124.

Shoji, J., H. Mitamura, K. Ichikawa, H. Kinoshita, and N. Arai.
2017. Increase in predation risk and trophic level induced by nocturnal visits of piscivorous fishes in a temperate seagrass bed. Sci. Rep. 7:3895.

Sudo, H., and M. Azeta.
1992. Selective predation on mature male *Byblis japonicus* (amphipoda: Gammaridea) by the barface cardinalfish, *Apogon semilineatus*. Mar. Biol. 114:211–217.

Tolimieri, N., K. Andrews, G. Williams, S. Katz, and P. S. Levin.
2009. Home range size and patterns of space use by lingcod, copper rockfish and quillback rockfish in relation to diel and tidal cycles. Mar. Ecol. Prog. Ser. 380:229–243.

Williams, E. H., and S. Ralston.
2002. Distribution and co-occurrence of rockfishes (family: Sebastidae) over trawlable shelf and slope habitats of California and southern Oregon. Fish. Bull. 100:836–855.

National Marine
Fisheries Service
NOAA

Fishery Bulletin
established in 1881

Spencer F. Baird
First U.S. Commissioner
of Fisheries and founder
of *Fishery Bulletin*

Elasmobranch bycatch of the shrimp trawl fishery along the Pacific coast of Guatemala

Julio Sánchez (contact author)[1]
Omar Santana Morales[1,2]
Rebeca Zertuche[2]
Elisa Areano[1]

Email address for contact author: jfsanchez89@gmail.com

[1] Fundación Mundo Azul
Boulevard Rafael Landívar 10-05 Paseo Cayalá zona 16
Edificio D1, Oficina 202
01016 Guatemala City, Guatemala

[2] Ecología Cielo, Mar y Tierra A.C.
Avenida del Puerto 2270
Colonia Hidalgo
22880 Ensenada, Baja California, Mexico

Abstract—In this study, the species composition of bycatch in the shrimp bottom-trawl fishery off the Pacific coast of Guatemala was examined. In total, 15 species of elasmobranchs, including 13 ray species and 2 shark species, were recorded. Of these taxa, 1 species is listed as critically endangered, 4 species are listed as near threatened, 7 species are listed as vulnerable, and 1 species is listed as a species of least concern by the International Union for Conservation of Nature. Currently, there is no official monitoring system for shrimp trawling in Guatemala; therefore, the abundance and biological characteristics of the elasmobranch species caught as bycatch are unknown. This information is lacking because only 5.5% of the registered elasmobranch bycatch was landed and traded for its economic value.

Worldwide, shrimp trawling has the highest discard rate of all fisheries (27% in 2005) (Kelleher, 2005). Although reducing bycatch is important from both economic and management standpoints, bycatch is economically valuable in developing countries and supports food security in many coastal communities (Gillett, 2010; Barreto et al., 2022). Nonetheless, in many Latin American countries, shrimp trawl fisheries are currently banned because they are unsustainable (TNC[1]). In Guatemala, cartilaginous and bony fish species are incidentally caught in the shrimp trawl fishery, which is still permitted. The species that are commercially valuable are retained, and the others are discarded at sea. Shrimp trawling for 5 shrimp species and 1 prawn species is conducted on both the Pacific and Caribbean coasts of Guatemala (TNC[1]). In the 1980s and into the mid-1990s, 60 large vessels and about 1500 artisanal vessels participated in this fishery. Between 1995 and 2000, a notable reduction in catch occurred and has continued to the present day. From 2010 through 2013, 750–1500 metric tons (t) of shrimp (plus 250 t of bycatch species) were landed, but only 150 t of shrimp were landed from 2014 through 2016. In 2016, bycatch (100 t) was greater than the catch of shrimp (50 t) (FAO, 2018).

Ixquiac Cabrera (1998) identified 148 species of bony fish and 11 species of elasmobranchs among the shrimp bycatch from the Pacific coast of Guatemala, although the study did not include a complete annual fishing cycle or information on the biological characteristics of incidentally caught elasmobranchs. Using data from both the artisanal and trawl fisheries operating on the continental shelf,

Manuscript submitted 15 December 2022.
Manuscript accepted 25 April 2023.
Fish. Bull. 121:78–83 (2023).
Online publication date: 25 May 2023.
doi: 10.7755/FB.121.3.2

The views and opinions expressed or implied in this article are those of the author (or authors) and do not necessarily reflect the position of the National Marine Fisheries Service, NOAA.

[1] TNC (The Nature Conservancy). 2018. Planificación espacial marina del Pacífico de Guatemala, 108 p. Proyecto conservación y uso sostenible de la biodiversidad en áreas protegidas marino-costeras. Ministerio de Ambiente y Recursos Naturales, Consejo Nacional de Áreas Protegidas, United Nations Development Programme, and Global Environment Facility. [Available from TNC, 4245 North Fairfax Dr., Ste. 100, Arlington, VA 22203-1606.]

Ixquiac Cabrera et al.[2] constructed a catalog of batoid species present in the Pacific Ocean off Guatemala and reported 15 species from the families Dasyatidae, Myliobatidae, Urotrygonidae, Rajidae, Rhinobatidae, and Narcinidae. Nonetheless, a notable information gap exists regarding the bycatch of the shrimp trawl fishery. In an effort to fill this gap, we developed a method to evaluate the bycatch of different shrimp trawlers. Some vessels systematically and voluntarily provided samples of their bycatch from each fishing trip so that the composition of the bycatch could be characterized. Through the results of this study, we provide herein a current description of the shrimp trawl fishery in Guatemala and characterize the species composition and biological characteristics of incidentally caught elasmobranchs. These data will aid in managing these species.

Materials and methods

Study area

Bottom trawling is conducted along the Pacific coast of Guatemala within the exclusive economic zone (83,000 km^2) between the 5- and 50-m isobaths (<30 km offshore) (TNC[1]). The low-temperature months are from January through March (28.6–29.1°C), and the high-temperature months are from April through December (29.2–30.2°C) (Ponce Hernández, 2015). Therefore, the temperature of the sea surface in this region is quite stable throughout the year.

The Directorate of Fisheries and Aquaculture Regulations (DIPESCA) of Guatemala conducts official inspections at the industrial landing sites of Puerto San José and Buena Vista. However, many trawlers and small vessels strategically use the alternative artisanal landing zone of Las Lisas, which is located approximately 150 km from the industrial landing sites and has its own fish market. During the rainy season (May–October) when catches are high, fishermen are paid the best prices at Las Lisas.

Monitoring of landings

Crew members of the vessels included in this study voluntarily collected and retained a portion of the organisms that are normally discarded at sea from each fishing trip. We then collected these retained organisms and used them to obtain biological data. Landings from 69 different fishing trips and 8 different trawl vessels were documented in Las Lisas from 2017 through 2022, and portions of elasmobranchs retained from the catches were sampled and photographed. Total length (for sharks, the natural extension of the caudal fin was used), disc width, disc length, and clasper length (in males) were recorded (to the nearest 0.5 cm). The maturity of males was verified by using clasper calcification. Eggs or embryos emerging from the cloaca in females were opportunistically recorded. In addition, trawler crews gathered the elasmobranchs that were to be discarded and collected one sample (5–7 kg) per trip. Each discard specimen was photographed, measured, and identified following Compagno (2001), Ebert and Fowler (2015), and Ebert et al. (2021). For all species, we summarized the main morphological characteristics, sex ratio, and size at first maturity obtained from the literature (Villavicencio Garyzar, 2000; Anislado-Tolentino and Robinson-Mendoza, 2001; López, et al.[3]; Payán et al., 2011; Torres-Huerta[4]; Castellanos Betancourt et al., 2013; Pincay-Espinoza and Romero-Calcedo, 2014; Torres Palacios, 2015; Vélez Tacuri, 2015; Carrera-Fernández et al., 2019; Ronquillo Moreira, 2019; Jiménez García, 2020), along with conservation status according to the International Union for Conservation of Nature (IUCN) Red List of Threatened Species (IUCN, 2022). Finally, length-frequency histograms were created for species for which data for more than 30 individuals were collected.

Results and discussion

Fishing activity

Five shrimp species, the seabob (*Xiphopenaeus kroyeri*), crystal shrimp (*Penaeus brevirostris*), yellowleg shrimp (*P. californiensis*), whiteleg shrimp (*P. vannamei*), and blue shrimp (*P. stylirostris*), and 1 prawn species, the pelagic red crab (*Pleuroncodes planipes*), are harvested along the Pacific coast of Guatemala (TNC[1]). Bony fish species, such as the bigmouth sanddab (*Citharichthys gilberti*), spotted rose snapper (*Lutjanus guttatus*), and Pacific sierra (*Scomberomorus sierra*) (Jolon-Morales et al.[5]), and shark species, such as the scalloped hammerhead (*Sphyrna lewini*) (FUNMZ[6]), are also caught, landed, and marketed. From 2017 through 2022, 16 active shrimp trawlers, with an average of 5 crew members, average length of 18.66 m (13.00–22.87 m), average net registered weight of 22.37 t [4–87 t], and average gross registered weight of 70.49 t (14–170 t), operated in the

[2] Ixquiac Cabrera, M., I. Franco, J. Lemus, S. Méndez, and A. López-Roulet. 2010. Identificación, abundancia, distribución espacial de batoideos (rayas) en el Pacífico Guatemalteco, 41 p. Informe finale. Proyecto Fodecyt 34-2006. Fondo Nac. Cienc. Tecnol., Cent. Estud. Mar Acuic., and Organ. Conserv. Medio Ambiente, Guatemala City, Guatemala. [Available from Cent. Estud. Mar Acuic., Univ. San Carlos Guatem., Ciudad Universitaria zona 12, Edificio T-14, 01012 Guatemala City, Guatemala.]

[3] López, J., P. A. Mejía-Falla, and A. F. Navia. 2009. Aspectos biológicos de la raya látigo *Dasyatis longa* (Pisces: Dasyatidae) de la zona central del Pacífico colombiano. Doc. Téc. Fund. SQUALUS FS0109, 39 p. [Available from SQUALUS, Calle 10A No. 72-35, Cali 760001, Colombia.]

[4] Torres-Huerta, A. M. 2012. Peces batoideos de la plataforma continental del Golfo de Tehuantepec, 68 p. Informe final. SNIB-CONABIO proyecto no. HJ031. Inst. Recur., Univ. Mar., Puerto Angel, Mexico. [Available from website.]

[5] Jolon-Morales, M. R., R. Sanchez-Castañeda, J. C. Villagrán-Colón, C. Mechel, and H. A. Kinh. 2005. Estudio sobre los recursos pesqueros (de escama) en el Litoral Pacifico y Mar Caribe de Guatemala, 128 p. Agencia Esp. Coop. Int. and Uni. Manejo Pesca Acuic., Guatemala City, Guatemala.

[6] FUNMZ (Fundación Mundo Azul). 2023. Informe anual 2022, 25 p. FUNMZ, Guatemala City, Guatemala. [Available from website.]

region (Morales[7]). There are no closed seasons to regulate commercial shrimp fishing; as a result, trawling is conducted year-round, although shrimp trawlers are more active during the rainy season (FUNCAGUA[8]). The shrimp trawling fleet requires 30-d permits granted by DIPESCA. Normally, trawling vessels work for 12–15 d at a time, and 4–5 trawl tows are conducted each day (3–4 h of operation in total per day). We observed that trawlers, preferring to reduce fuel costs, made partial landings in Las Lisas with the aid of smaller boats from the fishing community instead of returning to the official docks of Puerto San José and Buena Vista.

A limited number of trained DIPESCA personnel are available to conduct inspections and collect data of commercial shrimp landings to control fishing activities along the Pacific coast of Guatemala; therefore, data are limited and unreliable. High staff turnover within DIPESCA has also resulted in unreported or irregularly reported catches and unreliable data. No monitoring programs currently record the additional organisms captured as bycatch in shrimp trawling activities. Information on bycatch off Guatemala is lacking, although turtles and marine mammals, in addition to elasmobranchs, are known to be captured with shrimp trawling fishing gears.

[7] Morales, J. 2022. Personal commun. Dir. Fish. Aquac. Regul. Km. 22 Carretera al Pacífico, Edificio la Ceiba, tercer nivel, Guatemala City, Guatemala.

[8] FUNCAGUA (Fundación para la Conservación del Agua de la Región Metropolitana de Guatemala). 2020. Clima en Guatemala. [Available from website.]

Landings

In all, 43 trips (62.3% of trips) were conducted during the rainy season, and 26 trips (37.7% of trips) were conducted during the dry season. A total of 1330 elasmobranchs were recorded, belonging to 5 orders, 12 families, and 15 species. Of these 15 species, 1 species is listed as critically endangered, 4 species are listed as near threatened, 7 species are listed as vulnerable, and 1 species is listed as a species of least concern on the IUCN Red List (Table 1) (IUCN, 2022). Overall, 73 elasmobranch individuals (5.5% of the total number of elasmobranchs recorded) were considered commercially valuable and sold. The bycatch mainly comprised 3 ray species, the longtail stingray (*Hypanus longus*), golden cownose ray (*Rhinoptera steindachneri*), and Pacific eagle ray (*Aetobatus laticeps*), and 2 shark species, the scalloped hammerhead and bull shark (*Carcharhinus leucas*). The fins of large sharks (>1 m in total length) were dried and marketed.

Ten elasmobranch species were discarded (number of samples [*n*]=1257, 94.5% of the total number of individuals recorded; Table 1). Of these 10 species, the vermiculate electric ray (*Narcine vermiculata*) (*n*=426) was the most abundant, followed by the Panamic stingray (*Urotrygon aspidura*) (*n*=397), whitesnout guitarfish (*Pseudobatos leucorhynchus*) (*n*=182), giant electric ray (*N. entemedor*)

Table 1

Number of samples (*n*), ratio of males (M) to females (F), size range, and status on the International Union for Conservation of Nature and Natural Resources (IUCN) Red List of Threatened Species for elasmobranch species landed by shrimp trawlers in Las Lisas, Guatemala, during 2017–2022. Also noted is whether captured individuals of non-target species were traded in the market (bycatch) or had no commercial value and were returned to the sea dead or alive (discard). The measurement of size (MS) is either total length (TL) or disk width (DW). Sizes at first maturity are from the literature. No data (ND) on size at maturity were available in the literature for *Rostroraja equatorialis*.

Species	*n*	Sex ratio (M:F)	MS	Average size (cm)	Size range (cm)	Size at first maturity (cm)		IUCN status	Discard or Bycatch
						Males	Females		
Narcine vermiculata	426	151:275	TL	20.6	6.0–39.3	11.6	11.6	Least concern	Discard
Urotrygon aspidura	397	153:244	TL	32.9	9.0–94.2	23.0	25.0	Near threatened	Discard
Pseudobatos leucorhynchus	182	58:124	TL	38.2	18.0–63.4	51.2	48.5	Vulnerable	Discard
Narcine entemedor	127	34:93	TL	27.4	14.0–68	47.7	70.0	Vulnerable	Discard
Urotrygon chilensis	72	30:42	DW	18.3	10.0–29.2	16.5	16.0	Near threatened	Discard
Hypanus longus	38	9:29	DW	62.8	7.0–131.0	92.0	120.0	Vulnerable	Bycatch
Zapteryx xyster	27	10:17	TL	36.8	26.0–57.0	46.8	50.0	Vulnerable	Discard
Gymnura crebripunctata	22	15:7	DW	34.9	18.5–54.0	34.2	58.8	Near threatened	Discard
Sphyrna lewini	17	10:7	TL	49.8	42.0–54.0	170.0	190.0	Critically endangered	Bycatch
Rhinoptera steindachneri	15	0:15	DW	39.2	26.0–47.0	71.8	71.8	Near threatened	Bycatch
Aetobatus laticeps	2	0:2	DW	41.1	37.2–45.0	83.2	83.2	Vulnerable	Bycatch
Rostroraja equatorialis	2	0:2	DW	35.1	32.7–37.5	ND	ND	Vulnerable	Discard
Carcharhinus leucas	1	0:1	TL	–	262.0	157.0	180.0	Vulnerable	Bycatch
Gymnura sp.	1	0:1	DW	–	38.0	–	–	–	Discard
Zapteryx sp.	1	1:0	TL	–	38.0	–	–	–	Discard

(n=127]), blotched stingray (*U. chilensis*) (n=72), and longtail stingray (n=38). Other species were represented by less than 30 individuals (Table 1).

In this study, 13 ray species and 2 shark species were identified. About 90% of these species belong to 3 genera, *Narcine*, *Urotrygon*, and *Pseudobatos*, which accounted for 41.6%, 35.3%, and 13.7% of the identified species, respectively. According to the distribution of sizes and sexes recorded for the most abundant species (Fig. 1), trawling could be affecting the breeding areas of the vermiculate electric ray, Panamic stingray, and blotched stingray. At the same time, this trawl fishing zone could be a breeding area for the whitesnout guitarfish, giant electric ray, and longtail stingray. This probable breeding area extends along the Pacific coast of Guatemala, between the isobaths of 5 and 50 m (TNC[1]), where trawling activities take place throughout the year. However, it is necessary to continue monitoring this fishery to be able to determine the extent and temporality of this area according to the different species recorded.

The biological characteristics shared by elasmobranch species (e.g., late sexual maturity and low fecundity) make their populations vulnerable to instability when subjected to direct or incidental fishing pressure (Walker, 1992). The trawl nets used in the Pacific Ocean off Guatemala are not selective, although they have turtle excluding devices. The resulting bycatch is concerning because of the lack of records and data (Gillett, 2010), especially considering that bycatch exceeded the catch volume of targeted shrimp species in Guatemala in 2016 (FAO, 2018).

Conservation and management

In the General Law of Fisheries and Aquaculture of Guatemala, rays are not included as target species in coastal fisheries (MAGA, 2002). In 2021, the Ministry of Agriculture, Livestock, and Food, which oversees DIPESCA, approved the National Action Plan for the Conservation of Chondrichthyans of Guatemala by ministerial agreement (no. 280-2021) (MAGA, 2021) to investigate, manage, and conserve chondrichthyan species in the exclusive economic zones of Guatemala in the Atlantic and Pacific Oceans. Nonetheless, few studies on elasmobranchs that

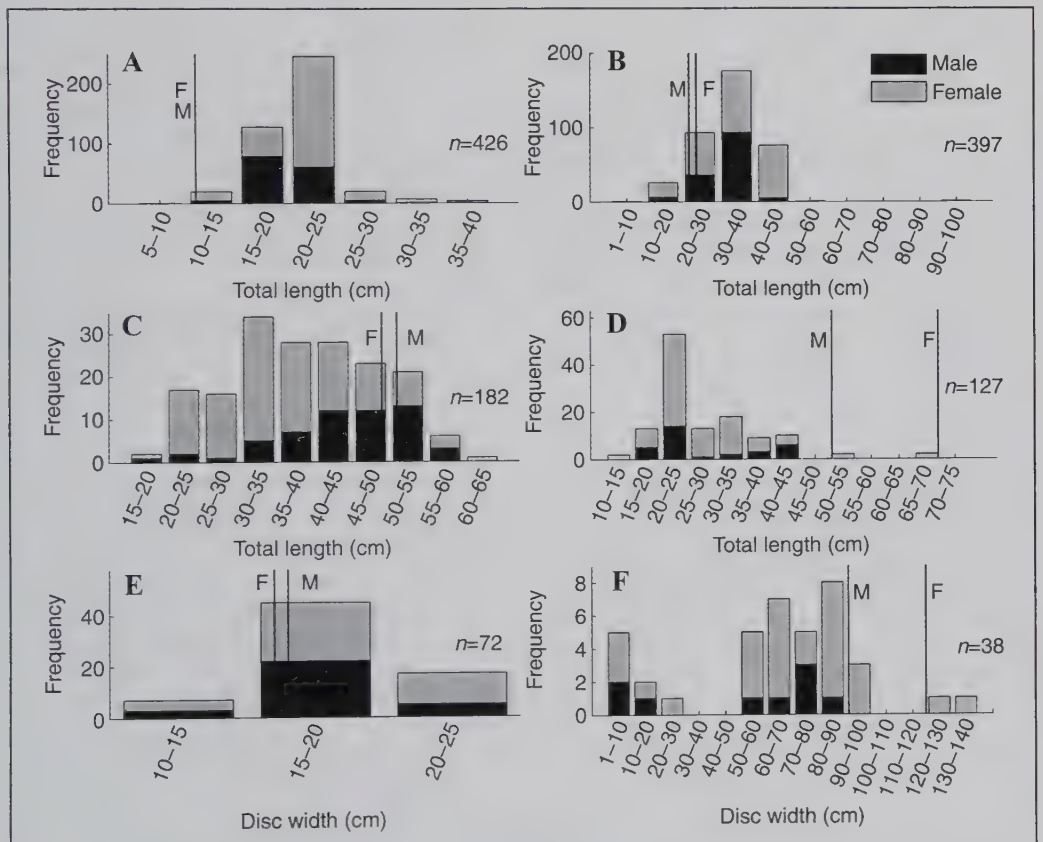

Figure 1

Size–frequency distributions of elasmobranch species landed by shrimp trawlers as bycatch from 2017 through 2022 in Las Lisas, Guatemala: (**A**) vermiculate electric ray (*Narcine vermiculata*), (**B**) Panamic stingray (*Urotrygon aspidura*), (**C**) whitesnout guitarfish (*Pseudobatos leucorhynchus*), (**D**) giant electric ray (*N. entemedor*), (**E**) blotched stingray (*U. chilensis*), and (**F**) longtail stingray (*Hypanus longus*). Histograms are based on the number of organisms sampled (n), not on the total number of individuals captured. The vertical lines indicate lengths at first maturity for males (M) and females (F).

are not commercially valuable, such as the Panamic stingray (Torres Palacios, 2015), which is listed as near threatened on the IUCN Red List (Kyne et al., 2020a), and the blotched stingray (Pincay-Espinoza and Romero-Calcedo, 2014), which also is listed as near threatened on the IUCN Red List (Kyne et al., 2020b), have been done. Therefore, little information is available to inform management decisions. Indeed, the composition and volume of ray bycatch are often unknown, and no research or monitoring efforts are directed at this group of elasmobranch species. As such, the results of this study provide an important characterization of the species composition of elasmobranchs that are normally discarded as bycatch during shrimp trawling activities off Guatemala.

Resumen

Se examinó la composición específica de la captura incidental en la pesquería de arrastre de camarón, en la costa del Pacífico de Guatemala. En total, se registraron 15 especies de elasmobranquios, incluidas 13 especies de rayas y 2 especies de tiburones. De estos taxones, 1 especie está enlistada como en riesgo crítico, 4 especies como casi amenazadas, 7 como vulnerables y 1 como de menor preocupación por la Unión Internacional para la Conservación de la Naturaleza. Actualmente, no existe un sistema oficial de monitoreo de la pesca de arrastre de camarón en Guatemala, por lo que se desconoce la abundancia y las características biológicas de las especies de elasmobranquios capturadas incidentalmente. Se carece de esta información debido a que sólo el 5.5% de la captura incidental de elasmobranquios registrada se desembarcó y comercializó por su valor económico.

Acknowledgments

This study was supported by the Shark Conservation Fund (grant no. G-21-2123555). We thank L. Trejo, J. Morales, M. Shoenbeck, T. Pereira, A. Lievana, and J. Rodríguez for their support. We also thank our community monitors in Las Lisas and the trawlers that operate along the Pacific coast of Guatemala for their collaboration during data collection.

Literature cited

Anislado-Tolentino, V., and C. Robinson-Mendoza.
2001. Age and growth for the scalloped hammerhead shark, *Sphyrna lewini* (Griffith and Smith, 1834) along the central Pacific coast of Mexico. Cienc. Mar. 27:501–520.

Barreto, G. C., M. A. Leite Lima, A. R. Carvalho, V. R. Cañete, F. H. Souza Lobato, Q. H. Pantoja Lobo, M. T. Cabrera, F. Escobar-Toledo, M. Rueda, Á. Hernández-Flores, et al.
2022. Cadenas de valor en las pesquerías de arrastre de América Latina y el Caribe—integración y análisis de estudios nacionales. FAO Doc. Téc. Pesca Acuic. 679, 70 p. FAO, Rome.

Carrera-Fernández, M., C. M. Tenelema-Delgado, and A. B. Zúñiga-Reinoso.
2019. Aspectos reproductivos de la raya mariposa, *Gymnura crebripunctata*, en el Pacífico ecuatoriano. *In* Libro de resúmenes. Primer congreso Latinoamericano de tiburones, rayas y quimeras: VIII Simposium Nacional de Tiburones y Rayas; Playa del Carmen, 27–29 March (E. C. Oñate González, A. W. Díaz Sánchez, O. Méndez, and E. E. Becerril García, eds.), p. 46. Soc. Mex. Peces Cartil., Mexico City, Mexico. [Available from website.]

Castellanos Betancourt, J. C., C. E. Ramírez Santiago, and J. L. Castillo Géniz.
2013. Catálogo de aletas, tronchos y cabezas de tiburones en el Pacífico Mexicano, 60 p. Inst. Nac. Pesca, Juarez, Mexico. [Available from website.]

Compagno, L.
2001. Sharks of the world. An annotated and illustrated catalogue of shark species known to date. Volume 2: Bullhead, mackerel and carpet sharks (Heterodontiformes, Lamniformes and Orectolobiformes). FAO Species Cat. Fish. Purp. 1, 269 p. FAO, Rome.

Ebert, D., and S. Fowler.
2015. A pocket guide to sharks of the world, 256 p. Princeton Univ. Press, Princeton, NJ.

Ebert, D. A., M. Dando, and S. Fowler.
2021. Sharks of the world: a complete guide, 608 p. Princeton Univ. Press, Princeton, NJ.

FAO (Food and Agriculture Organization of the United Nations).
2018. Diagnóstico del sector de la pesca y la acuacultura en Guatemala, 64 p. FAO, Guatemala City, Guatemala. [Available from website.]

Gillett, R.
2010. Estudio mundial sobre las pesquerías del camarón. FAO Doc. Téc. Pesca Acuic. 475, 386 p. FAO, Rome.

IUCN (International Union for Conservation of Nature and Natural Resources).
2022. The IUCN Red List of Threatened Species, vers. 2022-3. [Available from website, accessed November 2022.]

Ixquiac Cabrera, M.
1998. Análisis de la composición y distribución de la fauna de acompañamiento del camarón (FAC) en el Océano Pacífico guatemalteco dentro de las isóbatas de 10 al 100 m durante los cruceros de investigación enero 1996 a febrero 1998. B.S. thesis, 104 p. Cent. Estud. Mar Acuic., Univ. San Carlos Guatem., Guatemala City, Guatemala.

Jiménez García, Y. A.
2020. Demografía de *Rhinoptera steindachneri* (Evermann & Jenkins, 1891) y *Narcine entemedor* (Jordan & Starks, 1985); en Bahía de la Paz, BCS, México. M.S. thesis, 52 p. Cent. Interdiscip. Cienc. Mar, Inst. Politéc. Nac., La Paz, Mexico. [Available from website.]

Kelleher, K.
2005. Discards in the world's marine fisheries: an update. FAO Fish. Tech. Pap. 470, 152 p. FAO, Rome. [Available from website.]

Kyne, P. M., P. Charvet, E. M. Areano, A. Cevallos, M. Espinoza, A. González, K. Herman, P. A. Mejía-Falla, J. M. Morales-Saldaña, A. F. Navia, et al.
2020a. *Urotrygon aspidura*. The IUCN Red List of Threatened Species 2020: e.T161689A124528276. [Available from website.]

Kyne, P. M., P. Charvet, E. M. Areano, A. Cevallos, M. Espinoza, A. González, K. Herman, P. A. Mejía-Falla, J. M. Morales-Saldaña, A. F. Navia, et al.
2020b. *Urotrygon chilensis*. The IUCN Red List of Threatened Species 2020: e.T44647A124436667. [Available from website.]

MAGA (Ministerio de Agricultura, Ganadería y Alimentación).
2002. Ley general de pesca y acuicultura. Decreto no. 80-2002. Congreso de la Republica de Guatemala, Guatemala City, Guatemala. [Available from website.]
2021. Plan de acción nacional para la ordenación y conservación de tiburones, rayas y quimeras de Guatemala. Acuerdo Ministerial no. 280-2021, 2 p. Minist. Agric. Ganad. Aliment., Guatemala City, Guatemala. [Available from website.]

Payán, L. F., A. F. Navia, E. A. Rubio, and P. A. Mejía-Falla.
2011. Biología de la raya guitarra *Rhinobatos leucorhynchus* (Günther, 1867) (Rajiformes: Rhinobatidae) en el Pacífico colombiano. Lat. Am. J. Aquat. Res. 39:286–296.

Pincay-Espinoza, J., and A. Romero-Calcedo.
2014. Reproducción de la raya chilena *Urotrygon chilensis* en dos localidades del Pacífico ecuatoriano. *In* Primer Congreso Latinoamericano de Rayas y Quimeras; Manta, 10–12 March, p. 71–76. Secr. Tec. Mar., Manta, Ecuador.

Ponce Hernández, J. A.
2015. Relación entre la abundancia relativa del pez vela *Istiophorus platypterus* (Shaw, 1792) y la temperatura superficial del agua en el Pacífico de Guatemala. B.S. thesis, 29 p. Univ. San Carlos Guatem., Guatemala City, Guatemala.

Ronquillo Moreira, I. L.
2019. Distribución, abundancia, estructura de tallas y fidelidad del sitio de *Aetobatus laticeps*, mediante monitoreo participativo y foto-identificación I3S en la Reserva Marina El Pelado, Santa Elena. B.S. thesis, 57 p. Univ. Estatal Penín s. Santa Elena, Santa Elena, Ecuador. [Available from website.]

Torres Palacios, K.
2015. Edad y crecimiento de la raya espinosa *Utrotrygon aspidura* de la zona Centro-Sur del Pacífico colombiano. M.S. thesis, 59 p. Cent. Interdiscip. Cienc. Mar., Inst. Politéc. Nac., La Paz, Mexico. [Available from website.]

Vélez Tacuri, J.
2015. Aspectos reproductivos de la raya ocelada *Zapteryx xyster* (Jordan & Everman, 1896) en Santa Rosa, Salinas, Ecuador. B.S. thesis, 99 p. Univ. Laica Eloy Alfaro Manabí, Manta, Ecuador. [Available from website.]

Villavicencio Garayzar, C. J.
2000. Taxonomía abundancia estacional, edad y crecimiento y biología reproductiva de *Narcine entemedor* Jordan y Starks (Chondrichthyes; Narcinidae), en Bahía Almejas, B.C.S., México. Ph.D. diss., 136 p. Univ. Autónoma Nuevo León, San Nicolás de los Garza, Mexico. [Available from website.]

Walker, T. I.
1992. Fishery simulation model for sharks applied to the gummy shark, *Mustelus antarticus* Günther, from southern Australian waters. Mar. Freshw. Res. 43:195–212.

National Marine
Fisheries Service
NOAA

Fishery Bulletin
established in 1881

Spencer F. Baird
First U.S. Commissioner
of Fisheries and founder
of *Fishery Bulletin*

Updated reproductive parameters for the tiger shark (*Galeocerdo cuvier*) in the western North Atlantic Ocean

Lisa J. Natanson (retired) (contact author)[1]
William B. Driggers III[2]
Camilla T. McCandless[1]
Nancy E. Kohler (retired)[1]

Email address for contact author: mangrules@yahoo.ca

[1] Northeast Fisheries Science Center
National Marine Fisheries Service, NOAA
28 Tarzwell Drive
Narragansett, Rhode Island 02882

[2] Mississippi Laboratories
Southeast Fisheries Science Center
National Marine Fisheries Service, NOAA
3209 Frederic Street
Pascagoula, Mississippi 39567

Abstract—Reproductive data collected through anatomical dissection, from 48 female and 66 male tiger sharks (*Galeocerdo cuvier*) captured in the western North Atlantic Ocean, were used to assess stage of maturity. The fork length (FL) of examined females and males ranged from 88 to 318 cm and from 84 to 349 cm, respectively. Median length at maturity (L_{50}) was calculated by using binomial maturity data from dissections in addition to maturity assignments based on clasper condition examination of 320 males (46–280 cm FL) and published maturity data for 14 males (170–313 cm FL) and 28 females (242–312 cm FL). Further, sex-specific median age at maturity (A_{50}) was calculated by using direct age estimates and the aforementioned binomial maturity data from the dissected specimens. Females reached L_{50} at 261.4 cm FL and A_{50} at 11.6 years. Males reached L_{50} at 258.9 cm FL and A_{50} at 9.5 years.

Manuscript submitted 22 December 2022.
Manuscript accepted 2 June 2023.
Fish. Bull. 121:84–95 (2023).
Online publication date: 20 June 2023.
doi: 10.7755/FB.121.3.3

The views and opinions expressed or implied in this article are those of the author (or authors) and do not necessarily reflect the position of the National Marine Fisheries Service, NOAA.

The tiger shark (*Galeocerdo cuvier*) is a large, opportunistic predator that is common globally in warm temperate and tropical marine waters (Bigelow and Schroeder, 1948). Off the east coast of North America, within the western North Atlantic Ocean (WNA), the species ranges from Nova Scotia, Canada, to Texas, including in the Gulf of Mexico and the Caribbean Sea (Kohler and Turner, 2019).

In the WNA, tiger sharks are commonly caught in commercial and recreational fisheries but are usually released alive (Natanson et al., 1999). The WNA had an increase in recreational shark fishing in the 1970s, followed by the expansion of the directed shark fishery in the 1980s (Stone et al., 1998); these fisheries peaked in the late 1980s, after which abundance of tiger sharks declined by an estimated 80% into the early 1990s (Musick et al., 1993). After the implementation of the National Marine Fisheries Service Shark Management Plan in 1993, increases in tiger shark abundance were observed throughout the late 1990s and 2000s (Peterson, 2017). Although information is available on various aspects of the biology of tiger sharks, such as diet and growth dynamics, and the size of the smallest mature fish in the sample or *size at maturity* has been reported from several studies (Springer, 1960; Clark and von Schmidt, 1965; Branstetter et al., 1987; Castro, 2011), median length and age at maturity (L_{50} and A_{50}) have not been calculated for this species.

Information pertaining to the reproductive biology of tiger sharks is largely limited to reports of examined specimens or anecdotal observations included in other studies (e.g., Bigelow and Schroeder, 1948; Springer, 1960; Clark and von Schmidt, 1965). For example, worldwide, female tiger sharks are thought to reproduce biennially and reported brood sizes range from 6 to 104 embryos, although most commonly they have a brood size of 30–40 embryos (Springer, 1938; Baughman and Springer, 1950; Rivera-López, 1970;

Dodrill, 1977; Applegate et al., 1979; Simpfendorfer, 1992; Castro, 2011). Simpfendorfer (1992) found a significant relationship between litter size and maternal length, a result that, along with the possibility of spontaneous abortion due to capture, may explain the smaller litter sizes occasionally observed.

Reliable estimates of L_{50} and A_{50} are critical to gaining a complete understanding of ontogenetic shifts in behavior, migratory patterns, diet, and habitat utilization, including identification of pupping, nursery, and mating areas (e.g., Natanson et al., 2020). Of equal, and perhaps greater importance, is an understanding of the reproductive potential of the population and how long it will take an exploited population to rebuild under different management strategies. Reproductive information on the tiger shark in the WNA is primarily from Branstetter et al. (1987), who reported that maturity occurs at approximately 256.9–261.1*[1] cm fork length (FL) and 252.6* cm FL for females and males, respectively. Although size at maturity was not mentioned as different between the areas, ages at maturity differed between the Gulf of Mexico and the rest of the WNA because of growth rate differences in that study.

Shields (2018) studied the maturation of the tiger shark in the WNA, using plasma hormone concentrations supplemented by clasper calcification and ultrasonography methods for males and females, respectively. She reported that males mature between 210.2* and 244.2* cm FL and females mature between 218.7* and 252.6* cm FL, ranges that fall below those reported by Branstetter et al. (1987) for tiger sharks from this region. However, this difference in length at maturity could be related to differences between the 2 studies in the methods used to assess maturity (dissection versus noninvasive sampling), as the hormonal methods have yet to be validated. Although it is possible that size at maturity for tiger sharks has changed over the 3 decades separating the 2 studies, direct comparison between maturity estimates through the use of lethal (anatomical dissection) and nonlethal (sex steroid analysis) methods cannot be made until it has been validated that both sampling strategies accurately assign maturity status. For example, sperm has been observed in the tiger shark prior to maturation of requisite secondary sex characteristics, such as calcified claspers (Clark and von Schmidt, 1965). Although a metric, such as sex steroid concentration, from a nonlethal method could indicate the commencement of spermatogenesis, an immature male would not be capable of copulation without possessing calcified claspers. Similarly, a female could be undergoing vitellogenesis prior to the maturation of the reproductive tract and be erroneously considered mature through the use of sex steroid analysis when actually incapable of reproducing.

In this study, we updated the reproductive parameters of both male and female tiger sharks from the WNA, using measurements obtained through anatomical dissection. Additionally, we produced sex-specific, quantitatively derived estimates of L_{50} and A_{50} for the tiger shark that can be used to generate maturity schedules, which are a vital component of age-structured stock assessments.

Materials and methods

Tiger shark specimens were collected by using rod and reel during recreational fishing tournaments or longline gear during research surveys and commercial fishing operations. Upon landing, FL was measured (in centimeters) over the body (OTB) (Natanson et al., in press) from the tip of the snout to the fork in the caudal fin. Sex was assigned to all individuals on the basis of the presence or absence of claspers. Selected moribund or dead individuals were dissected to collect a suite of reproductive data upon which maturity status was assigned. All dissections were conducted by biologists from the Apex Predators Program, NOAA Northeast Fisheries Science Center, all of whom are experienced with reproductive dissection methods, using a standardized sampling protocol. We used standardized terminology for anatomical measurements from Hamlett (1999) and Hamlett and Koob (1999).

Because of difficulty in obtaining accurate weights for tissues collected aboard vessels, we relied upon linear measurements of various tissues within reproductive tracts and direct observation of external sexual characters (i.e., clasper condition) to assess the maturity of tiger sharks. All internal measurements (in millimeters) were taken from the right side of each shark at the widest portion of the organ and following the protocols detailed in Natanson and Gervelis (2013). For females, internal measurements included the anterior oviduct width, oviducal gland width, uterus width and length, ovary width and length, and diameter of the largest yolked oocyte. Internal measurements taken from male specimens included testis diameter and length, epididymis width, and ampulla epididymis width. Additionally, when functional, the right siphon sac length was measured. Siphon sacs are blind sacs between the dermis and the abdominal musculature and are requisite reproductive structures that are only functional when a male is mature or reaching a mature state. Further, the outer clasper length from the insertion to the posterior tip was measured and clasper condition was noted (i.e., uncalcified, transitional, or calcified). Assignment of male maturity for our study required fully calcified claspers that freely rotated 180° from their natural position and rhipidions that could be readily splayed opened (e.g., Clark and von Schmidt, 1965). Males that were approaching maturity as indicated by elongating yet flaccid claspers were considered to be transitional and classified as immature.

Pregnant and postpartum females, as indicated by the presence of embryos within the uteri or distended uteri, were assigned a mature status. Those that had given birth, with indications of recovery, were considered mature and in a resting (reproductively inactive) stage (Castro, 2009). Assignment of female maturity required ovaries capable of producing vitellogenic follicles and a fully developed

[1] An asterisk (*) denotes that the fork length has been converted from a total length.

reproductive tract (i.e., ovary, oviducts, oviducal glands, and uteri). Morphometric measurements of the reproductive organs of both sexes were plotted against FL to show how growth of the reproductive organs changed as an individual approached maturity. In most cases, determination of stage was made during dissection by using these criteria. For specimens that were not classified at the time of dissection, maturity status was later assigned by using the relationships between FL and organ measurements and the detailed notes taken at dissection. This process helped differentiate maturing or transitional nulliparous females from those that were truly mature.

Because of the overall small sample size and limited data for specific size classes, additional maturity data were obtained from the literature and used for analyses of L_{50}. All published data were carefully scrutinized to ensure that we agreed with the author's criteria for maturity and that the measured (i.e., not estimated) length and maturity status of individuals were explicitly stated. Published values originally reported in straight total length (TL_{STR}) were converted to FL_{OTB} by using a conversion from Natanson et al. (in press):

$$TL_{STR} = 11.90 + 1.18(FL_{OTB}),$$

coefficient of determination (r^2)=0.996,
number of samples (n)=605.

Converted values are denoted with an asterisk throughout the text. All measurements are presented in FL_{OTB} unless otherwise noted. Additional maturity data were obtained from live males tagged and released during bottom longline surveys conducted by the NOAA Southeast Fisheries Science Center between July and September off the east coast of Florida and in the northern Gulf of Mexico, with maturity status assigned solely on the basis of clasper condition.

For both sexes, L_{50} was estimated by using logistic regression fit to measured length and binomial maturity data (i.e., 0=immature, and 1=mature). Similarly, A_{50} was estimated by using a subset of the binomial maturity data that had corresponding ages from Kneebone et al. (2008), as both studies used many of the same specimens. Logistic models were fit to data for each sex separately through maximum likelihood methods by using functions available in R (vers. 4.1.3; R Core Team, 2022) as per Natanson et al. (2020). Confidence intervals (CIs) of 95% around L_{50} and A_{50} were bootstrapped from fits of a binomial generalized linear model to 1000 resamples of the maturity data (Harry et al., 2013) by using the boot package (vers. 1.3-28.1; Canty and Ripley, 2022) in R. For all models, normalized diagnostic plots of the residuals were examined visually to evaluate the appropriateness of model assumptions (Zuur et al., 2010).

Results

Dissections were conducted on 66 female and 48 male tiger sharks to assess their state of maturity and reproductive condition. Females and males ranged in size from 84.0 to 349.2 cm FL and from 88.3 to 318.0 cm FL, respectively (Fig. 1). The majority of specimens were collected between

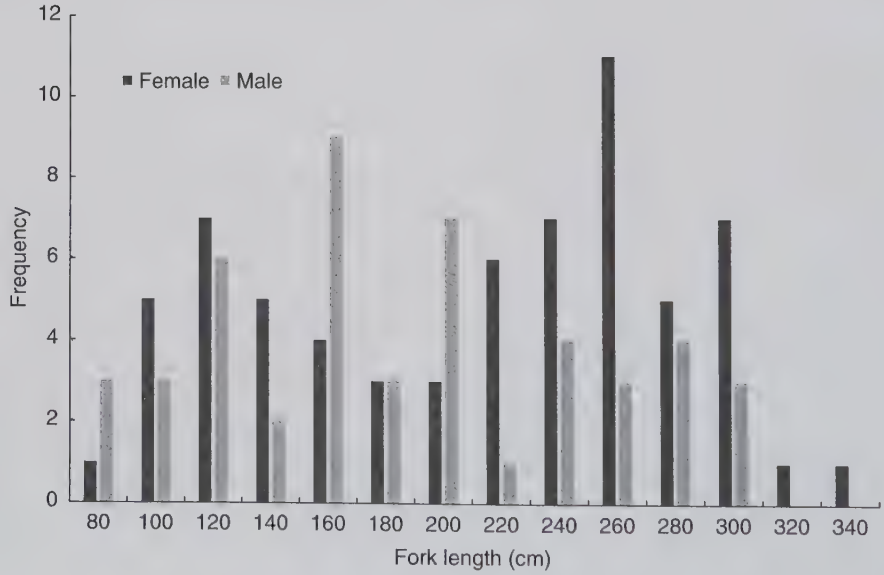

Figure 1

Size–frequency histogram for female and male tiger sharks (*Galeocerdo cuvier*) caught in waters from Massachusetts down along the Atlantic coast and into the Gulf of Mexico, between 1974 and 2019, and examined for reproductive condition.

1974 and 2019 from recreational anglers at shark fishing tournaments (60% of sexes combined, 59% of females, and 60% of males) and between May and June (78% of females and 85% of males) along the East Coast between Massachusetts and the west coast of Florida (Fig. 2). Females were caught from March through September, and males were caught from March through August.

Females

Among the females dissected, immature (n=50) and mature (n=16) specimens had size ranges of 84.0–279.4 cm FL and 270.0–349.2 cm FL, respectively. Results of regression analyses relating FL to reproductive organ measurements indicate that ovary width (F=393.61, P<0.01, r^2=0.87), ovary length (F=177.19, P<0.01, r^2=0.74), and uterus length (F=100.22, P<0.01, r^2=0.79) were not of value in assessing maturity as their relationships were linear and therefore isometric. The relationships between FL and anterior oviduct width (F=278.89, P<0.01, r^2=0.82; Fig. 3), oviducal gland width (F=847.35, P<0.01, r^2=0.93; Fig. 4), and uterus width (F=401.14, P<0.01, r^2=0.87; Fig. 5) were best fit with an exponential model and had inflection points at approximately 250 cm FL, indicating their utility for defining onset of maturation.

Immature females were characterized by undeveloped ovaries embedded within the epigonal organs, with the right ovary containing numerous macroscopically visible yet undeveloped oocytes that were white to clear in color. The left ovary appeared inactive in all specimens and remained undeveloped through ontogeny. The anterior oviduct was thin and tubular, and the immature oviducal gland presented as a slight but discrete widening approximately midway along the length of the anterior oviduct. In the smallest individuals, the uteri were not differentiated from the anterior and posterior oviducts and were only slightly differentiated from the rest of the reproductive tract prior to onset of maturation.

The transitional length range, where individuals are approaching maturity, is bracketed by the sizes of the smallest mature female and largest immature female. The smallest mature female in our sample was 270.0 cm FL, which is substantially larger than the smallest mature shark from the literature at 241.6* cm FL (Clark and von Schmidt, 1965). The largest immature female in our sample was 279.4 cm FL. Maximum follicle diameter in the transitional range was 7.5–14 mm (Table 1). Measurements from transitional individuals overlap those of mature and immature individuals, and variation in the development rates of different organs make it difficult to differentiate maturity from only one organ. However, anterior oviduct and oviducal gland sizes greater than 18.6 and 69.1 mm, respectively, could be considered to be from mature females and those below 4.0 and 25.0 mm, respectively, could be considered to be from immature females with reasonable certainty (Table 1).

Mature females ranged from 270.0 to 349.2 cm FL (n=16). Of those sampled, 1 specimen was pregnant, 7 sharks were

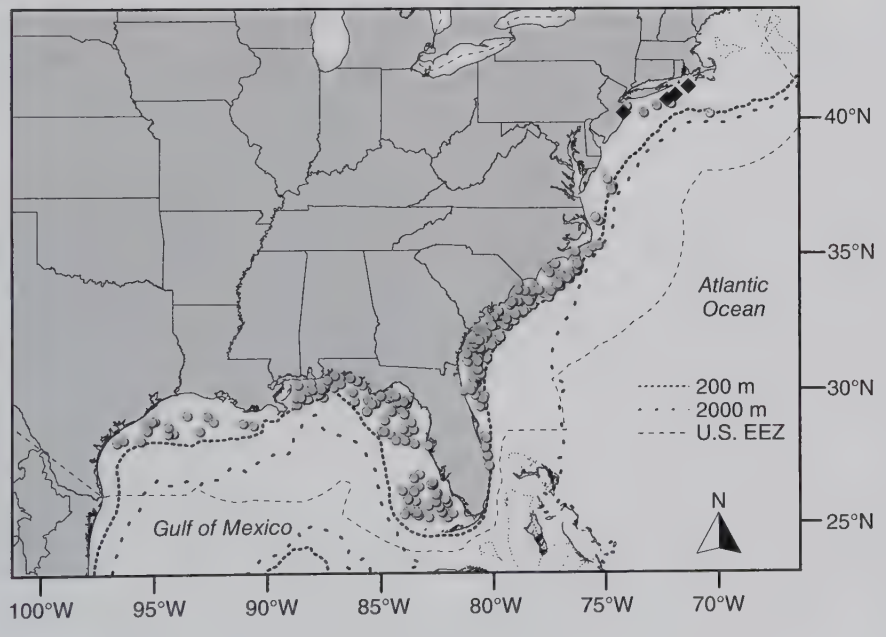

Figure 2

Map of the capture locations for tiger sharks (*Galeocerdo cuvier*) collected in the western North Atlantic Ocean, between 1974 and 2019, and examined for reproductive condition. Black diamonds represent the general locations where a total of 61 individuals were caught during 10 shark tournaments in the U.S. Northeast.

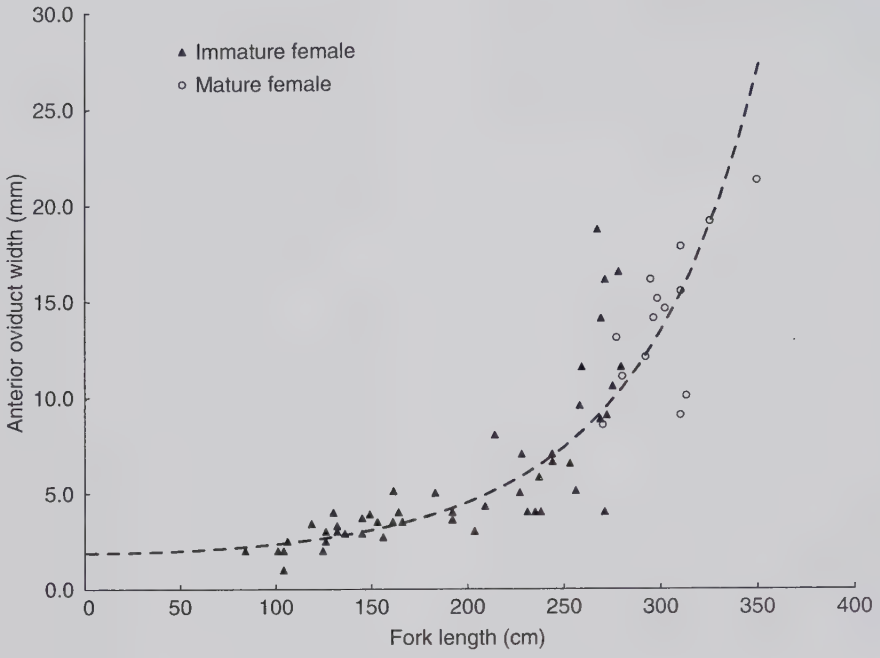

Figure 3

Relationship of anterior oviduct width (in millimeters) to fork length (FL, in centimeters) for female tiger sharks (*Galeocerdo cuvier*) (n=63) caught in waters from Massachusetts down along the Atlantic coast and into the Gulf of Mexico between 1974 and 2019. *Anterior oviduct width* (mm) = $exp(0.0637934 + (0.000022 \times FL^2\ (\text{cm})))$.

postpartum, and 8 females had just reached maturity or were resting. The pregnant female was 312.4 cm FL and was caught in June in the Gulf of Mexico with 19 embryos in each uterus. Postpartum females ranged in FL from 292.0 to 325.0 cm and were caught in June (n=1), July (n=5), and August (n=1). Five of the postpartum sharks were caught between Long Island, New York, and southern Massachusetts, and single individuals were caught off New Jersey and North Carolina and at an unknown location. Four of the 5 postpartum sharks were noted to be recently postpartum on the basis of the observation of flocculent materials in the uterus or organ condition (e.g., flaccid uteri), and no detailed information was available for the fifth one.

Males

Males that were dissected ranged in size from 88.3 to 318.0 cm FL. Immature (n=40) and mature (n=8) males had size ranges of 88.3–270.0 cm FL and 274.0–318.0 cm FL, respectively. The relationships between FL and testis length (F=273.52, P<0.01, r^2=0.87) and testes diameter (F=164.31, P<0.01, r^2=0.80) were significant but isometric and therefore not reliable in assigning maturity. The relationships between FL and epididymis width (F=112.78, P<0.01, r^2=0.75) and ampulla epididymis width (F=108.43, P<0.01, r^2=0.73) were exponential and also significant; however, there were no distinct inflection points to indicate onset of maturity, and the widths of both organs vary widely at larger body sizes because of known seasonal regression and recrudescence of these tissues. Hence, these measures were also considered of minimal value in assessing maturity.

There was a significant exponential relationship between FL and clasper length (F=1336.43, P<0.01, r^2=0.97; Fig. 6) with an abrupt inflection point indicative of the onset of maturation. Clasper length gradually increased in size relative to FL until approximately 225 cm FL, when the clasper length increased more rapidly in growth, particularly after 250 cm FL; however, the small sample size for sharks in this length range makes interpretation difficult (Fig. 6). Claspers were not completely calcified until they were over 200 mm in length, although clasper size was not entirely indicative of calcification status or maturity. The smallest fully calcified clasper was 210 mm on a 290-cm-FL male. In contrast, claspers on 4 males ranging from 268 to 297 cm FL were large (217–235 mm), but these males were considered immature because of incomplete clasper calcification. The siphon sacs were only partially formed until a male had reached approximately 200 cm FL, at which point siphon sac length grew isometrically with body length (Fig. 7). Although the measurements of clasper length and siphon sac length had some overlap between stages, claspers greater than 225 mm and siphon sacs greater than 430 mm could safely be considered to be from

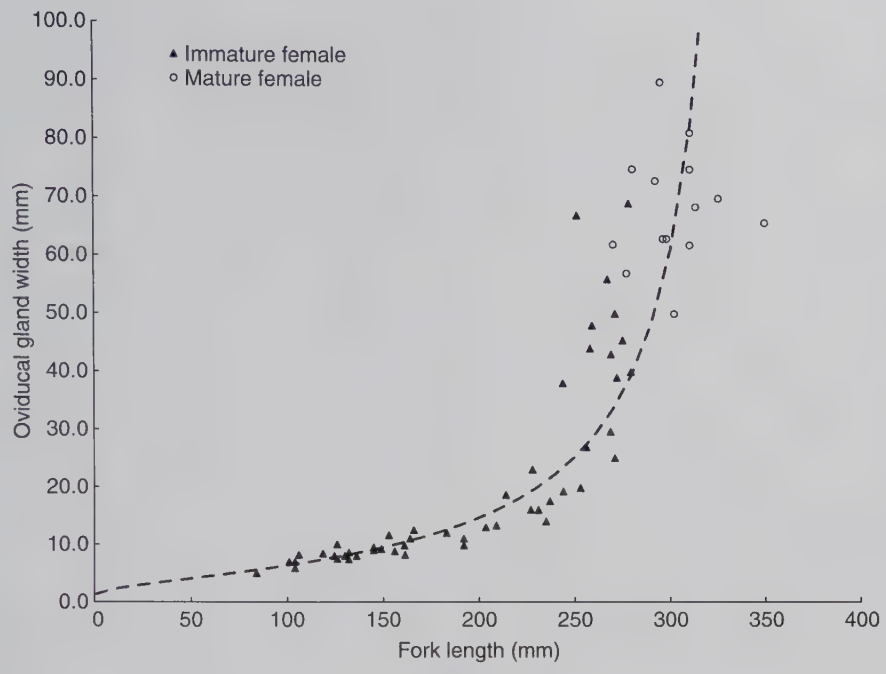

Figure 4

Relationship of oviducal gland width (in millimeters) to fork length (FL, in centimeters) for female tiger sharks (*Galeocerdo cuvier*) (n=63) caught in waters from Massachusetts down along the Atlantic coast and into the Gulf of Mexico between 1974 and 2019. *Oviducal gland width* (mm) = $1/(0.0747339 - (0.128163 \times \ln FL\ (\text{cm})))$.

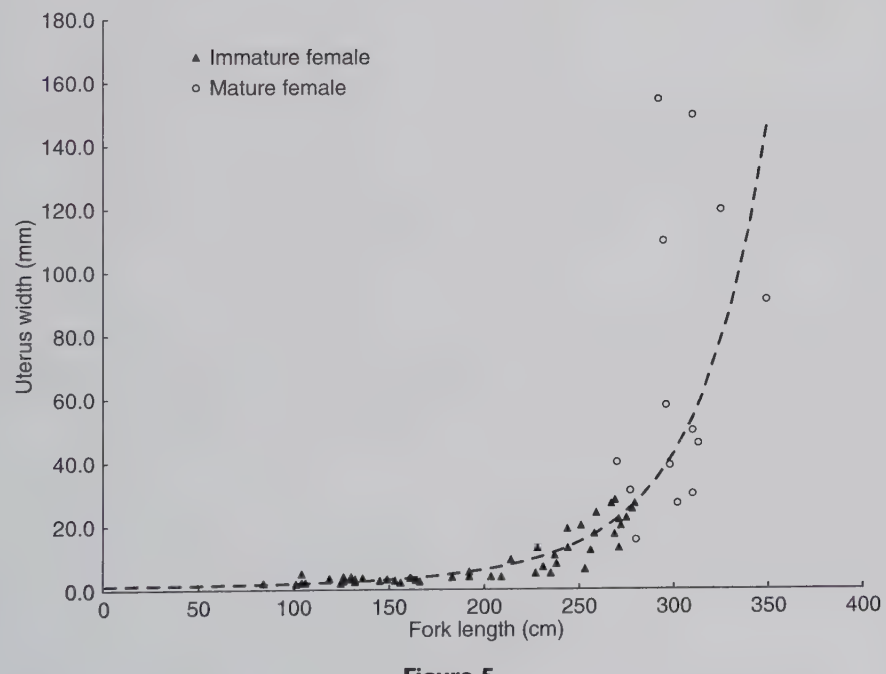

Figure 5

Relationship of uterus width (in millimeters) to fork length (FL, in centimeters) for female tiger sharks (*Galeocerdo cuvier*) (n=63) caught in waters from Massachusetts down along the Atlantic coast and into the Gulf of Mexico between 1974 and 2019. *Uterus width* (mm) = $exp(0.285987 + (0.00038 \times FL^2\ (\text{cm})))$.

Table 1

Comparison of measurements of female reproductive organs by stage for tiger sharks (*Galeocerdo cuvier*) collected in the western North Atlantic Ocean from 1974 through 2019. Stages are based on information from dissection. The measurements of the anterior oviduct, oviducal gland, and uterus are widths. FL=fork length; *n*=number of samples.

			Anterior oviduct (mm)			Oviducal gland (mm)			Uterus (mm)			Ovarian follicle diameter (mm)		
Maturity	Stage	Size range (cm FL)	Median	Range	*n*	Median	Range	*n*	Median	Range	*n*	Median	Range	*n*
Immature	Juvenile	<270.0	4.0	1.0–18.6	43	11.0	5.0–67.0	43	4.0	1.8–28.0	43	5.0	0.4–14.0	41
Immature	Transitional	≥270.0 to <279.4	10.5	4.0–16.4	7	50.0	25.0–69.1	7	22.4	13.0–40.0	7	9.6	7.5–14.0	6
Mature	Adult	≥279.4	14.5	9.0–21.1	13	68.5	40.0–90.0	13	50.0	15.5–155.0	13	10.0	6.0–14.7	13

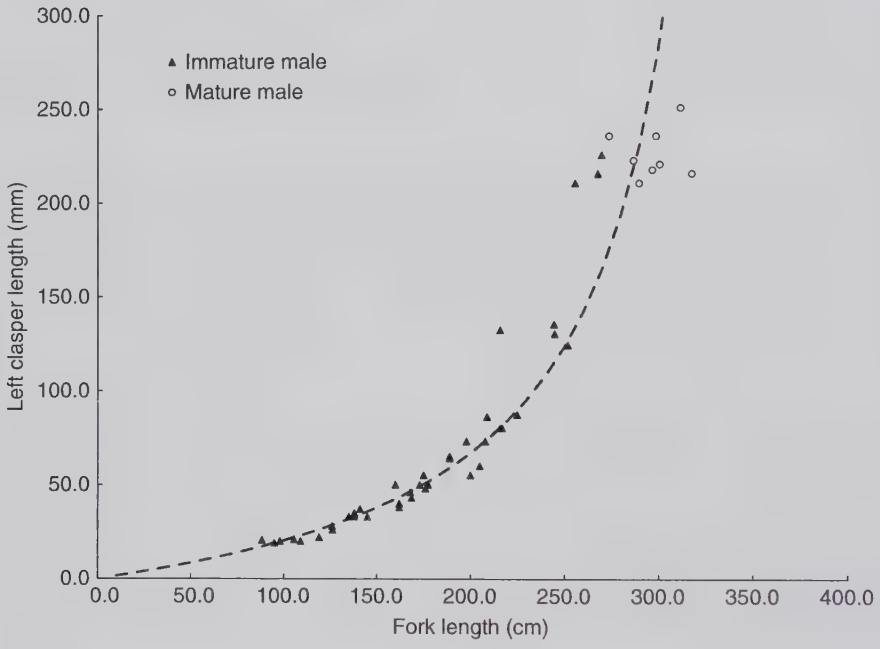

Figure 6

Relationship of left outer clasper length (in millimeters) to fork length (FL, in centimeters) for male tiger sharks (*Galeocerdo cuvier*) (*n*=48) caught in waters from Massachusetts down along the Atlantic coast and into the Gulf of Mexico between 1974 and 2014. *Left clasper length* (mm) = 1/(−0.192966 + (6.85822/*FL* (cm))).

mature fish, and those less than 210.0 and 390.0 mm, respectively, could be considered to be from immature fish, particularly if there was information on clasper calcification (Table 2).

Because of a lack of samples in the size range at which male tiger sharks appear to be maturing, the exact size range at which transition occurred could not be defined from dissection data alone. We therefore examined data for 325 males, collected during Southeast Fisheries Science Center bottom longline surveys (*n*=322) or discussed in the literature (*n*=3; Shields, 2018), that were staged on the basis of clasper condition alone. The fork lengths for 3 of these males (184.0, 210.2*, and 217.0 cm) were unrealistically low compared to dissection and published data and were therefore excluded from the ogive analysis. The remaining data indicate a lower size at maturity (232.0 cm FL) than previously published values, expanding the transitional maturity range to 232–280 cm FL, which is based on the size of the largest immature shark with uncalcified claspers (280 cm FL).

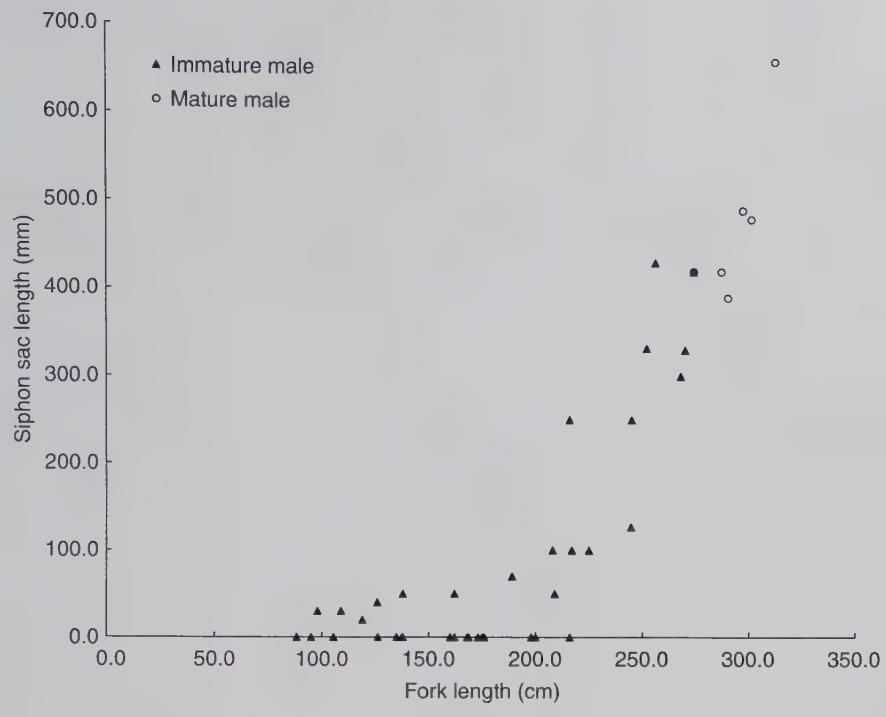

Figure 7

Relationship of siphon sac length (in millimeters) to fork length (in centimeters) for male tiger sharks (*Galeocerdo cuvier*) caught in waters from Massachusetts down along the Atlantic coast and into the Gulf of Mexico between 1974 and 2014.

Table 2

Comparison of length measurements of male reproductive organs by stage for tiger sharks (*Galeocerdo cuvier*) collected in the western North Atlantic Ocean from 1974 through 2019. Stages are based on information from dissection. Only one sample was determined to be in the transitional stage on the basis of our definition of the stage; therefore, data for this stage are not shown. FL=fork length; *n*=number of samples.

			Left clasper (mm)			Siphon sac (mm)		
Maturity	Stage	Size range (cm FL)	Median	Range	*n*	Median	Range	*n*
Immature	Juvenile	<274.0	50.0	19.0–225.0	40	25.0	0.0–430.0	34
Mature	Adult	≥280.0	220.0	210.0–250.0	7	480.0	390.0–660.0	5

Median length and age at maturity

Data for the L_{50} analysis included the 320 males (46.0–280.0 cm FL) staged on the basis of clasper condition. To fill in other important size classes for which data were limited or missing, we also included data from 42 tiger sharks (14 males and 28 females, 170.4*–312.8* cm FL and 241.6*–311.9* cm FL, respectively) obtained from 5 publications (Clark and von Schmidt, 1965; Rivera-López, 1970; Dodrill, 1977; Branstetter et al., 1987; Castro, 2011). Combining all data sources, the estimated L_{50} for females was 261.4 cm FL (95% CI: 251.6–270.6 cm FL) (Fig. 8A). For males, the estimated L_{50} was 258.9 cm FL (95% CI: 247.9–269.8 cm FL) (Fig. 8B). The A_{50} for females estimated by using direct age data was 11.5 years (95% CI: 10.2–14.2 years) (Fig. 9A). For males, the estimated A_{50} was 9.5 years (95% CI: 8.6–12.3 years) (Fig. 9B).

Discussion

The data presented herein represent the largest compilation of reproductive samples for tiger sharks thus far available for this species in the WNA. Unfortunately, sampling issues common for large migratory species create limitations to these data. It is difficult to obtain an adequate

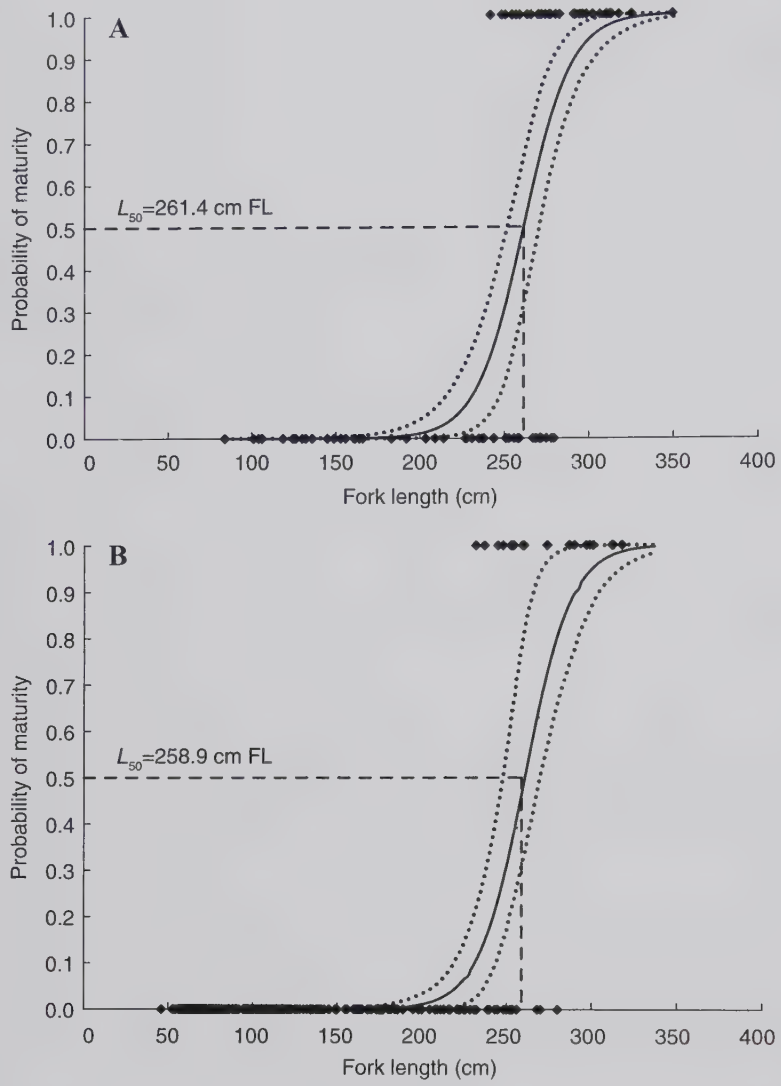

Figure 8

Maturity ogives based on length for (**A**) female and (**B**) male tiger sharks (*Galeocerdo cuvier*) caught in waters from Massachusetts down along the Atlantic coast and into the Gulf of Mexico between 1974 and 2019. The horizontal and vertical lines indicate median size at 50% maturity. The dotted curved lines are 95% confidence intervals. Females: *Probability mature* = $exp(-18.86125 + (0.07216 \times FL\ (\text{cm})))/(1 + exp(-18.86125 + (0.07216 \times FL\ (\text{cm}))))$. Males: *Probability mature* = $exp(-19.17472 + (0.07406 \times FL\ (\text{cm})))/(1 + exp(-19.17472 + (0.07406 \times FL\ (\text{cm}))))$. FL=fork length.

number of samples from all sizes and reproductive stages of a migratory shark, as access is often limited to shore-based or fishery-dependent sampling. Tiger sharks are known to be highly migratory and to have discrete pupping areas (Driggers et al., 2008; Kohler and Turner, 2019). Young tiger sharks are thought to be primarily coastal, and results from recent studies indicate that mature tiger sharks of both sexes are highly migratory (Hammerschlag et al., 2012; Lea et al., 2015; Rooker et al., 2019).

Our study was very fishery dependent. Over 60% of the sharks dissected were caught on recreational and commercial vessels that were primarily in coastal waters. Fishing location likely limits the catch to mostly juveniles, as seen in this study. The smaller sample size of the maturing and mature fish was likely influenced by catch location and the effects of a commercial fishery that caused an 80% decline in the population in the 1990s (Musick et al., 1993), and the limited number of these fish may bias the sample. We attempted to mitigate this issue by adding data from published studies and research surveys, although the coastal nature of these surveys is very similar to the locations of recreational and commercial fishing. Despite these sampling limitations, our data encompass the full known size range of the tiger shark (Fig. 1) and the coastal geographic coverage of the WNA (Fig. 2); therefore, our estimates represent the portion of the tiger shark population in this region.

The size of the smallest mature female in our sample (270.0 cm FL) is within the range of worldwide estimates for the tiger shark (220.4–286.5* cm FL) (Kauffman, 1950; Fourmanoir, 1961; Stevens, 1984; Simpfendorfer, 1992; Whitney and Cowe, 2007; Shields, 2018). Incorporating data from other trusted sources into our ogive analysis decreased the size of the smallest mature female to 241.6* cm FL, presented by Clark and von Schmidt (1965), resulted in a range that more accurately represents the species in the WNA and improved ogive analysis.

It is interesting to note that more recent data contain information on several mature males that were substantially smaller than the smallest size estimates for mature males presented in Branstetter et al. (1987) (252.6* cm FL). Aside from the 3 males with fork lengths that were not used in our ogive (from surveys: 184.0 and 217.0 cm; from Shields, 2018: 210.2* cm), an additional 4 males (232.0–248.0 cm) from this study were staged mature at sizes less than those presented in the literature (Stevens, 1984; Branstetter et al., 1987; Whitney and Crow, 2007; Shields, 2018). The lengths of the latter 4 males were within the parameters of the dissection data and were included in the ogive. Alternatively, the size of the smallest mature female in our study was much higher than previously reported for this species in the WNA by Clark and von Schmidt (1965). Although these differences could be due to a response to environmental and fishing pressure affecting the size at maturation of

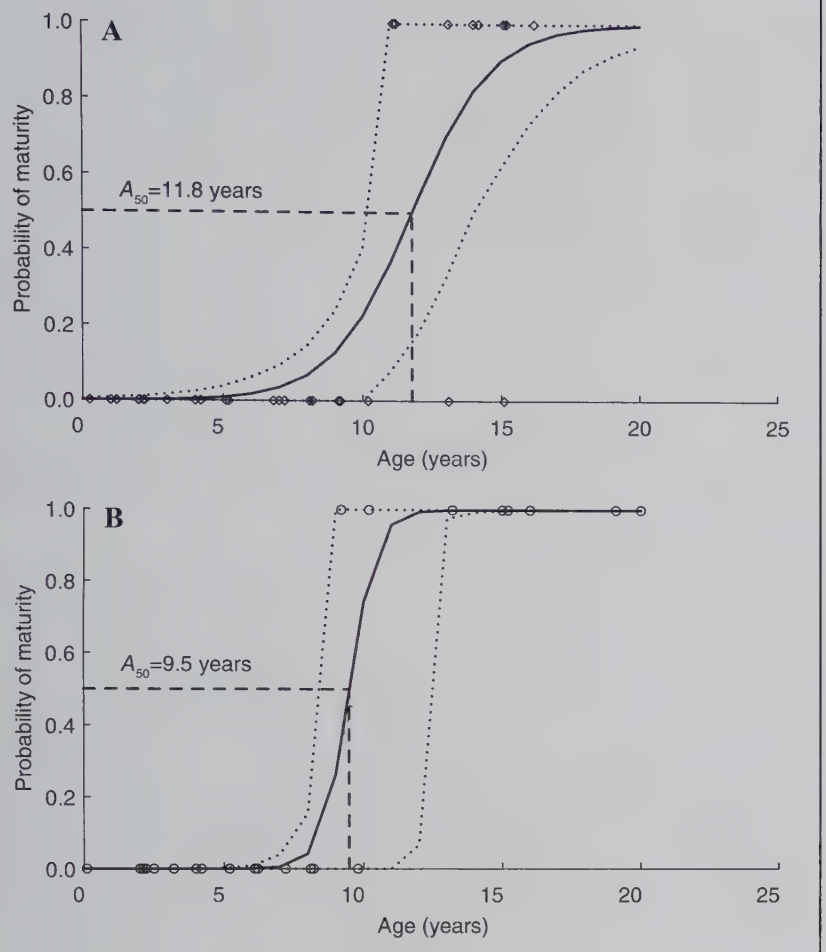

Figure 9

Age ogives based on length for (**A**) female and (**B**) male tiger sharks (*Galeocerdo cuvier*) caught in waters from Massachusetts down along the Atlantic coast and into the Gulf of Mexico between 1974 and 2019. The horizontal and vertical lines indicate median size at 50% maturity. The dotted curved lines are 95% confidence intervals. Females: *Probability mature* = $exp(-8.1803 + (0.6947 \times age\ (\text{years})))/(1+ exp(-8.1803 + (0.6947 \times age\ (\text{years}))))$. Males: *Probability mature* = $exp(-19.906 + (2.097 \times age\ (\text{years})))/(1 + exp(-19.906 + (2.097 \times age\ (\text{years}))))$.

the tiger shark over time, they could also be due to sampling bias as discussed previously.

As is commonly the case for males, use of a combination of clasper length and stage of calcification is the most accurate method of determining maturity, and it is nonlethal (Clark and von Schmidt, 1965; Natanson and Gervelis, 2013). Mature males have rigid claspers, with the ability of the clasper to rotate freely and of the rhipidion to splay, whereas immature males have soft or plastic claspers that do not easily open or rotate (Clark and von Schmidt, 1965). Clasper calcification appears to be the last phase of maturation for the tiger shark on the basis of males that did not have fully rigid claspers having all of their other reproductive organs be visibly mature. Either the internal reproductive organs of the male tiger shark grew isometrically or there was no distinct inflection in their measurement, making them of little value in quantitatively assessing maturity. In contrast, there was a very distinct inflection in siphon sac length at approximately 250 cm FL. The distinct siphon sac inflection has also been observed in the shortfin mako (*Isurus oxyrinchus*) and the porbeagle (*Lamna nasus*) (senior author, unpubl. data). Because of the presence of external reproductive organs in males, and the tendency for clasper calcification to be the last stage of maturation, assessing clasper condition is a viable alternative to lethal sampling. Nonlethal hormonal studies, however, still need to be validated, for both sexes, but particularly for females who have no external reproductive organs and go through several distinct stages.

Determining maturity from individual organ measurements can be complex. Quantitative overlap between organ measurements occurs between stages (Tables 1 and 2), and there is variation in organ growth between individuals. The internal reproductive organs of the female tiger shark were of varying use as indicators of maturity; therefore, the results from using one organ as an indicator of maturity could be misleading. Additionally, there is overlap in the measurements of individual reproductive organs between stages; in the transitional stage, maturity is particularly difficult to determine from examination of a single organ (Tables 1 and 2). Overlap in measurements between maturity stages is not uncommon and has been found in the sandbar shark (*Carcharhinus plumbeus*) and the common thresher shark (*Alopias vulpinus*) (Baremore and Hale, 2012; Natanson and Gervelis, 2013), among others. It is best to use a combination of observations and measurements when assessing maturity (Baremore and Hale, 2012); however, if that is not possible, measurements from multiple reproductive organs need to be examined in concert. Additionally, the relationship of organ development to body length is species specific (e.g., in female common thresher sharks, measurements of all internal reproductive organs except the oviducal gland had an inflection [Natanson and Gervelis, 2013], but in the study described herein, the oviducal gland width did have an inflection). Although clasper development and calcification appear to be consistent indicators of maturity among species, a full analysis of species reproduction for both sexes is vital in determining maturity.

The estimates of L_{50} and A_{50} for the tiger shark provide information for management of this species and improve on previous information. Using updated reproductive data and direct estimates from paired ages and maturities, we

have refined the estimates and present A_{50} as 11.5 and 9.5 years for females and males, respectively. These estimates are similar to those of Kneebone et al. (2008), who estimated that the smallest mature female and male tiger sharks reached maturity at the age of 10 years on the basis of their validated growth curves and maturity estimates from Branstetter et al. (1987).

Brood size information was limited in this study to 1 shark with 38 young, but data from the WNA indicate a range of 18–70 young (Springer, 1938; Baughman and Springer, 1950; Dodrill, 1977; Castro, 2011). Worldwide, estimates of brood size reach 104 young (Applegate et al., 1979).

Conclusions

We examined the reproductive characteristics of the tiger shark in the WNA. Results of our analysis indicate that the values of L_{50} and A_{50} are similar to sizes and ages of the smallest mature individuals found in previous studies (Springer, 1960; Clark and von Schmidt, 1965; Branstetter et al., 1987; Kneebone et al., 2008; Castro 2011; Shields, 2018). Females reached L_{50} at 261.4 cm FL and A_{50} at 11.6 years. Males reached L_{50} at 258.9 cm FL and A_{50} at 9.5 years. This information can be used for input into species management in terms of maturity schedules and reproductive potential. These data are also useful in essential fish habitat analyses that may lead to management through the use of open and closed areas.

Resumen

Para evaluar el estado de madurez de tiburón tigre (*Galeocerdo cuvier*), se utilizaron datos reproductivos colectados mediante disección anatómica de 48 hembras y 66 machos capturados en el océano Atlántico noroeste. La longitud furcal (FL) de las hembras y machos examinados varió de 88 a 318 cm y de 84 a 349 cm, respectivamente. La longitud mediana de la madurez (L_{50}) se calculó utilizando datos binomiales de madurez a partir de disecciones en conjunto con asignaciones de madurez basadas en la condición del gonopterigios (cláspers) de 320 machos (46–280 cm FL) y datos de madurez publicados para 14 machos (170–313 cm FL) y 28 hembras (242–312 cm FL). Además, para cada sexo, se calculó edad mediana de madurez (A_{50}) utilizando estimaciones directas de la edad y los datos binomiales de madurez antes mencionados de los especímenes disectados. Las hembras alcanzaron la L_{50} a los 261.4 cm FL y la A_{50} a los 11.6 años. Los machos alcanzaron la L_{50} a los 258.9 cm FL y la A_{50} a los 9.5 años.

Acknowledgments

We thank the officials and participants of the many shark tournaments along the U.S. northeast coast as well as commercial and recreational fishermen for allowing us to sample their landed tiger sharks. M. Winton provided some of the R code used during this study. We also appreciate all the people who helped get us references during the pandemic: N. Hammerschlag, N. Whitney, J. Kneebone, and J. Castro. We are grateful for the efforts of M. Passerotti, K. Zewinski, and K. Hannan in locating data.

Literature cited

Applegate, S. P., L. Espinosa-Arrubarrena, L. B. Menchaca-López, and F. Sotelo-Macías.
1979. Tiburones mexicanos, 150 p. Dir. Gen. Ciencia Tecnol. Mar, Subsecr. Educ. Investig. Techol., Secr. Educ. Pública, Mexico City, Mexico.

Baremore, I. E., and L. F. Hale.
2012. Reproduction of the sandbar shark in the western North Atlantic Ocean and Gulf of Mexico. Mar. Coast. Fish. 4:560–572.

Baughman, J. L., and S. Springer.
1950. Biological and economic notes on the sharks of the Gulf of Mexico, with reference to those of Texas, and with a key for their identification. Am. Midl. Nat. 44:96–152.

Bigelow, H. B., and W. C. Schroeder.
1948. Sharks. *In* Fishes of the western North Atlantic. Part 1: lancelets, cyclostomes, sharks (J. Tee-Van, C. M. Breder, S. F. Hildebrand, A. E. Parr, and W. C. Schroeder, eds.), p. 59–546. Sears Found. Mar. Res., Yale Univ., New Haven, CT.

Branstetter, S., J. A. Musick, and J. A. Colvocoresses.
1987. A comparison of the age and growth of the tiger shark, *Galeocerdo cuvier*, from off Virginia and from the northwestern Gulf of Mexico. Fish. Bull. 85:269–279.

Canty, A., and B. Ripley.
2022. boot: bootstrap R (S-Plus) functions. R package, vers. 1.3-28.1. [Available from website, accessed March 2023.]

Castro, J. I.
2009. Observations on the reproductive cycles of some viviparous North American sharks. Aqua Int. J. Ichthyol. 15:205–222.
2011. The sharks of North America, 640 p. Oxford Univ. Press, New York.

Clark, E., and K. von Schmidt.
1965. Sharks of the central Gulf Coast of Florida. Bull. Mar. Sci. 15:13–83.

Dodrill, J. W.
1977. A hook and line survey of the sharks found within five hundred meters of shore along Melbourne Beach, Brevard County, Florida. M.S. thesis, 304 p. Florida Inst. Technol., Melbourne, FL.

Driggers, W. B., III, G. W. Ingram Jr., M. A. Grace, C. T. Gledhill, T. A. Henwood, C. N. Horton, and C. M. Jones.
2008. Pupping areas and mortality rates of young tiger sharks *Galeocerdo cuvier* in the western North Atlantic Ocean. Aquat. Biol. 2:161–170.

Fourmanoir, P.
1961. Requins de la côte ouest de Madagascar. Mem. Inst. Sci. Madagascar, Ser. F (Oceanogr.) 4, 81 p.

Hamlett, W. C.
1999. Male reproductive system. *In* Sharks, skates, and rays: the biology of elasmobranch fishes (W. C. Hamlett, ed.), p. 444–470. Johns Hopkins Univ. Press, Baltimore, MD.

Hamlett, W. C., and T. J. Koob.
1999. Female reproductive system. *In* Sharks, skates, and rays: the biology of elasmobranch fishes (W. C. Hamlett, ed.), p. 398–443. Johns Hopkins Univ. Press, Baltimore, MD.

Hammerschlag, N., A. J. Gallagher, J. Wester, J. Luo, and J. S. Ault.
2012. Don't bite the hand that feeds: assessing ecological impacts of provisioning ecotourism on an apex marine predator. Funct. Ecol. 26:567–576.

Harry, A. V., A. J. Tobin, and C. A. Simpfendorfer.
2013. Age, growth and reproductive biology of the spot-tail shark, *Carcharhinus sorrah*, and the Australian black-tip shark, *C. tilstoni*, from the Great Barrier Reef World Heritage Area, north-eastern Australia. Mar. Freshw. Res. 64:277–293.

Kauffman, D. E.
1950. Notes on the biology of the tiger shark (*Galeocerdo atcticus*) from Philippne waters. U.S. Fish Wildl. Serv. Res. Rep. 16, 10 p.

Kneebone J., L. J. Natanson, A. H. Andrews, and W. H. Howell.
2008. Using bomb radiocarbon analyses to validate age and growth estimates for the tiger shark, *Galeocerdo cuvier*, in the western North Atlantic. Mar. Biol. 154:423–434.

Kohler, N. E., and P. A. Turner.
2019. Distributions and movements of Atlantic shark species: a 52-year retrospective atlas of mark and recapture data. Mar. Fish. Rev. 81(2):1–93.

Lea, J. S. E., B. M. Wetherbee, N. Queiroz, N. Burnie, C. Aming, L. L. Sousa, G. R. Mucientes, N. E. Humphries, G. M. Harvey, D. W. Sims, et al.
2015. Repeated, long-distance migrations by a philopatric predator targeting highly contrasting ecosystems. Sci. Rep. 5:11202.

Musick, J. A., S. Branstetter, and J. A. Colvocoresses.
1993. Trends in shark abundance from 1974 to 1991 for the Chesapeake Bight region of the U.S. Mid-Atlantic Coast. *In* Conservation biology of elasmobranchs (S. Branstetter, ed.), p. 1–18. NOAA Tech. Rep. NMFS 115.

Natanson, L. J., and B. J. Gervelis.
2013. The reproductive biology of the common thresher shark in the western North Atlantic Ocean. Trans. Am. Fish. Soc. 142:1546–1562.

Natanson, L. J., J. G. Casey, N. E. Kohler, and T. Colket IV.
1999. Growth of the tiger shark, *Galeocerdo cuvier*, in the western North Atlantic based on tag returns and length frequencies; and a note on the effects of tagging. Fish. Bull. 97:944–953.

Natanson, L. J., M. Winton, H. Bowlby, W. Joyce, B. Deacy, R. Coelho, and D. Rosa.
2020. Updated reproductive parameters for the shortfin mako (*Isurus oxyrinchus*) in the North Atlantic Ocean with inferences of distribution by sex and reproductive stage. Fish. Bull. 118:21–36.

Natanson, L. J., C. T. McCandless, M. S. Passerotti, C. N. Belcher, H. Bowlby, W. B. Driggers III, B. S. Frazier, J. Gelsleichter, S. J. B. Gulak, J. M. Hendon, et al.
In press. Morphometric conversions for 33 shark species from the western North Atlantic Ocean. Mar. Fish. Rev. 84(3–4).

Peterson, C. D., C. N. Belcher, D. M. Bethea, W. B. Driggers III, B. S Frazier, and R. J. Latour.
2017. Preliminary recovery of coastal sharks in the south-east United States. Fish Fish. 18:845–859.

R Core Team.
2022. R: a language and environment for statistical computing. R Foundation for Statistical Computing, Vienna, Austria. [Available from website, accessed March 2022.]

Rivera-López, J.
1970. Studies on the biology of the nurse shark, *Ginglymostoma cirratum* Bonneterre and the tiger shark, *Galeocerdo cuvieri* Peron and Le Sueur. M.S. thesis, 80 p. Univ. Puerto Rico, Mayaguez, Puerto Rico.

Rooker, J. R., M. A. Dance, R. J. D. Wells, M. J. Ajemian, B. A. Block, M. R. Castleton, J. M. Drymon, B. J. Falterman, J. S. Franks, N. Hammerschlag, et al.
2019. Population connectivity of pelagic megafauna in the Cuba-Mexico-United States triangle. Sci. Rep. 9:1663.

Shields, C.
2018. Reproductive biology of the tiger shark in the western North Atlantic Ocean. M.S. thesis, 68 p. Univ. North Fla., Jacksonville, FL. [Available from website.]

Simpfendorfer, C.
1992. Biology of tiger sharks (*Galeocerdo cuvier*) caught by Queensland Shark Meshing Program off Townsville, Australia. Mar. Freshw. Res 43:33–43.

Springer, S.
1938. Notes on the sharks of Florida. Proc. Fla. Acad. Sci. 3:9–41.
1960. Natural history of the sandbar shark *Eulamia milberti*. Fish. Bull. 61:1–38.

Stevens, J. D.
1984. Biological observations on sharks caught by sport fishermen off New South Wales. Mar. Freshw. Res. 35:573–590.

Stone, R. B, C. M. Bailey, S. A. McLaughlin, P. M. Mace, and M. B. Schulze.
1998. Federal management of US Atlantic shark fisheries. Fish. Res. 39:215–221.

Whitney, N. M., and G. L. Crow.
2007. Reproductive biology of the tiger shark (*Galeocerdo cuvier*) in Hawaii. Mar. Biol. 151:63–70.

Zuur, A. F., E. N. Ieno, and C. S. Elphick.
2010. A protocol for data exploration to avoid common statistical problems. Methods Ecol. Evol. 1:3–14.

National Marine
Fisheries Service
NOAA

Fishery Bulletin
established in 1881

Spencer F. Baird
First U.S. Commissioner
of Fisheries and founder
of *Fishery Bulletin*

Timing and environmental drivers of spawning migrations of alewife (*Alosa pseudoharengus*) and blueback herring (*A. aestivalis*) in rivers of Chesapeake Bay

Henry D. Legett (contact author)
Robert Aguilar
Keira Heggie
Kimberly D. Richie
Matthew B. Ogburn

Email address for contact author: legetth@si.edu

Smithsonian Environmental Research Center
647 Contees Wharf Road
Edgewater, Maryland 21037

Abstract—Annual life history events, such as migration and spawning in fish, are often timed to match seasonal fluctuations in environmental conditions. Understanding phenological patterns and their drivers is needed to conserve vulnerable fish populations, particularly as climate change is disrupting seasonal transitions. In this study, we examined the phenology of spring spawning migrations of river herring, the alewife (*Alosa pseudoharengus*) and the blueback herring (*A. aestivalis*), in 4 rivers of Chesapeake Bay over 7 years (2013–2019). We used imaging sonar and weekly biological samples to estimate species-specific hourly fish counts in the Choptank River, Deer Creek (a tributary of Susquehanna River), Marshyhope Creek (a tributary of Nanticoke River), and the Patapsco River. Our results indicate that patterns of water temperature in spring drive spawning migrations at seasonal, daily, and hourly scales. The relationship between fish counts and other environmental factors, such as streamflow, lunar phase, turbidity, wind stress, and tides, were annually inconsistent, and their influences on migrations may be river specific. For both species, distinct diel patterns in movement were observed. Migrations were diurnal in the Choptank River and Marshyhope Creek but nocturnal in Deer Creek and the Patapsco River. Observed interannual and inter-river variation in phenology and the influence of non-temperature factors on migrations highlight the need for long-term, multi-river monitoring of river herring in Chesapeake Bay.

Manuscript submitted 4 January 2023.
Manuscript accepted 24 July 2023
Fish. Bull. 121:96–111 (2023).
Online publication date: 24 August 2023.
doi: 10.7755/FB.121.3.4

The views and opinions expressed or implied in this article are those of the author (or authors) and do not necessarily reflect the position of the National Marine Fisheries Service, NOAA.

The life history strategies of many plants and animals depend on specific environmental conditions and resource levels that fluctuate with seasons (Forrest and Miller-Rushing, 2010). Annual migration events, for example, are often timed to match spatiotemporal shifts in resources. However, species across taxa are altering the timing of their life history events in response to climate change (Root et al., 2003), disrupting such phenological linkages (e.g., Staudinger et al., 2019). As species respond differently to changes in environmental regimes and seasonal transitions, asynchrony in biotic interactions can result in extirpations and extinctions (Parmesan, 2007; Bellard et al., 2012). Therefore, understanding phenology and how environmental conditions drive life history events is critical for the conservation of vulnerable populations and development of climate adaptation management strategies.

River herring, which is the collective term for the alewife (*Alosa pseudoharengus*) and the blueback herring (*A. aestivalis*), are anadromous fish species that range along the Atlantic coast of North America. Adult river herring annually migrate between marine and freshwater habitats, spending most of their adult lives at sea and returning to freshwater systems in spring to spawn. These migrations connect different aquatic ecosystems by moving energy and nutrients among ocean, estuarine, and freshwater food webs and support a diverse community of higher trophic level fishes, birds, and mammals (MacAvoy et al., 2009; Dias et al., 2019). In addition, the predictable timing of these migrations historically made river herring a valuable resource for coastal human communities (Hall et al., 2012). Through the 19th and 20th centuries, however, severe declines in abundance of river herring occurred across the range of these taxa, and by the 2010s commercial harvests had decreased to <2% of their historical peaks (ASMFC, 2017). These declines were driven by overfishing, bycatch in other fisheries, the destruction and degradation of freshwater spawning habitats, and the damming of waterways that obstruct spawning migrations (Atkins and Foster, 1868; Limburg and Waldman, 2009; Hall et al., 2012; Hasselman et al., 2016).

Although restoration efforts, such as fishing moratoria and dam removals, have resulted in increasing abundance of river herring in some rivers (e.g., Wippelhauser, 2021), many populations remain at historic lows. Furthermore, these low abundances make river herring vulnerable to the detrimental effects of climate change (Hare et al., 2021). Loss of suitable spawning habitat, northward shifts in distributions, and temporal shifts in migration and spawning patterns due to warming temperatures have already been documented for river herring and other diadromous fishes (Nye et al., 2009; Peer and Miller, 2014; Lynch et al., 2015; Lombardo et al., 2019; Nack et al., 2019; Staudinger et al., 2019).

The sensitivity of river herring to climate change is, in part, due to a link between their life cycles and water temperature. The results of previous behavioral experiments and counts of adults migrating upstream indicate that changes in water temperature drive their spring spawning migrations at both seasonal and daily scales (Collins, 1952; Saila et al., 1972; Richkus, 1974; Ogburn et al., 2017a; Rosset et al., 2017; Lombardo et al., 2019; Legett et al., 2021). Taken in aggregate, river herring begin migrating into freshwater systems when water temperatures reach 9–10°C and stop at temperatures around 20–21°C (Kissil, 1974; Loesch, 1987; Ellis and Vokoun, 2009; Ogburn et al., 2017a,; Rosset et al., 2017). Within this thermal threshold, alewife typically migrate earlier in the spring in colder water (approximately 9–16°C) (Greene et al., 2009; ASMFC, 2017). Alewife are also more abundant than blueback herring in the northern extent of their range in the Labrador Sea and Gulf of Maine. Blueback herring, in comparison, migrate later in the spring in warmer water (approximately 15–21°C) and range farther south into Georgia and northern Florida.

The link between migration and water temperature also results in latitudinal variation in the annual timings of migrations that correspond with the seasonal transitions to spring and summer. In the southern extent of the range of river herring, migrations span from January through April, and in the more northern extent of their range, migrations typically span from March through June (ASMFC, 2017). As climate change is causing the transitions between seasons to occur earlier in the year (Friedland et al., 2015; Henderson et al., 2017), migrations of river herring also have begun to occur earlier (Huntington et al., 2003; Ellis and Vokoun, 2009; Lombardo et al., 2019; Cobb, 2020). More concerning, is that climate change may be shortening the window of time (i.e., phenophase) during which temperatures are suitable for migration and spawning. This compression of the thermal window for migration (a threshold of 9–21°C) has already been observed in long-term studies in some regions, for example, in southern New England (Ellis and Vokoun, 2009) and in Albemarle Sound, North Carolina (Lombardo et al., 2019). Therefore, the increasing rate at which temperatures change throughout the spring can temporally restrict reproduction of river herring. In addition, if thermal shifts are not uniform across that window, alewife and blueback herring may be affected differently.

Although there is a growing body of literature on the phenology of the spawning migrations of river herring (e.g., Huntington et al., 2003; Ellis and Vokoun, 2009; Rosset et al., 2017; Lombardo et al., 2019; Cobb, 2020; Legett et al., 2021; Dalton et al., 2022), the timing of migrations in many regions and rivers is not well known (ASMFC, 2012, 2017). Furthermore, the environmental drivers of migration and spawning other than water temperature, such as streamflow and lunar cycle, can be inconsistent among rivers in a region (Rosset et al., 2017; Legett et al., 2021; Bi et al., 2021). Given the threat of climate change to river herring, understanding the timing and environmental drivers of their spawning migrations has been identified as a key research need for preservation and restoration efforts (Nelson et al., 2020; Hare et al., 2021). This need is especially high in regions like Chesapeake Bay, where air and water temperatures are warming faster than global averages (IPCC, 2013; Hinson et al., 2022) and where some of the most severe declines in populations of alewife and blueback herring have occurred (Palkovacs et al., 2014).

In the early 20th century, the fishery targeting river herring (alewife and blueback herring combined) was the largest fishery by quantity in Chesapeake Bay, with an estimated annual catch of over 10,000 metric tons (over 22 million pounds) (Hildebrand and Schroeder, 1928). Because of subsequent declines in abundance, a moratorium was imposed in 2012 on the commercial and recreational fisheries of river herring in Maryland and Virginia to prevent the extirpation of these species (ASMFC, 2017). In 2013, a fisheries-independent monitoring program was established by the Smithsonian Environmental Research Center (SERC) to assess the stock status, population dynamics, and ecology of river herring in the Upper and Middle Chesapeake Bay regions. In an initial analysis of spawning run counts from this monitoring effort, runs from a single year in a single river were examined (Choptank River in 2014; Ogburn et al., 2017a).

In this study, we examined the phenology of spawning migrations of alewife and blueback herring in Chesapeake Bay, expanding on initial analyses of the SERC monitoring program (Ogburn et al., 2017a) by analyzing multi-year, multi-river fish counts. From 2013 through 2019, hourly counts of upstream migrations were collected by using imaging sonar in the Choptank River (over 4 years); Deer Creek, a tributary of the Susquehanna River (over 1 year); Marshyhope Creek, a tributary of the Nanticoke River (over 2 years); and the Patapsco River (over 4 years) to characterize spatial and interannual variability in spawning runs. We assessed migration timing and environmental drivers at 3 temporal scales: seasonal, daily, and hourly.

At a seasonal scale, we examined the start and end dates of the runs and how those metrics align with previously observed temperature thresholds (9–21°C; Ogburn et al., 2017a). We predicted that the timing of migrations of river herring would match the time when these temperatures occurred across river systems, with runs starting and ending earlier in warmer years and later in cooler

years. At a daily scale, we examined the relationship between migration and environmental factors that fluctuate daily throughout the spring, including water temperature, streamflow (also referred to as *discharge*), lunar phase, turbidity, and wind stress. Given that daily changes in water temperature are a consistent predictor of daily movements of river herring in other regions (Legett et al., 2021), we predicted that temperature would be the primary driver of upstream migrations in the rivers of Chesapeake Bay. At an hourly scale, we compared the diel cycles of migrations of river herring in each river and examined the relationship between migration and environmental factors with diel patterns, including water temperature, tides, and solar elevation. Because migrations of river herring often fluctuate on a 24-h cycle (Saila et al., 1972; Richkus, 1974; Ogburn et al., 2017a), we predicted solar elevation to be a primary driver of hourly movement. Herein, we discuss our results in the context of monitoring and management of river herring in Chesapeake Bay.

Materials and methods

Fish counts

We collected counts of adult river herring during their spawning migrations in the Choptank River (during 2014–2017), Deer Creek (in 2015), Marshyhope Creek (in 2013 and 2014), and the Patapsco River (during 2016–2019) (Fig. 1). The study sites were located just upstream of the tidal influence in each river system. Fish were counted for the duration of the spawning runs, from March through late May or early June (Suppl. Table 1) (online only), by using a dual-frequency identification sonar unit (DIDSON[1] unit with DIDISON V5.25.52 software, Sound Metrics Corp., Bellevue, WA). Imaging sonar video recordings were collected and processed following established protocols (Ogburn et al., 2017a). The sonar unit was set to a high resolution (1.8 mHz) to record a 10-m field of view. Construction fencing was used to block fish from swimming outside the field of view on the near and far side of the stream during normal and low flow conditions. Sonar video recordings were collected for 10-min segments every hour, with a randomized hourly start time. A sampling effort at the rate of 10 min/h is common for estimating the passage of anadromous fish during their migrations and can result in low variation (coefficient of variation: ~5.5%) between estimated fish counts and real passage (Xie and Martens, 2014).

We used these counting protocols consistently across the time period of this study in the Choptank River, Deer Creek, and the Patapsco River. In Marshyhope Creek, hourly recordings were collected and analyzed for 1 month during the spawning season in 2013 (27 March–2 May). For the rest of the season in 2013 (14 March–26 March and 3 May–30 May) in Marshyhope Creek, and for the entire season in 2014 (11 April–27 May), sonar video recordings were analyzed every other hour each day from 0600 to 1800 GMT as opposed to every hour.

Individual fish moving upstream were manually counted from playbacks of the sonar video recordings by using DIDSON V5.25.52 software. Fish were digitally measured in the recordings by using a straight line, and only fish in the size range of adult river herring (200–350 mm in total length [TL]) were counted (Ogburn et al., 2017a). For each river, 1–7 observers counted fish; each observer was trained by using a standard set of files. For quality

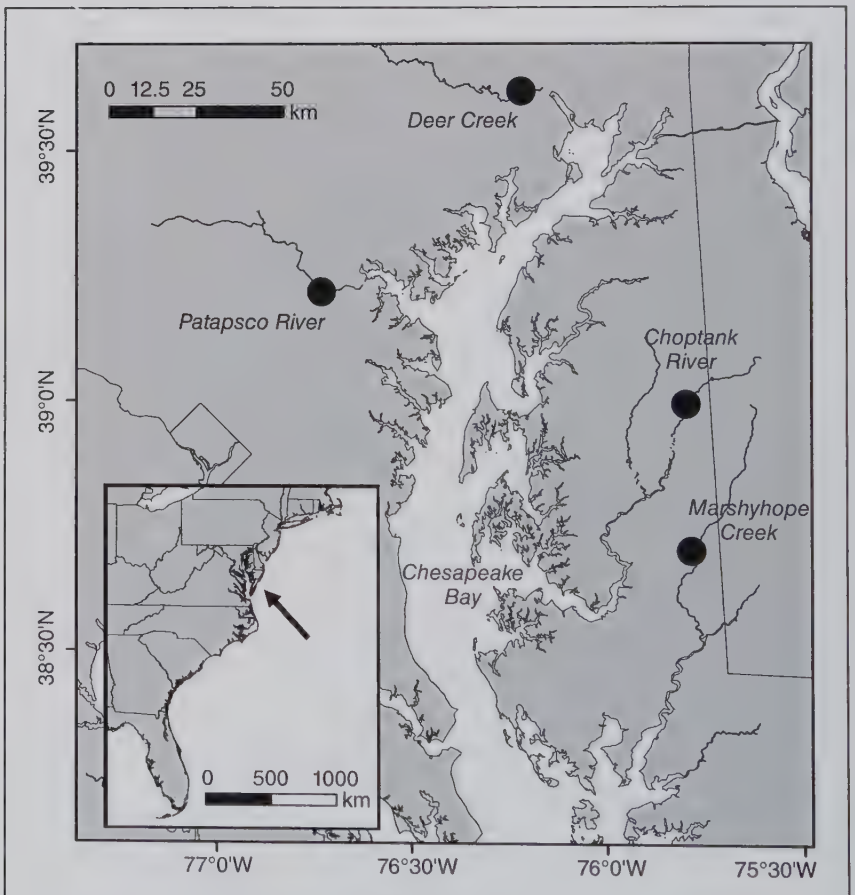

Figure 1

Map of Chesapeake Bay in Maryland showing the locations of the 4 sites where counts of adult alewife (*Alosa pseudoharengus*) and blueback herring (*A. aestivalis*) were collected from 2013 through 2019. The geographic coordinates for each site can be found in Supplementary Table 1 (online only).

[1] Mention of trade names or commercial companies is for identification purposes only and does not imply endorsement by the National Marine Fisheries Service, NOAA.

assurance, multiple observers reviewed at least 20 files from each river and year. Results from a previous study on observer variability indicate that there is no significant difference among trained observers counting fish during migrations in recordings made by using imaging sonar (Petreman et al., 2014; but see Keefer et al., 2017). To generate hourly estimates, counts from the 10-min recordings were multiplied by a factor of 6.

During this study, high flow events in the rivers sometimes disrupted the sonar or changed the field of view of the recordings such that fish could not be counted. In several instances, when an extreme event such as a large storm was expected, equipment was preemptively removed from the river to prevent its loss. These disruptions and removals created gaps in the counts of fish during spawning runs and was a particular problem in the Patapsco River, which had extreme flooding during the study period (Doheny and Nealen[2]).

Species-specific estimates

The 2 species of river herring, alewife and blueback herring, and similarly sized individuals of other species cannot be differentiated in the sonar video recordings. To measure the relative abundance of each species and estimate species-specific counts, weekly biological samples were collected by using backpack or boat electrofishing (in the Choptank River, Marshyhope Creek, and the Patapsco River) or fyke nets (in Deer Creek) within 500 m of the sonar sites. These collections were approved by the Maryland Department of Natural Resources (MDNR) and the SERC Institutional Animal Care and Use Committee. All fish within the size range of 200–350 mm TL were counted and identified to species. The proportions of alewife and blueback herring were calculated for each biological sample, and daily proportions for each species were calculated by using linear interpolation (Hughes and Hightower, 2015; Ogburn et al., 2017a). Daily species compositions were calculated in this way to smooth day-to-day changes in species composition rather than having sharp breaks week to week. These daily proportions were then applied to the hourly sonar counts for each date to generate species-specific hourly counts.

Environmental factors

Hourly measurements of water temperature were collected by using either HOBO U20-001-2-Ti or HOBO U24-002-C data loggers (Onset Computer Corp., Bourne, MA). The loggers were housed in PVC pipping and anchored underwater next to the sonar unit. Measures of streamflow were obtained for U.S. Geological Survey monitoring stations from the National Water Dashboard (data available from website, accessed August 2021). Stations were located upstream of the sonar unit site in each river (Choptank River: gauge 01491000, ~0.5 km upstream; Deer Creek: gauge 01580520, ~50 m upstream; Marshyhope Creek: gauge 01488500, ~20 km upstream; Patapsco River: gauge 01589035, ~2 km upstream). Measures of turbidity were obtained from the National Water Dashboard for the monitoring station in the Patapsco River, which was the only site for which these data were available for the time frame of the study.

Lunar cycle data were obtained by using the fisheries stock assessment model MULTIFAN-CL and the associated R4MFCL scripts for use in statistical software R (Hoyle et al.[3]). Tidal data were obtained from water level measurements relative to mean lower low water recorded at NOAA stations (data available from website, accessed August 2021). The closest NOAA station downstream to each site was used for each river. These stations were located either at the mouth of each river (Choptank River: station 8571892, ~67 km downstream; Patapsco River: station 8574680, ~14 km downstream) or in Chesapeake Bay (Deer Creek: station 8573364, ~60 km downstream; Marshyhope Creek: station 8571421, ~75 km downstream).

Hourly measures of wind speed and wind direction were also obtained for these same NOAA stations. Daily measures of wind stress (τ) were calculated from wind speed and wind direction at 45° intervals by using the following equation (Wilson, 1960; Large and Pond, 1981):

$$\tau = C_d \times \rho_{air} \times U^2, \quad (1)$$

where C_d = a dimensionless drag coefficient that was set at 0.0012;
ρ_{air} = 1.2 kg/m^3, the mass density of air; and
U = the wind magnitude.

Solar elevation (measured in degrees above the horizon) was obtained from the solar geometry calculator of the NOAA Earth System Research Laboratories (data available from website, accessed August 2021), with angles corrected for atmospheric refraction. All data were set to the standardized time of GMT.

Statistical analyses

Counts of alewife and blueback herring were analyzed at seasonal, daily, and hourly scales by using R, vers. 4.0.3 (R Core Team, 2020). The estimated hourly counts for each species were used to calculate the mean daily rate of upstream migration (number of fish per hour) and the overall annual counts. At a seasonal scale, run initiation and end dates were calculated as the days when the estimated counts exceeded 5% and 95% of the total run (Ellis and Vokoun, 2009). The duration of each run was the number of days between the initiation and end

[2] Doheny, E. J., and C. W. Nealen. 2021. Storms and floods of July 30, 2016, and May 27, 2018, in Ellicott City, Howard County, Maryland. U.S. Geolog. Surv., Fact Sheet 2021-3025, 6 p. [Available from website.]

[3] Hoyle, S., D. Fournier, P. Kleiber, J. Hampton, F. Bouyé, N. Davies, and S. Harley. 2009. Update of recent developments in MULTIFAN-CL and related software for stock assessment. West. Cent. Pac. Fish. Comm., WCPFC-SC5-2009/SA-IP-07, 16 p. [Available from website.]

dates. For the run initiation and end dates, we calculated the daily average and maximum water temperature for each species, river, and year. We also calculated the 7-day average water temperature for each initiation and end date (average of the 7 days leading up to the date). The thermal transition dates for the combined migrations of both species of river herring each year were calculated as the first days the average temperature exceeded 9°C and 21°C, and the thermal season length was the number of days between these dates.

At a daily scale, the relationship between counts of river herring and daily changes in environmental factors was assessed by using cross-correlation analysis at lags of ±4 days with 95% confidence intervals (CIs) (Ogburn et al., 2017a); CIs were calculated following Brockwell and Davis (2002). For this analysis, $\log_{10}+1$ of the mean daily rate of upstream migration (number of fish per hour per day) was compared to the change in daily mean water temperature, mean streamflow, lunar phase, and mean wind stress. Mean daily turbidity was also assessed for the Patapsco River. Because temperature generally increases day to day throughout the spring, water temperature data needed to be detrended to separate daily from seasonal changes (Wu et al., 2007). A weighted index of change in mean daily water temperature, therefore, was used for this analysis and was calculated by using this equation (following Ogburn et al., 2017a):

$$\Delta T = [(T_0 - T_1) \times 3 + (T_1 - T_2) \times 2 + (T_2 - T_3)] / 6, \quad (2)$$

where T_0 = the mean daily temperature, and
$T_{1\text{–}3}$ = the mean temperatures 1–3 days earlier.

By considering changes in temperatures up to 3 days earlier, this index both detrends temperature on a seasonal scale and reflects multiday warming and cooling trends.

Hourly patterns in migrations of river herring were analyzed by using the R package circular (vers. 0.4-95; Agostinelli and Lund, 2022). The parameters of the von Mises distribution, mean (μ) and dispersion (κ), of estimated counts for each species were calculated from maximum-likelihood estimates. A Rayleigh test of uniformity was used to test the null hypothesis that counts were randomly distributed by hour (Humphreys and Ruxton, 2017). Cyclical patterns at an hourly scale were additionally assessed by using wavelet analyses in the R package WaveletComp (vers. 1.1; Rösch and Schmidbauer[4]), with 95% CIs used to identify period lengths associated with hourly variability in the fish counts (Torrence and Compo, 1998). The relationships between counts of river herring and hourly changes in environmental factors were assessed by using cross-correlation analysis at lags up to ±4 h with 95% CIs. For this analysis, the $\log_{10}+1$ of estimated hourly counts (number of fish) were compared with hourly measures of water temperature, tide, and solar elevation. Hourly patterns in Marshyhope Creek were analyzed for only the time period in the 2013 season when 24-h counts were available (27 March 27–2 May). Data supporting this study are publicly available on Figshare at website.

[4] Rösch, A., and H. Schmidbauer. 2018. WaveletComp 1.1: a guided tour through the R package, 58 p. [Available at website.]

Results

Species composition of biological samples

A total of 5451 fish within the size range of 200–350 mm TL, representing 24 species, were collected by using boat electrofishing or fyke nets. River herring were the dominant species in these samples and typically composed >80% of the collection during the peaks of the runs. Overall, 34% of the total samples were alewife, and 39% were blueback herring. Other abundant species included white perch (*Morone americana*) (9%), gizzard shad (*Dorosoma cepedianum*) (5%), yellow perch (*Perca flavescens*) (3%), hickory shad (*A. mediocris*) (2%), striped bass (*Morone saxatilis*) (2%), and white sucker (*Catostomus commersonii*) (2%). In Deer Creek, all sampled fish within the required size range were alewife.

Estimated sonar counts of river herring

A total of 1.35 million fish within the required size range were counted in 10-min sonar video recordings. After multiplying these counts by a factor of 6 to generate hourly estimates and adjusting for daily species composition, an estimated 2.69 million alewife and 3.06 million blueback herring migrated upstream across the 4 rivers and 7 years of this study (Table 1). Species-specific estimates ranged from 800,000 of each species in the Choptank River in 2015 to less than 10,000 of each species in the Patapsco River in 2019. Although low counts in the Patapsco River can be partially attributed to inconsistent collection efforts caused by weather related disruptions, the counts were notably lower in this river in 2016 when efforts to collect recordings were consistent.

Seasonal patterns in migrations

Alewife began migrating approximately 22 d (standard deviation [SD] 12) earlier in the season compared with the timing of migration by blueback herring (day of year: 52–105 versus 91–121; Table 1). Alewife also stopped migrating 22 d (SD 7) earlier than blueback herring (day of year: 105–132 versus 126–144). The earlier migrations of alewife occurred in colder waters, starting at the average daily water temperature of 11.2°C (SD 1.1), compared with the temperature at which migrations of blueback herring started, 15.2°C (SD 0.9) (Suppl. Table 2) (online only). The migrations ended at an average daily water temperature of 15.4°C (SD 1.2) for alewife and 18.9°C (SD 1.1) for blueback herring. Overall, the migrations of both species generally occurred within the thermal window of 9–21°C, and the durations of the migrations roughly corresponded with the duration of this thermal window (Table 1, Fig. 2). Migrations occurred earlier

Table 1

Seasonal phenology of spawning runs of alewife (AW) (*Alosa pseudoharengus*) and blueback herring (BBH) (*A. aestivalis*) from 2013 through 2019 in 4 rivers of Chesapeake Bay in Maryland. Start day (first 5% of the run), end day (95% of the run), and total counts of fish were calculated from the estimated hourly upstream counts (the symbol > or < indicates that counting either started after the run had begun or ended before the run ended). The thermal window range (i.e., the thermal thresholds in which river herring migrations typically occur) is the first day that the average water temperature exceeded 9°C and the first day that it exceeded 21°C (the symbol < indicates that counting began after temperatures crossed the threshold).

River	Year	Species	Total count (000s)	Start date (day of year)	End date (day of year)	Run duration (d)	Thermal window range (days of year)
Choptank River	2014	AW	552	79	115	37	71–133
		BBH	757	104	135	32	
	2015	AW	796	89	112	24	76–129
		BBH	793	106	132	27	
	2016	AW	232	<60	105	>46	55–147
		BBH	477	91	>138	>48	
	2017[1]	AW	326	<52	111	>59	50–119
		BBH	259	96	>140	>45	
Deer Creek	2015[1]	AW	418	107	122	16	92–131
		BBH	–	–	–	–	
Marshyhope Creek[2]	2013[1]	AW	255	<87	107	>20	79–142
		BBH	321	103	126	24	
	2014[1]	AW	60	<102	116	>15	<101–133
		BBH	303	<107	>133	>27	
Patapsco River	2016	AW	17	87	132	46	<70–147
		BBH	50	121	144	24	
	2017[1]	AW	12	88	117	30	67–119
		BBH	18	112	137	26	
	2018[1]	AW	11	105	118	14	88–124
		BBH	71	115	133	19	
	2019[1]	AW	5	89	106	18	74–140
		BBH	9	103	138	36	

[1] Counts were not collected, or were inconsistently collected, for large portions of the season. Total upstream counts for both river herring species are underestimated.
[2] In Marshyhope Creek, hourly sonar video recordings were collected and analyzed for 1 month during the season in 2013 (27 March–2 May). For the rest of the season in 2013 and for the season in 2014, recordings were collected and analyzed every other hour each day from 0600 to 1800 GMT.

in years when spring water temperatures reached 9°C earlier, and migrations ended later in years when water temperatures reached 21°C later.

There were inter-river differences in water temperatures at the start of migrations of alewife, particularly between the Choptank River and the other 3 systems (Suppl. Table 2) (online only). Alewife began migrating in colder water (8.6°C [SD 1.1]) in the Choptank River compared with the average water temperatures in Deer Creek (15.7°C [SD 1.2]), Marshyhope Creek (12.7°C [SD 1.0]), and the Patapsco River (12.2°C [SD 1.3]). Temperatures at which migrations of alewife ended were more similar among all the rivers (Choptank River: 15.6°C [SD 0.8]; Deer Creek: 14.5°C [SD 1.6]; Marshyhope Creek: 16.9°C [SD 1.2]; Patapsco River: 14.8°C [SD 1.4]). The migration of alewife in Deer Creek in 2015 (the only year during which river herring were monitored in this river) was unique in that it started and ended at around the same temperature. Water temperatures during migrations of blueback herring were similar among the rivers at their starts (Choptank River: 16.5°C [SD 1.1]; Marshyhope Creek: 14.3°C [SD 0.8]; Patapsco River: 14.5°C [SD 0.6]) and endings (Choptank River: 19.3°C [SD 0.8]; Marshyhope Creek: 17.7°C [SD 0.5]; Patapsco River: 18.9°C [SD 1.6]).

Daily patterns in migrations

Increases in the daily rates of migration for both alewife and blueback herring were consistently associated with increases in weighted mean change in water temperature (Suppl. Tables 3–6) (online only). This relationship occurred most often between lags from –1 to 0 d, such that days with peaks in upstream migration rates occurred on days, or followed days, with increased water temperatures. In an exception to this trend, daily migration of alewife in the Patapsco River in 2018 was strongly negatively correlated with changing water temperature (correlation <–0.80) –1 to 0 d before peaks in counts (Suppl. Table 6) (online only).

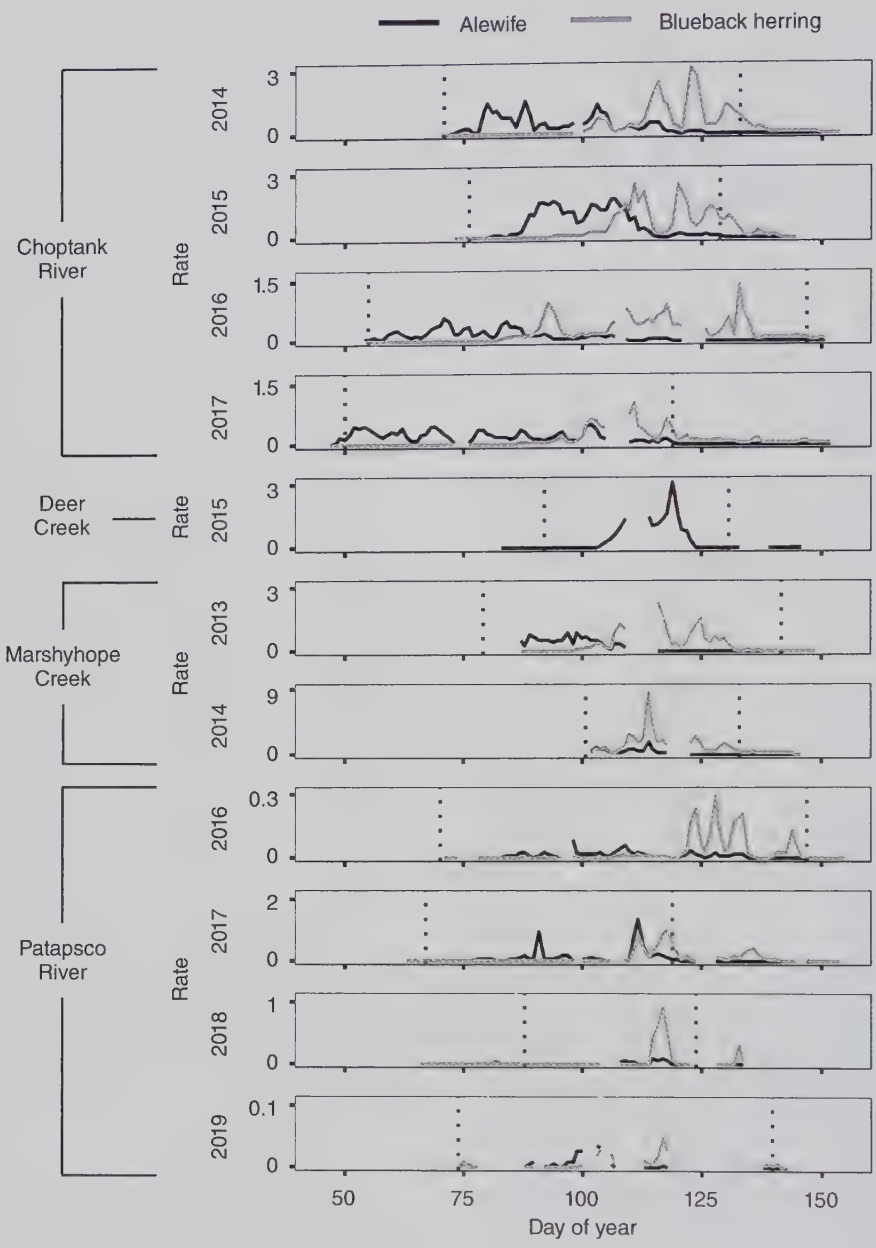

Figure 2

Daily mean estimated rates of upstream migration (number of fish per hour in thousands) of alewife (*Alosa pseudoharengus*) and blueback herring (*A. aestivalis*) in each year from 2013 through 2019 in 4 rivers of Chesapeake Bay in Maryland. Vertical dotted lines indicate the thermal window, with the first line at the first day the mean water temperature reached 9°C and the second line at the first day the mean temperature reached 21°C. Gaps in plots are days on which counts were not collected. Note the differences in scales among plots.

Streamflow, lunar phase, and turbidity were also often associated with daily migration patterns. However, these associations and the direction of the relationship were more inconsistent than they were for water temperature.

In the Choptank River, streamflow was significantly negatively correlated with migrations of alewife in 2015 and with migrations of both alewife and blueback herring in 2017 (lags from –2 to 2 d; Suppl. Table 3 [online only]). In Deer Creek, streamflow was negatively correlated with migrations of alewife (lag of 3 d; Suppl. Table 4 [online only]). In Marshyhope Creek, streamflow was positively correlated with migrations of alewife in 2013 (lag of –2 d) but negatively correlated with

migrations of blueback herring in 2013 and alewife in 2014 (lags from –1 to 1 d) (Suppl. Table 5) (online only). In the Patapsco River, streamflow was positively correlated with migrations of blueback herring in 2016 and 2018 (lags from –2 to 0 d) but negatively correlated with migrations of blueback herring in 2017 (lags from 1 to 4 d) and with migrations of both alewife and blueback herring in 2019 (lags from –4 to –2 d) (Suppl. Table 6) (online only).

Lunar phase in the Choptank River was positively correlated with migrations of alewife and blueback herring in 2016 (lags from –4 to 4 d) but negatively correlated with migrations of blueback herring in 2017 (lags from 1 to 4 d) (Suppl. Table 3) (online only). In Deer Creek, lunar phase was positively correlated with migrations of alewife (lags from 1 to 3 d; Suppl. Table 4 [online only]). In Marshyhope Creek, lunar phase was negatively correlated with migrations of blueback herring in 2014 (lags from 0 to 4 d; Suppl. Table 5 [online only]). In the Patapsco River, lunar phase was negatively correlated with migrations of alewife in 2017 and blueback herring in 2016, 2017, and 2019 (lags from –3 to 4 d) but positively correlated with migrations of alewife in 2016 and 2019 and blueback herring in 2018 (lags from –1 to 4 d) (Suppl. Table 6) (online only).

Turbidity in the Patapsco River was positively correlated with migrations of alewife in 2016 and 2019 and migrations of blueback herring in 2016 and 2018 (lags from –3 to 0 d). In this river, turbidity was negatively correlated with migrations of alewife in 2016 and blueback herring in 2017 (lags from 1 to 3 d).

Wind stress also had a variable relationship with daily migration patterns among rivers and years (Suppl. Figs. 1–4) (online only). In the Choptank River, wind stress from the southwest was strongly positively correlated with migrations of alewife and blueback herring in 2014 at lags from –3 to 0 d before peaks in counts, but it was strongly negatively correlated with migrations of blueback herring in 2018 at the same lags (Suppl. Fig. 1) (online only). The only consistent trend related to wind stress was observed in the Patapsco River. There, wind stress originating from the south was negatively associated with migrations of alewife in all 4 years of this study (2016–2019) and with migrations of blueback herring in 2016 (lag of 0 d) but positively associated with migrations of alewife and blueback herring from –4 to –2 d before peaks in counts (Suppl. Fig. 4) (online only).

Hourly patterns in migrations

Distinct diel patterns in migrations of both alewife and blueback herring were observed in each river (Rayleigh test of uniformity: $P<0.001$ in all cases). In the Choptank River during 2014–2017, counts were diurnal and most concentrated in the afternoons, with alewife moving slightly later in the day (μ=15.52, κ=0.48) compared with blueback herring (μ=12.73, κ=0.62; Fig. 3). In Deer Creek in 2015, most of the alewife migration occurred at night (μ=21.17, κ=0.40; Fig. 3). In Marshyhope Creek in 2013, counts were diurnal, with alewife most concentrated in the early afternoon (μ=13.77, κ=0.50) and blueback herring most concentrated in the later morning (μ=10.47, κ=1.08) (Fig. 3). In the

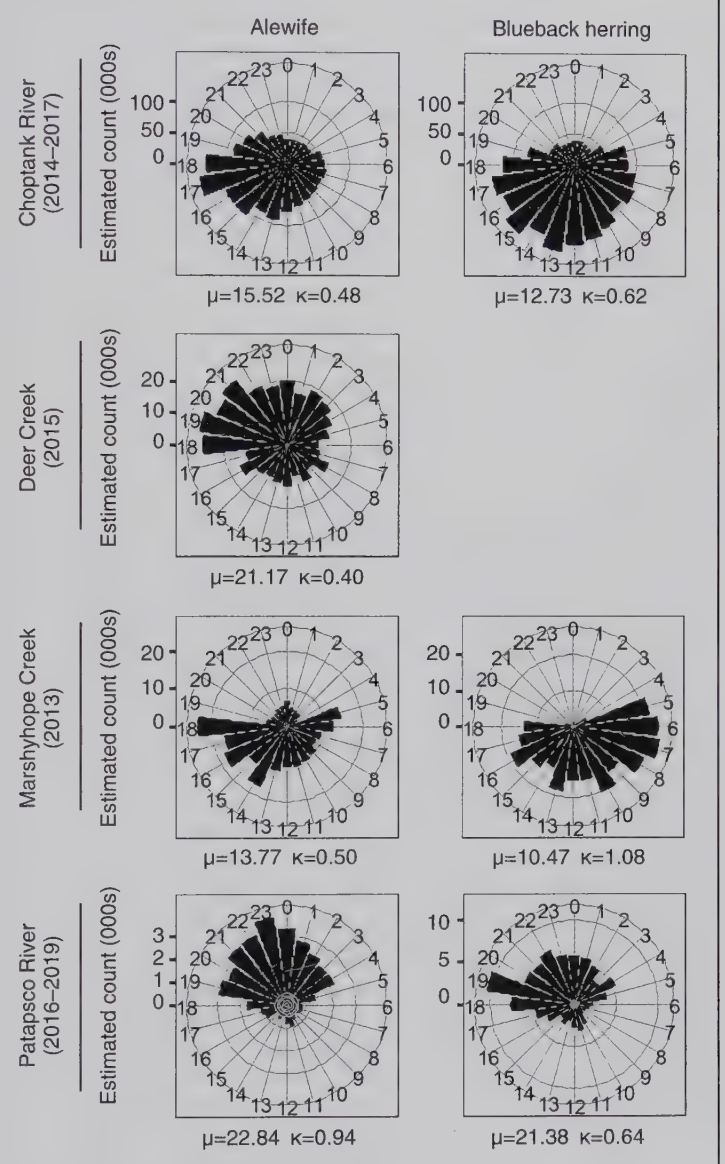

Figure 3

Circular histograms representing estimated fish counts (number of fish per hour in thousands) by time of day for alewife (*A. pseudoharengus*) and blueback herring (*A. aestivalis*) in 4 rivers of Chesapeake Bay in Maryland: the Choptank River in 2014–2017, Deer Creek in 2015, Marshyhope Creek in 2013, and the Patapsco River in 2016–2019. Note the differences in scales among histograms. The mean (μ) and dispersion (κ) values for the von Mises distribution are given below each histogram. Only alewife were detected in Deer Creek. Circular histograms for each year in the Choptank and Patapsco Rivers can be found in Supplementary Figures 5 and 6 (online only).

Patapsco River during 2016–2019, migrations occurred at night for both alewife (μ=22.84, κ=0.94) and blueback herring (μ=21.38, κ=0.64) (Fig. 3). Migrations in Marshyhope Creek and the Patapsco River were generally more concentrated than in the other 2 river systems, with a greater majority of counts restricted almost exclusively to daytime hours (Marshyhope Creek) or nighttime hours (Patapsco River). Circular histograms representing the time of day of estimated upstream migrations for each year in the Choptank and Patapsco Rivers can be found in Supplementary Figures 5 and 6 (online only).

Corresponding to these diel patterns, hourly increases in estimated counts were consistently correlated with solar elevation at all measured lags (from −4 to 4 h) across rivers and years (Suppl. Tables 7–10) (online only). This relationship with solar elevation was positive in the Choptank River and Marshyhope Creek, where the migrations were diurnal, but the relationship was negative in Deer Creek and the Patapsco River, where the majority of the migrations were nocturnal.

Generally, there was a positive correlation between hourly counts and water temperature. Exceptions to this trend include a negative correlation between temperature and counts of alewife in the Choptank River in 2015 (lags from −4 to −2 h), blueback herring in the Patapsco River in 2018 and 2019 (lags from −4 to 4 h), and alewife and blueback herring in Marshyhope Creek in 2013 (lags from −4 to 1 h). In the Patapsco River, the correlation with temperature was still positive for counts of alewife in all 4 years of the study (2016–2019) and for counts of blueback herring in 2016 and 2017, despite migrations occurring at night when daily temperatures were lowest. Similarly, in Deer Creek, hourly counts were positively correlated with temperature despite nocturnal migrations.

Hourly counts were often correlated with tides; however, the direction of the relationship was not consistent. Tides in the Choptank River were positively correlated with migrations of alewife in 2017 (lags from −4 to 1 h) and blueback herring in 2015 and 2016 (lags from 0 to 4 h), but tides were negatively correlated with migrations of alewife in 2015 (lags from −4 to 4 h) and blueback herring in 2017 (lags from 3 to 4 h) (Suppl. Table 7) (online only). Tides were negatively correlated with migrations of alewife in Deer Creek (lags from −1 to 0 h; Suppl. Table 8 [online only]) and with migrations of alewife and blueback herring in Marshyhope Creek (lags from 2 to 4 h; Suppl. Table 9 [online only]). In the Patapsco River, counts were positively correlated with tides in migrations of alewife in 2018 (lags from 3 to 4 h) and blueback herring in 2016 and 2018 (lags from −4 to 4 h), but they were negatively correlated with migrations of alewife in 2016 (lags from −4 to 2 h) and blueback herring in 2017 and 2019 (lags from −4 to 4 h) (Suppl. Table 10) (online only).

In wavelet analyses, significant peaks in power of the global wavelet spectrum occur at a period of approximately 24 h (corresponding to diel patterns) for migrations of both alewife and blueback herring in all years and rivers (Fig. 4). An additional significant peak around 10–14 h (corresponding to the ~12-h tidal cycle) occurred in all migrations of alewife in the Choptank River in 2014–2017, in migrations of alewife and blueback herring in Marshyhope Creek in 2013, in migrations of alewife in the Patapsco River in 2016 and 2019, and in migrations of blueback herring in the Patapsco River in

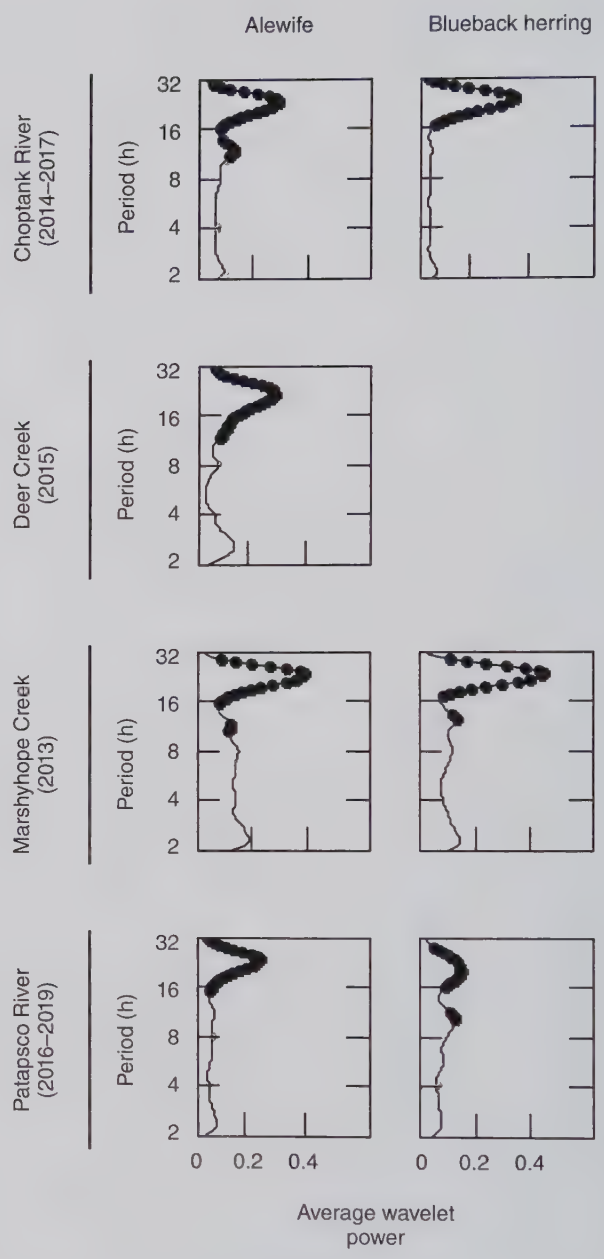

Figure 4

Global spectra from wavelet analyses of hourly estimated fish counts of alewife (*Alosa pseudoharengus*) and blueback herring (*A. aestivalis*) in 4 rivers of Chesapeake Bay in Maryland: the Choptank River in 2014–2017, Deer Creek in 2015, Marshyhope Creek in 2013, and the Patapsco River in 2016–2019. Black dots represent statistically significant points that exceed the 95% confidence interval. Only alewife were detected in Deer Creek. Results from wavelet analyses for each year in the Choptank and Patapsco Rivers can be found in Supplementary Figure 7 (online only).

2016–2018. Results of wavelet analyses for each year in the Choptank and Patapsco Rivers can be found in Supplementary Figure 7 (online only).

Discussion

Seasonal migration patterns: correspondence with water temperature

Counts at a seasonal scale indicate that the duration of migrations of river herring in rivers of Upper and Middle Chesapeake Bay are bounded by a known temperature threshold, approximately 9–21°C. This thermal tolerance window is generally consistent across rivers in Chesapeake Bay and in other regions (Kissil, 1974; Loesch, 1987; Ellis and Vokoun, 2009; Rosset et al., 2017; Bi et al., 2021). Interspecific differences in seasonal migration patterns were also consistent across river systems and align with long-established and range-wide reports of behavior of river herring, with alewife migrating earlier in the spring in cooler water temperatures and blueback herring migrating later in warmer temperatures (ASMFC, 2017). Our results indicate some inter-river differences in this temperature threshold, specifically in the Choptank River, where alewife began migrating in slightly colder water compared with their migrations in the other 3 rivers (~8°C versus ~12°C).

In Deer Creek, our biological sampling efforts captured only alewife, and the phenology of migration at a seasonal scale was unique compared to those of the migrations in the other 3 rivers. As a tributary of the Susquehanna River, Deer Creek is one of the most northern spawning locations for river herring in Chesapeake Bay. This farther distance from the mouth of Chesapeake Bay may result in fish arriving at Deer Creek later in the year in warmer water temperatures and leaving earlier in colder temperatures compared to their behavior in other rivers in this region. Monitoring was conducted in only 1 year (2015) in this system. Blueback herring have been collected in biological samples from Deer Creek in other years (e.g., blueback herring were collected by the Maryland Department of Natural Resources in 2014; R. Aguilar, personal commun.), but additional monitoring is needed to confirm the interannual presence–absence of blueback herring in this system, to distinguish any species-specific timings of migrations, and to examine river-specific patterns in environmental drivers.

Daily migration patterns: correspondence with water temperature

Increases in daily mean water temperature were consistently followed by increased migration rates for both species of river herring. This link between daily migration patterns and temperature has also been observed in other regions (Saila et al., 1972; Richkus, 1974; Rosset et al., 2017). For example, in long-term (8–28 years) fish counts conducted across 12 streams in Massachusetts, water temperature was a predictor of both daily presence–absence and abundance of river herring (Legett et al., 2021). An exception to this pattern was in the Patapsco River in 2018, where the majority of the migrations of both species occurred in a single large pulse negatively correlated with water temperature, indicating that in some systems under certain conditions, other environmental factors may override the influence of water temperature.

The correlations between fish counts and streamflow and turbidity in the Patapsco River indicate that river herring may increase in abundance in this system following heavy rains. This result is further supported by our analysis of wind stress: high wind stress in the Patapsco River, indicating a storm event, may have led to a decrease in fish counts the day of the event and an increase in fish counts 2–4 d after the event. However, it is important to note that extreme flooding events in the Patapsco River during the study period (Doheny and Nealen[2]) disrupted counting efforts during events with some of the highest streamflow in this system. Additional years of monitoring, particularly the collection of counts during storm events, are needed to confirm the relationship between fish counts and streamflow, turbidity, and wind stress and to determine whether this relationship is specific to the Patapsco River.

Overall, across all 4 rivers, the relationships between daily migration rates of river herring and non-temperature environmental factors (streamflow, lunar phase, turbidity, and wind stress) were inconsistent, similar to the interannual and inter-river inconsistencies reported in previous fish count studies (Saila et al., 1972; Richkus, 1974; Legett et al., 2021). The influence of non-temperature factors may be river specific, as we observed with southerly wind stress in the Patapsco River.

The various ways in which individual environmental factors may influence migrations of river herring need to be considered. For example, changes in streamflow may motivate fish to migrate, but this influence may be separate from accessibility thresholds, where streamflow is so low or so high that fish are physically limited from moving upstream. The interactions between environmental factors also need to be considered. Increased wind stress from a storm event might correspond with increased streamflow from precipitation and changes in water temperature from runoff. It is possible that environmental factors are important only in how they shift water temperature. For instance, increased streamflow from stormwater runoff may have a positive or negative influence on fish migrations depending on the degree to which that runoff changes the water temperature. Therefore, further studies that consider the direct and indirect relationships between environmental factors are needed, and such examination may be achieved by using structural equation modeling (Malaeb et al., 2000; Fan et al., 2016). Such analysis requires data sets from long-term monitoring because of the degree of interannual variation in migration dynamics within and between river systems.

Hourly migration patterns: indication of inter-river variability

We observed divergent diel patterns in migrations of river herring among rivers. Migrations of both alewife and blueback herring were diurnal in the Choptank River and Marshyhope Creek but nocturnal in Deer Creek and the Patapsco River. On the basis of previous analyses of fish counts, the following have been reported: diurnal patterns in upstream migrations (Cooper, 1961; Saila et al., 1972; Kissil, 1974; Richkus, 1974; Mullen et al., 1986; Andrews, 2014; Rillahan, et al. 2021), nocturnal patterns (McCartin et al., 2019), crepuscular patterns (Alcott et al., 2021), and bimodal peaks in movement from dawn to noon and dusk to midnight (Tyus, 1974). The cause of this diel variation is not well known.

Nocturnal activity may be a strategy to avoid diurnal predators, such as ospreys (*Pandion haliaetus*), bald eagles (*Haliaeetus leucocephalus*), and striped bass (Bendall et al., 2005; McCartin et al., 2019; Alcott et al., 2021). This hypothesis of predator avoidance is supported by differences in water clarity between the rivers in our study, as the Choptank River and Nanticoke River (downstream of Marshyhope Creek) are tannic coastal plain systems located on the Delmarva Peninsula and are typically more turbid (secchi depth <0.5 m) compared with the Susquehanna River (downstream of Deer Creek) and Patapsco River (secchi depth >0.5 m), whose watersheds are located largely on the piedmont (turbidity data used in this study are from 4 water-quality stations of the Eyes on the Bay Program, Maryland Department of Natural Resources, the Choptank River station ET5.1, Nanticoke River station XDJ9007, Susquehanna River station CB1.1, and Patapsco River station WT5.1; available from website, accessed May 2022). Therefore, fish migrating in Deer Creek and the Patapsco River during the day are more visible to predators compared with fish migrating in the Choptank River and Marshyhope Creek and may migrate at night to reduce this exposure. Highlighting the predator avoidance hypothesis, large numbers of bald eagles have been observed at the sampling location in Deer Creek during the short 2-week period when alewife were present (R. Aguilar and K. Heggie, personal observ.), indicating that avian predators target river herring during their spawning migration.

Diel patterns in migrations of river herring most strongly correlated with solar elevation, but migrations were also positively correlated with water temperatures at an hourly scale. This relationship was expected for the Choptank River, where migrations are diurnal and solar elevation and temperature are colinear. However, this relationship was also present in Deer Creek and the Patapsco River, where migrations are nocturnal and consequently concentrated at times when water temperatures are at their coldest each day. This result indicates that, to some extent, hourly patterns in water temperature may drive hourly migration patterns independent of solar elevation. Exceptions to this relationship of hourly patterns, similar to the exceptions to the relationship of daily patterns in migrations and water temperatures, may indicate that the influence of water temperature can also be overridden by other conditions at this scale.

Our results also indicate a potential influence of changing tides on hourly migration patterns, but this relationship was inconsistent within and between rivers and years. In previous studies, it has been found that tidal transitions can influence diel movement patterns of river herring in systems where higher water levels are needed for fish to pass through anthropogenic structures, such as culverts or tide gates (Rillahan et al., 2021). Tidal influence may also change throughout the season depending on streamflow and overall water levels, and as with streamflow, there is a need to separate accessibility thresholds from the general influence of tides on movement rates. This variable influence and these potential interactions between environmental factors may explain why inconsistent results have similarly been found in previous studies of the effects of tides and lunar cycles on migrations of river herring (Ogburn et al., 2017a; Legett et al., 2021). A limitation of our study is that tides were not measured near the sampling sites in each river. For the Choptank River and Patapsco River, the NOAA stations where tide data were collected were located inside the mouth of each river. For Deer Creek and Marshyhope Creek, the nearest station was located beyond the river in Chesapeake Bay. The tidal cycles immediately downstream of the tidal or non-tidal boundary nearer to the sampling sites would have lagged behind the water levels recorded at the stations.

Inter-river variations in phenology and environmental drivers of migrations

Inter-river differences in migrations of river herring observed in our study, and in other multi-river studies (e.g., Legett et al., 2021; Dalton et al., 2022), may be due to the morphology and ecohydrological characteristics of each river. The Patapsco River, for example, is a rocky piedmont system in a narrow river valley with higher annual streamflow than the flow of coastal plain systems like the Choptank River and Marshyhope Creek (Suppl. Table 1) (online only). The comparative influence of streamflow and wind stress on daily migration patterns in the Patapsco River may be a result of these environmental differences. Inter-river differences in patterns of migration by river herring may also be a result of the specific locations where fish are monitored in each river. Because water temperature patterns can vary spatially within a watershed (e.g., Isaak et al., 2014; Steel et al., 2016), we expect the timing and dynamics of migrations of river herring to similarly vary. In the Choptank River, for example, we observed that alewife began their migrations in comparatively colder water temperatures. It is unknown if this inter-river difference in seasonal timing would persist if counts were collected from other locations in the Choptank River. Further studies in which water temperatures are monitored and river herring are tracked throughout a river, by using passive integrated transponder tags or acoustic telemetry (McCartin et al., 2019), would allow for the examination

of spatial variability in temperature and spawning migration phenology.

Finally, inter-river differences in migrations may also be species specific, as our results indicate that differences in temperature among rivers were not as great for blueback herring as they were for alewife. In other studies of migrations of river herring, in which the 2 species are not distinguished (e.g., Legett et al., 2021; Dalton et al., 2022), observed inter-river variability in phenology may similarly have been species specific. Therefore, our results highlight the need to differentiate between counts of alewife and blueback herring in studies of phenology of river herring.

Management implications

The thermal window for migrations of river herring is a concern for the management of these species, particularly as water temperatures in Chesapeake Bay are warming faster than global averages (Hinson et al., 2022). Changes in the timing of migrations of river herring due to warmer spring temperatures have been observed in other regions, occurring at rates of 0.3–1.2 d earlier in a year (Huntington et al., 2003; Ellis and Vokoun, 2009; Lombardo et al., 2019; Cobb, 2020). Although our study was not long enough for observation of trends in the seasonal timing of migrations, we expect that similar shifts are occurring for migrations of river herring in Chesapeake Bay, threatening the persistence of these species in this region and undermining restoration efforts.

Continued monitoring is needed to identify shifts in migration timing and the rate at which the thermal window for migrations is shortening, to identify whether changes in the thermal window are uneven or uniform, and to observe how populations of alewife and blueback herring are responding to these changes. Given the critical role of water temperature for river herring, management and conservation practices that reduce seasonal water temperatures in streams and rivers may benefit these species. For example, the establishment and maintenance of riparian buffers can provide shade and prevent direct runoff from agricultural lands, potentially mitigating the warming effects of climate change in streams and providing thermal habitat for spawning (Palone and Todd, 1998; Bowler et al., 2012; Albertson et al., 2018; Timm et al., 2021). Use of thermal mitigation practices for urban stormwater runoff may also help to maintain thermal habitat (Timm et al., 2020), especially in urban systems like the Patapsco River, which flows through the Baltimore metropolitan area.

Differences in diel patterns of migrations of river herring among rivers may have implications for restocking efforts. It is unclear whether the nocturnal migrations of river herring in Deer Creek and the Patapsco River are the result of behavioral plasticity or adaptation. If a nocturnal strategy is adaptive, river herring from a population with diurnal migrations may fail when stocked in a nocturnal system because nocturnality is driven by selective pressure and because the migrations and spawning activity of restocked fish will not temporally overlap with those of the native nocturnal population. Therefore, for restocking efforts, the respective phenologies of both the stocked and native populations may have to be considered. Furthermore, in genetic analyses of previous studies in the Upper Chesapeake Bay, genetically distinct spawning populations of river herring among rivers have been found (Ogburn et al., 2017b). Differences in diel patterns between populations may serve as a behavioral barrier limiting straying rates between rivers and preventing gene flow.

Viability of imaging sonar for monitoring migrations

As demonstrated in this study, imaging sonar, when combined with biological sampling, can be an effective tool for monitoring migrations of specific species in unobstructed natural waterways, especially in the turbid coastal streams common in the Chesapeake Bay watershed. Other methods used to monitor anadromous fish migrations, such as electronic resistivity counters and video recordings, require narrow fish passage structures (e.g., fish ladders) that can restrict upstream migration rates. In addition, video recordings are not effective in turbid waters or at night, and electronic counters can be inaccurate when fish are abundant or migrating at high densities (Hiebert et al., 2000; Sheppard and Bednarski, 2015).

A drawback of imaging sonar is its high cost, both in terms of the equipment and the time needed to count fish. Some automatic methods, such as passive acoustic monitoring of the natural sounds fish produce while spawning, may offer a less accurate but more cost-effective way to assess phenology of river herring (Staples et al., 2023). Another drawback to the use of imaging sonar in natural waterways is that high streamflow events can disrupt sonar video recordings at times when data are most needed. In the Patapsco River, which flows through the Patapsco Valley, extreme flooding was a reoccurring challenge during this study, especially in 2018 and 2019 (Doheny and Nealen[2]). When heavy rainfall was expected, equipment was removed from the river to prevent its destruction or loss; as a result, the dynamics of the migration of river herring immediately prior, during, and after the high streamflow event could not be assessed. In rivers with less variability in streamflow, such as the Choptank River, this issue was not as common.

Finally, although counts of fish made with imaging sonar are useful for examining relative changes in migration at fine temporal resolutions, counts alone are an inaccurate method for estimating abundances of river herring. Individual river herring may "oscillate" in a river throughout a season, migrating upstream and downstream between estuaries and spawning grounds multiple times (McCartin et al., 2019). Upstream counts of fish, including the count data analyzed in this study, are therefore likely an overestimation of run size. Pairing counts with tracking data of individuals, such as data from passive integrated transponder tags or acoustic telemetry, can account for milling behavior and upstream–downstream oscillations and may produce more accurate estimates of run sizes (e.g., Raabe and Hightower, 2014). There is a need to monitor

how populations of river herring in specific rivers respond to restoration activities, changes in management, climate change, and other anthropogenic factors (Hare et al., 2021). By accounting for oscillations, interannual changes in behavior (i.e., number of oscillations per individual) can be separated from changes in abundance.

Conclusions

Migrations of river herring were monitored every spring during 2013–2019 in 4 rivers of Chesapeake Bay: the Choptank River, Deer Creek, Marshyhope Creek, and the Patapsco River. Hourly estimates of fish counts, made by using imaging sonar combined with weekly biological sampling, allowed the assessment of the phenology of alewife and blueback herring. At a seasonal scale, migrations occurred within a temperature threshold (9–21°C), and annual shifts in the timing and duration of migrations corresponded to annual shifts in the timing and duration of this thermal window. Therefore, as climate change alters the shape and size of the thermal window in Chesapeake Bay, we expect migrations of river herring to be similarly altered.

At a daily scale, migration rates were positively correlated with changes in temperature, but the relationships between migration and non-temperature factors (streamflow, lunar phase, turbidity, and wind stress) were inconsistent among the rivers. Increased streamflow and turbidity following storm events may disrupt the relationship of temperature and migrations in the Patapsco River; however, long-term monitoring is needed to assess the interactions between the environmental variables and the extent to which the influence of non-temperature factors is river specific. At an hourly scale, we observed both diurnal (Marshyhope Creek and the Choptank River) and nocturnal (Deer Creek and the Patapsco River) patterns in spawning migrations. This divergence in diel patterns is potentially the result of inter-river differences in water clarity and therefore pressure from diurnal predators. In addition to solar elevation, hourly changes in counts were also correlated with water temperature and tides.

Overall, our results add to the body of literature supporting the strong link between water temperature and migrations and spawning of river herring at multiple temporal scales across their range (e.g., Collins, 1952; Saila et al., 1972; Richkus, 1974; Rosset et al., 2017; Lombardo et al., 2019; Legett et al., 2021). Therefore, although there may be some interannual and inter-river variability in the influence of non-temperature factors on the migrations of alewife and blueback herring, practices that reduce seasonal water temperatures and conserve and restore thermal habitat in rivers could be broadly applied to benefit these species.

Resumen

Los eventos anuales del ciclo vital de los peces, como la migración y el desove, suelen coincidir con las fluctuaciones estacionales de las condiciones ambientales. Es necesario comprender los patrones fenológicos y sus causas para conservar las poblaciones de peces vulnerables, sobre todo teniendo en cuenta que el cambio climático está alterando las transiciones estacionales. En este estudio, examinamos la fenología de las migraciones primaverales de desove del arenque de río, la pinchagua (*Alosa pseudoharengus*) y el arenque azul (*A. aestivalis*), en 4 ríos de la bahía de Chesapeake durante 7 años (2013–2019). Utilizamos un sonar de imágenes y muestras biológicas semanales para estimar los recuentos de peces de cada especie por hora en el Río Choptank, Deer Creek (un afluente del Río Susquehanna), Marshyhope Creek (un afluente del Río Nanticoke) y el Río Patapsco. Nuestros resultados indican que los patrones de temperatura del agua en primavera determinan las migraciones de desove a escala estacional diaria y por hora. La relación entre los recuentos de peces y otros factores ambientales, como el caudal, la fase lunar, la turbidez, la fuerza del viento y las mareas, fue anualmente inconsistente, y sus influencias en las migraciones pueden ser específicas de cada río. Para ambas especies se observaron distintos patrones de movimiento diurnos. Las migraciones fueron diurnas en el Río Choptank y el Arroyo Marshyhope, pero nocturnas en el Arroyo Deer y el Río Patapsco. La variación interanual e interfluvial observada en la fenología y la influencia de factores distintos de la temperatura en las migraciones, destacan la necesidad de un seguimiento a largo plazo del arenque de río en varios ríos de la bahía de Chesapeake.

Acknowledgments

We thank Patapsco Valley State Park, Maryland Park Service, MDNR, U.S. Army Corps of Engineers, F. Wothers, and Henry's Furniture for providing access to study sites. We thank W. McBurney, M. Goodison E. Kinnebrew, M. Kramer, G. Marafino, P. Roberts, H. Soulen, and J. Spires for counting fish in sonar video recordings. Funding was provided by the National Fish and Wildlife Foundation (award nos. 34809, 40321, 45567, and 50023), Smithsonian Environmental Research Center, and MDNR.

Literature cited

Agostinelli, C., and U. Lund.
2022. R package 'circular': circular statistics. Version 0.4-95. [Available from website, accessed September 2022.]

Albertson, L. K., V. Ouellet, and M. D. Daniels.
2018. Impacts of stream riparian buffer land use on water temperature and food availability for fish. J. Freshw. Ecol. 33:195–210.

Alcott, D., E. Goerig, C. Rillahan, P. He, and T. Castro-Santos.
2021. Tide gates form physical and ecological obstacles to river herring (*Alosa* spp.) spawning migrations. Can. J. Fish. Aquat. Sci. 78:869–880.

Andrews, S. N.
2014. Fishway efficiency and passage behaviour of Alewife in three fishways on Tantramar Marsh near Amherst, Nova Scotia. M.S. thesis, 98 p. Acadia Univ., Wolfville, Canada. [Available from website.]

ASMFC (Atlantic States Marine Fisheries Commission).
2012. River herring benchmark stock assessment, vol. 1. ASMFC, Stock Assess. Report 12-02, 207 p. [Available from website.]
2017. River herring stock assessment update. Volume 2: state-specific reports, 680 p. ASMFC, Arlington, VA. [Available from website.]

Atkins C. G., and N. Foster.
1868. First report of the commissioners of fisheries of the state of Maine, 1867, 128 p. Owen and Nash, Augusta, ME. [Available from website.]

Bellard, C., C. Bertelsmeier, P. Leadley, W. Thuiller, and F. Courchamp.
2012. Impacts of climate change on the future of biodiversity. Ecol. Lett. 15:365–377.

Bendall, B., A. Moore, and V. Quayle.
2005. The post-spawning movements of migratory brown trout *Salmo trutta* L. J. Fish Biol. 67:809–822.

Bi, R., Y. Jiao, L. A. Weaver, B. Greenlee, G. McClair, J. Kipp, K. Wilke, C. Haas, and E. Smith.
2021. Environmental and anthropogenic influences on spatiotemporal dynamics of *Alosa* in Chesapeake Bay tributaries. Ecosphere 12:e03544.

Bowler, D. E., R. Mant, H. Orr, D. M. Hannah, and A. S. Pullin.
2012. What are the effects of wooded riparian zones on stream temperature? Environ. Evid. 1, article 3.

Brockwell, P. J., and R. A. Davis.
2002. Introduction to time series and forecasting, 3rd ed., 425 p. Springer Nature, Cham, Switzerland.

Cobb, C. K.
2020. The impact of climate change on the migration phenology of New England's anadromous river herring and American Shad. Honors thesis, 32 p. Colby College, ME. [Available from website.]

Collins, G. B.
1952. Factors influencing the orientation of migrating anadromous fishes. Fish. Bull. 52:375–396.

Cooper, R. A.
1961. Early life history and spawning migration of the alewife, *Alosa pseudoharengus*. M.S. thesis, 58 p. Univ. Rhode Island, Kingston, RI. [Available from website.]

Dalton, R. M., J. J. Sheppard, J. T. Finn, A. Jordaan, and M. D. Staudinger.
2022. Phenological variation in spring migration timing of adult alewife in coastal Massachusetts. Mar. Coast. Fish. 14:e10198.

Dias, B. S., M. G. Frisk, and A. Jordaan.
2019. Opening the tap: increased riverine connectivity strengthens marine food web pathways. PLoS ONE. 14:e0217008.

Ellis, D., and J. C. Vokoun.
2009. Earlier spring warming of coastal streams and implications for alewife migration timing. North Am. J. Fish. Manag. 29:1584–1589.

Fan, Y., J. Chen, G. Shirkey, R. John, S. R. Wu, H. Park, and C. Shao.
2016. Applications of structural equation modeling (SEM) in ecological studies: an updated review. Ecol. Process. 5, article 19.

Forrest, J., and A. J. Miller-Rushing.
2010. Toward a synthetic understanding of the role of phenology in ecology and evolution. Philos. Trans. R. Soc. B. 365:3101–3112.

Friedland, K. D., R. T. Leaf, J. Kane, D. Tommasi, R. G. Asch, N. Rebuck, R. Ji, S. I. Large, C. Stock, and V. S. Saba.
2015. Spring bloom dynamics and zooplankton biomass response on the US Northeast Continental Shelf. Cont. Shelf Res. 102:47–61.

Greene, K. E., J. L. Zimmerman, R. W. Laney, and J. C. Thomas-Blate.
2009. Atlantic coast diadromous fish habitat: a review of utilization, threats, recommendations for conservation, and research needs. Atl. States Mar. Fish. Comm., Habitat Manag. Ser. 9, 463 p. [Available website.]

Hall, C. J., A. Jordaan, and M. G. Frisk.
2012. Centuries of anadromous forage fish loss: consequences for ecosystem connectivity and productivity. BioScience 62:723–731.

Hare, J. A., D. L. Borggaard, M. A. Alexander, M. M. Bailey, A. A. Bowden, K. Damon-Randall, J. T. Didden, D. J. Hasselman, T. Kerns, R. McCrary, et al.
2021. A review of river herring science in support of species conservation and ecosystem restoration. Mar. Coast. Fish. 13:627–664.

Hasselman, D. J., E. C. Anderson, E. E. Argo, N. D. Bethoney, S. R. Gephard, D. M. Post, B. P. Schondelmeier, T. F. Schultz, T. V. Willis, and E. P. Palkovacs.
2016. Genetic stock composition of marine bycatch reveals disproportional impacts on depleted river herring genetic stocks. Can. J. Fish. Aquat. Sci. 73:951–963.

Henderson, M. E., K. E. Mills, A. C. Thomas, A. J. Pershing, and J. A. Nye.
2017. Effects of spring onset and summer duration on fish species distribution and biomass along the Northeast United States continental shelf. Rev. Fish Biol. Fish. 27:411–424.

Hiebert, S., L. A. Helfrich, D. L. Weigmann, and C. Liston.
2000. Anadromous salmonid passage and video image quality under infrared and visible light at Prosser Dam, Yakima River, Washington. North Am. J. Fish. Manag. 20:827–832.

Hildebrand, S. F., and W. C. Schroeder.
1928. Fishes of Chesapeake Bay. Fish. Bull. 43:1–366.

Hinson, K. E., M. A. M. Friedrichs, P. St-Laurent, F. Da, and R. G. Najjar.
2022. Extent and causes of Chesapeake Bay warming. J. Am. Water Resour. Assoc. 58:805–825.

Hughes, J. B., and J. E. Hightower.
2015. Combining split-beam and dual-frequency identification sonars to estimate abundance of anadromous fishes in the Roanoke River, North Carolina. North Am. J. Fish. Manag. 35:229–240.

Humphreys, R. K., and G. D. Ruxton.
2017. Consequences of grouped data for testing for departure from circular uniformity. Behav. Ecol. Sociobiol. 71, article 167.

Huntington, T. G., G. A. Hodgkins, and R. W. Dudley.
2003. Historical trend in river ice thickness and coherence in hydroclimatological trends in Maine. Clim. Change 61:217–236.

IPCC (Intergovernmental Panel on Climate Change).
2013. Climate change 2013: the physical science basis. Contribution of working group 1 to the fifth assessment report of the Intergovernmental Panel on Climate Change, 1535 p. (T. F. Stocker, D. Qin, G.-K. Plattner, M. Tignor, S. K. Allen, J. Boschung, A. Nauels, Y. Xia, V. Bex, and P.M. Midgley, eds.) Cambridge Univ. Press, Cambridge, UK. [Available from website.]

Isaak, D. J., E. E. Peterson, J. M. Ver Hoef, S. J. Wenger, J. A. Falke, C. E. Torgersen, C. Sowder, E. A. Steel, M.-J. Fortin, C. E. Jordan, et al.
2014. Applications of spatial statistical network models to stream data. Wiley Interdiscip. Rev. Water 1:277–294.

Keefer, M. L., C. C. Caudill, E. L. Johnson, T. S. Clabough, C. T. Boggs, P. N. Johnson, and W. T. Nagy.
2017. Inter-observer bias in fish classification and enumeration using dual-frequency identification sonar (DIDSON): a Pacific lamprey case study. Northwest Sci. 91:41–53.

Kissil, G. W.
1974. Spawning of the anadromous alewife, *Alosa pseudoharengus*, in Bride Lake, Connecticut. Trans. Am. Fish. Soc. 103:312–317.
Large, W. G., and S. Pond.
1981. Open ocean momentum flux measurements in moderate to strong winds. J. Phys. Oceanogr. 11:324–336.
Legett, H. D., A. Jordaan, A. H. Roy, J. J. Sheppard, M. Somos-Valenzuela, and M. D Staudinger.
2021. Daily patterns of river herring (*Alosa* spp.) spawning migrations: environmental drivers and variation among coastal streams in Massachusetts. Trans. Am. Fish. Soc. 150:501–513.
Limburg, K. E., and J. R. Waldman.
2009. Dramatic declines in North Atlantic diadromous fishes. BioScience 59:955–965.
Loesch, J. G.
1987. Overview of life history aspects of anadromous alewife and blueback herring in freshwater habitats. Am. Fish. Soc. Symp. 1:89–103.
Lombardo, S. M., J. A. Buckel, E. F. Hain, E. H. Griffith, and H. White.
2019. Evidence for temperature-dependent shifts in spawning times of anadromous alewife (*Alosa pseudoharengus*) and blueback herring (*Alosa aestivalis*). Can. J. Fish. Aquat. Sci. 77:741–751.
Lynch, P. D., J. A. Nye, J. A. Hare, C. A. Stock, M. A. Alexander, J. D. Scott, K. L. Curti, and K. Drew.
2015. Projected ocean warming creates a conservation challenge for river herring populations. ICES J. Mar. Sci. 72:374–387.
MacAvoy, S. E., G. C. Garman, and S. A. Macko.
2009. Anadromous fish as marine nutrient vectors. Fish. Bull. 107:165–174.
Malaeb, Z. A., J. K. Summers and B. H. Pugesek.
2000. Using structural equation modeling to investigate relationships among ecological variables. Environ. Ecol. Stat. 7:93–111.
McCartin, K., A. Jordaan, M. Sclafani, R. Cerrato, and M. G. Frisk.
2019. A new paradigm in Alewife migration: oscillations between spawning grounds and estuarine habitats. Trans. Am. Fish. Soc.148:605–619.
Mullen, D. M., C. W. Fay, and J. R. Moring.
1986. Species profiles: life histories and environmental requirements of coastal fishes and invertebrates (North Atlantic)—alewife/blueback herring. U.S. Fish Wildl. Serv. Biol. Rep. 82 (11.56), 21 p. U.S. Army Corps Eng. TR EL-82-4. [Available from website.]
Nack, C. C., D. P. Swaney, and K. E. Limburg.
2019. Historical and projected changes in spawning phenologies of American Shad and Striped Bass in the Hudson River estuary. Mar. Coast. Fish. 11:271–284.
Nelson, G. A., B. I. Gahagan, M. P. Armstrong, A. Jordaan, and A. Bowden.
2020. A life cycle simulation model for exploring causes of population change in Alewife (*Alosa pseudoharengus*). Ecol. Model. 422:109004.
Nye, J. A., J. S. Link, J. A. Hare, and W. J. Overholtz.
2009. Changing spatial distribution of fish stocks in relation to climate and population size on the Northeast United States continental shelf. Mar. Ecol. Prog. Ser. 393:111–129.
Ogburn, M. B., J. Spires, R. Aguilar, M. R. Goodison, K. Heggie, E. Kinnebrew, W. McBurney, K. D. Richie, P. M. Roberts, and A. H. Hines.
2017a. Assessment of river herring spawning runs in a Chesapeake Bay coastal plain stream using imaging sonar. Trans. Am. Fish. Soc. 146:22–35.
Ogburn, M. B., D. J. Hasselman, T. F. Schultz, and E. P. Palkovacs.
2017b. Genetics and juvenile abundance dynamics show congruent patterns of population structure for depleted river herring populations in the upper Chesapeake Bay. North Am. J. Fish. Manag. 37:1083–1092.
Palkovacs, E. P., D. J. Hasselman, E. E. Argo, S. R. Gephard, K. E. Limburg, D. M. Post, T. F. Schultz, and T. V. Willis.
2014. Combining genetic and demographic information to prioritize conservation efforts for anadromous alewife and blueback herring. Evol. Appl. 7:212–226.
Palone, R. S., and A. H. Todd (eds.).
1998. Chesapeake Bay riparian handbook: a guide for establishing and maintaining riparian forest buffers. USDA Forest Service NA-TP-02-97, rev., 48 p. [Available from website.]
Parmesan, C.
2007. Influences of species, latitudes and methodologies on estimates of phenological response to global warming. Global Change Biol. 13:1860–1872.
Peer, A. C., and T. J. Miller.
2014. Climate change, migration phenology, and fisheries management interact with unanticipated consequences. North Am. J. Fish. Manag. 34:94–110.
Petreman, I. C., N. E. Jones, and S. W. Milne.
2014. Observer bias and subsampling efficiencies for estimating the number of migrating fish in rivers using Dual-frequency IDentification SONar (DIDSON). Fish. Res. 155:160–167.
R Core Team.
2020. R: a language and environment for statistical computing. R Foundation for Statistical Computing, Vienna, Austria. [Available from website, accessed October 2020.]
Raabe, J. K., and J. E. Hightower.
2014. Assessing distribution of migratory fishes and connectivity following complete and partial dam removals in a North Carolina river. North Am. J. Fish. Manag. 34:955–969.
Richkus, W. A.
1974. Factors influencing the seasonal and daily patterns of alewife (*Alosa pseudoharengus*) migration in a Rhode Island river. J. Fish. Res. Board Can. 31:1485–1497.
Rillahan, C. B., D. Alcott, T. Castro-Santos, and P. He.
2021. Activity patterns of anadromous fish below a tide gate: observations from high-resolution imaging sonar. Mar. Coast. Fish. 13:200–212.
Root, T. L., J. T. Price, K. R. Hall, S. H. Schneider, C. Rosenzweig, and J. A. Pounds.
2003. Fingerprints of global warming on wild animals and plants. Nature 421:57–60.
Rosset, J., A. H. Roy, B. I. Gahagan, A. R. Whiteley, M. P. Armstrong, J. J. Sheppard, and A. Jordaan.
2017. Temporal patterns of migration and spawning of river herring in coastal Massachusetts. Trans. Am. Fish. Soc. 146:1101–1114.
Saila, S. B., T. T. Polgar, D. J. Sheehy, and J. M. Flowers.
1972. Correlations between alewife activity and environmental variables at a fishway. Trans. Am. Fish. Soc. 101:583–594.
Sheppard, J. J., and M. S. Bednarski.
2015. Utility of single-channel electronic resistivity counters for monitoring river herring populations. North Am. J. Fish. Manag. 35:1144–1151.
Staples, A., H. D. Legett, J. L. Deichmann, K. Heggie, M. B. Ogburn.
2023. Automated acoustic detection of river herring (Alewife and Blueback Herring) spawning activity. North Am. J. Fish. Manag. 43:869–881.

Staudinger, M. D., K. E. Mills, K. Stamieszkin, N. R. Record, C. A. Hudak, A. Allyn, A. Diamond, K. D. Friedland, W. Golet, M. E. Henderson, et al.
2019. It's about time: a synthesis of changing phenology in the Gulf of Maine ecosystem. Fish. Oceanogr. 28:532–566.
Steel, A. E., C. Sowder, and E. E. Peterson.
2016. Spatial and temporal variation of water temperature regimes on the Snoqualmie River network. J. Am. Water Resour. Assoc. 52:769–787.
Timm, A., V. Ouellet, and M. Daniels.
2020. Swimming through the urban heat island: can thermal mitigation practices reduce the stress? River Res. Appl. 36:1973–1984.
2021. Riparian land cover, water temperature variability, and thermal stress for aquatic species in urban streams. Water 13:2732.
Torrence, C., and G. P. Compo.
1998. A practical guide to wavelet analysis. Bull. Am. Meteorol. Soc. 79:61–78.
Tyus, H. M.
1974. Movements and spawning of anadromous alewives, *Alosa pseudoharengus* (Wilson) at Lake Mattamuskeet, North Carolina. Trans. Am. Fish. Soc. 103:392–396.
Wilson, B. W.
1960. Note on surface wind stress over water at low and high wind speeds. J. Geophys. Res. Atmos. 65:3377–3382.
Wippelhauser, G.
2021. Recovery of diadromous fishes: a Kennebec River case study. Trans. Am. Fish. Soc. 150:277–290.
Wu, Z., N. E. Huang, S. R. Long, and C.-K. Peng.
2007. On the trend, detrending, and variability of nonlinear and nonstationary time series. Proc. Natl. Acad. Sci. U.S.A. 104:14889–14894.
Xie, Y., and F. J. Martens.
2014. An empirical approach for estimating the precision of hydroacoustic fish counts by systematic hourly sampling. North Am. J. Fish. Manag. 34:535–545.

National Marine
Fisheries Service
NOAA

Fishery Bulletin
established in 1881

Spencer F. Baird
First U.S. Commissioner
of Fisheries and founder
of *Fishery Bulletin*

Effect of reduction in spatial survey effort on indices of bottom temperature for the eastern Bering Sea

Cynthia Yeung
Stan Kotwicki
Sean K. Rohan

Email address for contact author: cynthia.yeung@noaa.gov

Resource Assessment and Conservation Engineering Division
Alaska Fisheries Science Center
National Marine Fisheries Service, NOAA
7600 Sand Point Way NE
Seattle, Washington 98115

Abstract—Bottom temperature is routinely measured as part of the bottom-trawl survey conducted every summer on the continental shelf of the eastern Bering Sea by the NOAA Alaska Fisheries Science Center. These data are widely used in ecosystem, stock assessment, and ocean modeling. We assessed the effect of alternative sampling designs and effort reduction on the quality of bottom-temperature information from the survey. Simple-random and stratified-random sampling were simulated and compared with the systematic sampling of fixed stations in the regular grid used in the standard survey, with respect to the use of survey data in the estimation of bottom temperatures and related indices. The effort simulated ranged from 34% to 100% of the full effort. In the simulated surveys, the use of each of the 3 sampling designs resulted in values of bottom-temperature metrics that are close to those from the real survey, even with as little as half the effort. Lower effort resulted in larger and more variable prediction errors of the indices. The decrease in prediction performance is most noticeable at the 34% effort level. Systematic sampling performed slightly better than simple-random and stratified-random sampling. One reason for this difference in performance is that random sampling may have been less effective than the standard sampling in capturing a small cold pool that is characteristic of the current warm ocean state.

Manuscript submitted 17 January 2023.
Manuscript accepted 1 August 2023.
Fish. Bull. 121:112–123 (2023).
Online publication date: 28 August 2023.
doi: 10.7755/FB.121.3.5

The views and opinions expressed or implied in this article are those of the author (or authors) and do not necessarily reflect the position of the National Marine Fisheries Service, NOAA.

All physiological rates of aquatic invertebrate and teleost fish species depend on body temperatures (Brown et al., 2004). Therefore, temperature is the principal driver of aquatic ecosystem dynamics (Kooijman, 2000; Poloczanska et al., 2016). The continental shelf of the eastern Bering Sea (EBS) is one of the most productive ecosystems in the world (Hood and Calder, 1981), supporting major groundfish fisheries, such as those that target walleye pollock (*Gadus chalcogrammus*) (Loughlin and Ohtani, 1999). Bottom water temperature is a key indicator of ecosystem state because of its pivotal role in the spatial distribution of groundfish species (Eisner et al., 2020; Kotwicki and Lauth, 2013), predator–prey interactions (Grüss et al., 2021), and demographic rates (Cooper et al., 2020).

The bottom temperature of the EBS is determined by an interplay between winter cooling, mixing due to wind and tide, and the spatial extent and persistence of ice cover (Sullivan et al., 2014). Bottom temperature is used to map the *cold pool*—a term typically used to refer to the layer of cold (<2°C) bottom water that forms below the pycnocline when sea ice freezes in the winter and extends southward over the middle of the shelf (at depths of 50–100 m) in summer in the EBS (Wyllie-Echeverria and Wooster, 1998; Stabeno et al., 2012). The size of the cold pool depends on the extent of sea ice during the previous winter. Under climate change, the area and thickness of sea ice are diminishing; ice forms later in the fall and retreats earlier in the spring (Overland et al., 2018; Stabeno and Bell, 2019). Since a warm thermal stanza across the Bering Sea began in late 2013 (NPFMC, 2016), there has been a series of record-breaking high water temperatures (Stabeno et al., 2019), and the cold pool has retracted northward, to the point of disappearing almost entirely from the EBS in 2018 (Rohan et al., 2022).

Bottom temperature in the EBS and cold pool indices are significant climate change indicators (Mueter and Litzow, 2008; Kotwicki and Lauth, 2013; Hollowed et al., 2020;) and environmental covariates in ecosystem and groundfish stock assessment (Thorson, 2019; Kearney et al., 2020; Rooper et al., 2021). In a cursory search in Google Scholar (website, accessed January 2023), about 8320 articles published since 2010 contained the phrase *eastern Bering Sea*, and in 10% and

7% of those articles *bottom temperature* and *cold pool* were also mentioned, respectively.

The primary source of data on summer bottom temperature for the EBS shelf is the bottom-trawl survey conducted every summer (June–August) since 1971 by the NOAA Alaska Fisheries Science Center for the assessment of groundfish stocks (Armistead and Nichol, 1993). The survey area includes the entire continental shelf at the depths of 20–200 m, and a regular grid of fixed stations is used for systematic sampling (Fig. 1). Temperature has been routinely recorded with each trawl sample in the standard survey since 1982. Survey temperature data are used to calibrate and validate the Bering10K Modeling Suite (Capotondi et al., 2019; Kearney et al., 2020). Although the cold pool is most commonly defined as bottom water colder than 2°C, 0°C and 1°C have also been used in the study of the spatial dynamics of fish populations (Kotwicki and Lauth, 2013; Thorson et al., 2017; Nichol et al., 2019).

Long-term ecological studies and resource surveys are expensive and complex to conduct. Worldwide, these programs are vulnerable to reductions in effort due to financial, logistical, or natural obstacles (ICES, 2020). The increasing disparity between funding allocation for the NOAA bottom-trawl survey and rising costs is also a reality that prompts considerations of effort reduction. Alternative sampling strategies under the constraint of reduced effort are often simulated to evaluate how the quality of survey data would be affected and whether program objectives could be achieved (e.g., Liu et al., 2011; Del Vecchio et al., 2019). In this study, we simulated surveys with systematic, simple-random, or stratified-random sampling and with different levels of effort, measured as the number of stations sampled, and compared estimation of bottom temperatures and related indices based on values from those simulated surveys with estimation based on data from the real standard surveys for which systematic sampling of fixed stations in a regular grid was used. The effort levels simulated ranged from 34% to 100% of the full effort of sampling 350 stations.

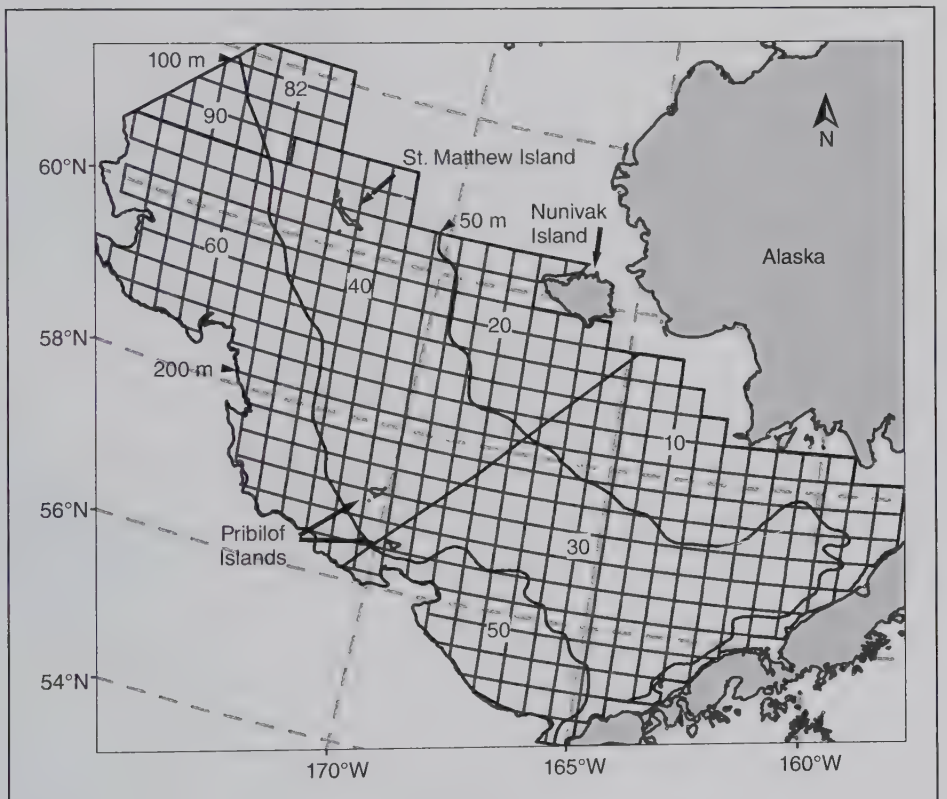

Figure 1

Map showing the regular grid used in the systematic sampling of the bottom-trawl survey conducted every summer on the continental shelf of the eastern Bering Sea by the NOAA Alaska Fisheries Science Center and used in the simulations of surveys in this study. Trawl samples are collected at stations located approximately at the center of each cell, each 20 × 20 nautical miles (37 km^2), in the grid. The survey area is divided into strata based on latitude and depth (strata are outlined with black lines and labeled with their assigned numbers), with the offshore boundaries of strata aligned with the 50-m, 100-m, and 200-m isobaths. The major islands on the shelf are indicated.

Materials and methods

Observations of bottom temperature

The bottom-trawl survey on the continental shelf of the EBS (hereafter referred to as *the survey*) has a systematic, regular-grid sampling design consisting of 350 cells of 20 × 20 nautical miles (nmi) (37.0 × 37.0 km) each (Fig. 1). The grid is divided into several strata that correspond to a combination of latitudinal and depth-associated biophysical domains that fall in 3 groups: inner shelf (depths <50 m), middle shelf (depths of 50–100 m), and outer shelf (depths >100 and ≤200 m) (Kinder and Schumacher, 1981; Coachman, 1986). Each stratum is assigned a number so that they can be referenced for management purposes (Fig. 1). Sampling during the survey progresses through the grid from the southeast corner to the northwest corner over an average of 57 days from late May to early August (Rohan et al., 2022). A standard trawl sample is taken from a location (or *station*) at approximately the center of each cell. The station configuration currently used for the survey was adopted in 1987 (Conner and Lauth, 2017). Bottom temperature (hereafter referred to as *temperature*) is recorded at each station. The various instruments used over the years, including an expendable bathythermograph and a digital temperature-depth recorder, are detailed in Rohan et al. (2022). Since 1996, the instrument for recording temperature has been attached to the head rope of the trawl net.

A spatial map of summer temperatures in the Bering Sea is produced annually as part of the survey and is a composite of observations from the survey duration of more than 2 months (Rohan et al., 2022). In this study, for each year from 1987 through 2019, temperature was simulated for the subset of stations that was considered the full effort: the 350 stations (Fig. 1) at the centers of cells, excluding the 26 stations located at the corners of cells around St. Matthew Island and the Pribilof Islands that are used in assessment of local populations of blue king crab (*Paralithodes platypus*) (Armistead and Nichol, 1993).

Simulated surveys of temperature

Spatial analyses were conducted by using popular spatial packages in the R statistical computing environment (vers. 3.6.3; R Core Team, 2020): gstat (vers. 2.1-1; Gräler et al., 2016), raster (vers. 3.3-13; Hijmans, 2020), sf (vers. 1.0-12; Pebesma, 2018), and sp (vers. 1.6-0; Pebesma and Bivand, 2005).

A regular grid of 494 rows and 565 columns (279,110 pixels) and with a 2-km resolution was superimposed over the survey area. Observed temperature at the standard set of 350 stations was interpolated over the grid by using ordinary kriging with Stein's Matérn autocovariance model (Stein, 1999), as implemented in the R package gstat, to produce annual temperature spatial surfaces (*rasters*). This process is the standard method for calculating temperature data products with information from the bottom-trawl survey in the Bering Sea (Rohan et al., 2022). The Matérn model was fitted to the sample variogram (smoothness=0.5; the sill and range automatically fitted by using gstat; Gräler et al., 2016). The variogram was used to interpolate pixel values over the raster. Only the pixels that partially or entirely overlapped the survey area were assigned values to interpolate the raster (R):

$$R = \left\{r_l\right\}_{l=1}^{N_r=123,274}, \quad (1)$$

where r_l = pixel l, and
N_r = the total number of pixels in R.

The raster produced from observed temperatures was defined as the "true" thermal state of the EBS shelf.

Several combinations of sampling design and effort were applied to resample the raster based on observed temperatures of each year in the set of years (Y) to simulate surveys:

$$Y = \{1987, 1988, \ldots, 2019\} = \left\{y_i\right\}_{i=1}^{N_y=33}, \quad (2)$$

where y_i = year i, and
N_y = the total number of years in Y.

The following sampling designs were used: 1) systematic, regular-grid (also referred to as *regular*), 2) simple-random (also referred to as *random*), and 3) stratified-random with proportionate allocation by area of stratum (also referred to as *stratified*) (Fig. 1). For random and stratified sampling, 4 effort levels (E), equivalent to 34%, 46%, 66%, and 100% of the full effort, were simulated as follows:

$$E = \{120, 160, 230, 350 \text{ stations}\} = \left\{e_j\right\}_{j=1}^{N_e=4}, \quad (3)$$

where e_j = effort j, and
N_e = the total number of levels in E.

The 3 reduced regular sampling efforts that were simulated were based on grid cell size: 35 nmi^2 (64.0 km^2) for the effort of 120 stations, 30 nmi^2 (55.6 km^2) for the effort of 163 stations, and 25 nmi^2 (46.3 km^2) for the effort of 226 stations. The full regular sampling effort of 350 stations is that of the actual survey with the cell size of 20 nmi^2 (37.0 km^2). The expected number of stations in the simulated set with regular effort is practically equivalent to the sets with random and stratified effort based on the exact number of stations.

For each combination of sampling design and effort, 100 replicate sets of different station locations were drawn from the survey grid with the spsample function in the R package sp (Bivand et al., 2013), with the replicate sets (S) defined as follows:

$$S = \left\{s_k\right\}_{k=1}^{N_s=100}, \quad (4)$$

where s_k = replicate set k, and
N_s = the total number of replicate sets in S.

Each replicate set represents a simulated survey. Temperature values were extracted (predicted temperature) at each

station from the raster based on observed temperatures. The point values of predicted temperature are used to interpolate a predicted temperature raster by using the same aforementioned methods for generating an observed temperature raster. The steps of the simulation are summarized schematically in Figure 2.

Performance evaluation

The performance of the simulated surveys in replicating temperatures from the real annual surveys was evaluated on the basis of the bias (ε) and the root mean squared error (RMSE) of each of the predicted temperature indices by using these general equations:

$$\varepsilon = \frac{1}{N}\sum_{t=1}^{N}\left(\hat{x}_t - x_t\right), \text{ and} \quad (5)$$

$$RMSE = \sqrt{\frac{1}{N}\sum_{t=1}^{N}\left(\hat{x}_t - x_t\right)^2}, \quad (6)$$

where $\hat{x}_t$ = the predicted temperature index for t=1, . . .,N, where the total number of samples, N, depends on the index.

The term *error* will hereafter refer generally to both bias and RMSE. The fundamental unit is the temperature value in each pixel of a raster, from which temperature indices are constructed. We examined the following indices: mean temperatures of the whole shelf (*shelf*) and shelf stratum (*stratum*), total cold pool area, the offshore (western-most longitude) and southern (southern-most latitude) extents of the cold pool, and the depth at the offshore extent of the cold pool. In addition to the common definition of the cold pool as bottom water with temperature <2°C (CP2), definitions with temperature thresholds of <1°C (CP1) and <0°C (CP0) were also evaluated. These indices comprehensively describe the general thermal state of the shelf and the location of the cold pool for a given year for the purposes of ecosystem and fishery management (Nichol et al., 2019; Siddon, 2021; Thorson et al., 2017; Uchiyama et al., 2020).

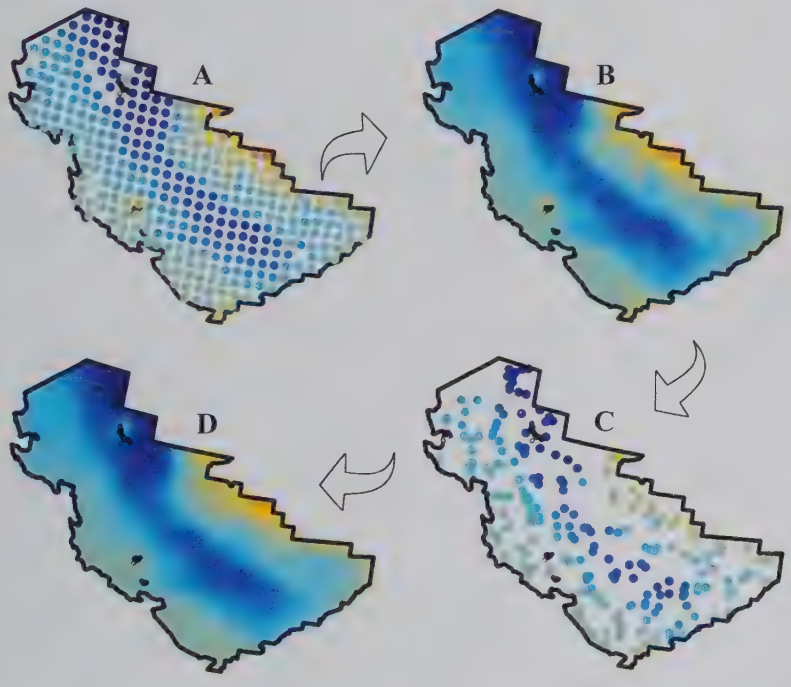

Figure 2

Schematic of the 4 main steps used to simulate a survey of bottom temperature on the continental shelf of the eastern Bering Sea. The steps are as follows: (**A**) start with temperatures observed at 350 regularly spaced stations of the real bottom-trawl survey from 1987 through 2019 (points indicate stations), (**B**) interpolate point values to generate a raster surface for observed temperature, (**C**) superimpose on the observed temperature raster stations simulated by using 1 of 3 sampling designs (regular, simple random [shown here], or stratified random) and 1 of 4 effort levels (number of stations: 120, 160, 230, or 350) and extract predicted temperatures at those stations, and (**D**) interpolate point values to generate a raster surface for predicted temperature. Values for corresponding pixels (simulated stations) in the rasters of predicted and observed temperature and related temperature indices were compared to evaluate prediction performance of the sampling designs used to simulate surveys.

Temperature rasters

To evaluate the prediction performance of a single raster, the error was calculated for each pixel l, and then the mean pixel error of the raster was determined across all pixels of the raster (N=123,274). To evaluate the variability among replicate rasters of a given combination of effort and year (or *treatment*) for each sampling design, the mean error of pixel l was calculated across the 100 replicates by using these equations:

$$\varepsilon_{ij.l} = \frac{1}{N_s}\sum_{k=1}^{N_s}\varepsilon_{kl}, \quad (7)$$

where $\varepsilon_{ij.l}$ = mean bias of pixel l for year i and effort j, and
ε_{kl} = mean bias of pixel l across all k replicate sets; and

$$RMSE_{ij.l} = \sqrt{\frac{1}{N_s}\sum_{k=1}^{N_s}\left(\varepsilon_{kl}\right)^2}, \quad (8)$$

where $RMSE_{ij.l}$ = mean RMSE of pixel l for year i and effort j.

The overall mean error of a given design and effort combination was averaged

across all years as follows ($N=N_y \times N_r=33 \times 123{,}274=4{,}068{,}042$):

$$\varepsilon_{j..} = \frac{1}{N_y N_r} \sum_{i=1}^{N_y} \sum_{l=1}^{N_r} \varepsilon_{ij.l}, \text{and} \quad (9)$$

$$RMSE_{j..} = \frac{1}{N_y N_r} \sum_{i=1}^{N_y} \sum_{l=1}^{N_r} RMSE_{ij.l}. \quad (10)$$

The standard deviation (SD) of the overall bias was determined with this equation:

$$SD(\varepsilon) = SD(\varepsilon_{ij..}) = \sqrt{\frac{1}{N_y N_r - 1} \sum_{i=1}^{N_y} \sum_{l=1}^{N_r} \left(\varepsilon_{ij.l} - \varepsilon_{j..}\right)^2}. \quad (11)$$

Mean temperatures of shelf and stratum

Predicted and observed annual mean temperatures of the whole shelf and individual stratum in the EBS were calculated by averaging all pixelated temperature values within the unit (shelf or stratum) in each raster. The error in annual mean shelf or stratum temperature was evaluated between each replicate raster based on predicted or observed temperatures.

Cold pool indices

The area of the cold pool was calculated as the number of pixels of the cold pool multiplied by the pixel size (2 km^2), for each of the 3 definitions of cold pool based on different boundaries (temperature thresholds) of the cold pool (0°C, 1°C, or 2°C). The error of the area was also expressed as a percentage of the observed area to evaluate their correlation. The offshore and southern extents of the cold pool are defined as the western-most longitude, and southern-most latitude of the cold pool identified on the raster. The depth of the cold pool at the geographic coordinates of its offshore extent was extracted from a bathymetry raster of the entire part of the U.S. exclusive economic zone off Alaska. The original raster with a 20-m resolution was compiled from 18.6 billion bathymetric soundings obtained from the NOAA National Center for Environmental Information (Lewis[1]). For this analysis, the raster was resampled to a 2-km resolution and clipped to the survey grid by using the Database Management Toolbox for raster processing in ArcMap[2], part of ArcGIS Desktop, vers. 10.7. (Esri, Redlands, CA).

Results

Within a sampling design, lower effort resulted in larger and more variable prediction errors in temperature metrics. Only exceptions will be mentioned hereafter.

[1] Lewis, S. 2018. Personal commun. Sustain. Fish. Div., Alsk. Reg. Off., Natl. Mar. Fish. Serv., NOAA, P.O. Box 21668, Juneau, AK 99802-1668.

[2] Mention of trade names or commercial companies is for identification purposes only and does not imply endorsement by the National Marine Fisheries Service, NOAA.

Temperature rasters

Prediction errors of individual rasters and among replicate sets of rasters were both low regardless of the combination of sampling design and effort. The overall mean values of pixel bias of the rasters for all combinations were ≤0.01°C (SD <0.3), and the overall mean values of pixel RMSE of the rasters for all combinations were <0.3°C (SD <0.2) (Table 1). The difference in prediction performance among designs for the same effort was small. Random sampling resulted in slightly higher RMSE values by magnitudes of tenths of degrees Celsius. Replicate rasters of predicted temperature within a treatment were similar to each other and to the corresponding raster of observed temperature. The similarity between annual observed temperature rasters (Fig. 3A) and mean predicted temperature rasters (N_s=100) from the survey simulation with random sampling and an effort of 230 stations (Fig. 3B) exemplifies the close visual resemblance of temperature rasters regardless of design and effort combination.

Mean temperatures

Shelf The means for bias in temperature on the entire shelf for all treatments were ≤±0.02°C (SD ≤0.06). The RMSE values in shelf temperatures for all treatments were <0.4°C. In almost all cases, predicted annual mean

Table 1

Overall mean bias ($\bar{\varepsilon}$) and overall root mean squared error (RMSE) and the standard deviation (SD) of the overall mean bias in the prediction of bottom temperature on the continental shelf of the eastern Bering Sea in rasters created by simulating bottom-trawl surveys for the years from 1987 through 2019. The statistics summarize the variability among replicates within a given combination of sampling design and survey effort (N=123,274 pixels per mean annual raster×33 years=4,068,042). The 3 sampling designs used in simulations were systematic (regular), simple random (random), and stratified random (stratified). Effort is given as the number of stations sampled to interpolate a raster of predicted temperature.

		Bias		
Design	Effort	$\bar{\varepsilon}$	SD	RMSE
Regular	120	−0.011	0.230	0.195
Regular	160	−0.008	0.190	0.155
Regular	230	−0.006	0.147	0.113
Random	120	−0.010	0.285	0.291
Random	160	−0.008	0.243	0.244
Random	230	−0.006	0.195	0.192
Random	350	−0.004	0.147	0.141
Stratified	120	−0.011	0.253	0.237
Stratified	160	−0.009	0.212	0.193
Stratified	230	−0.006	0.165	0.147
Stratified	350	−0.004	0.121	0.103

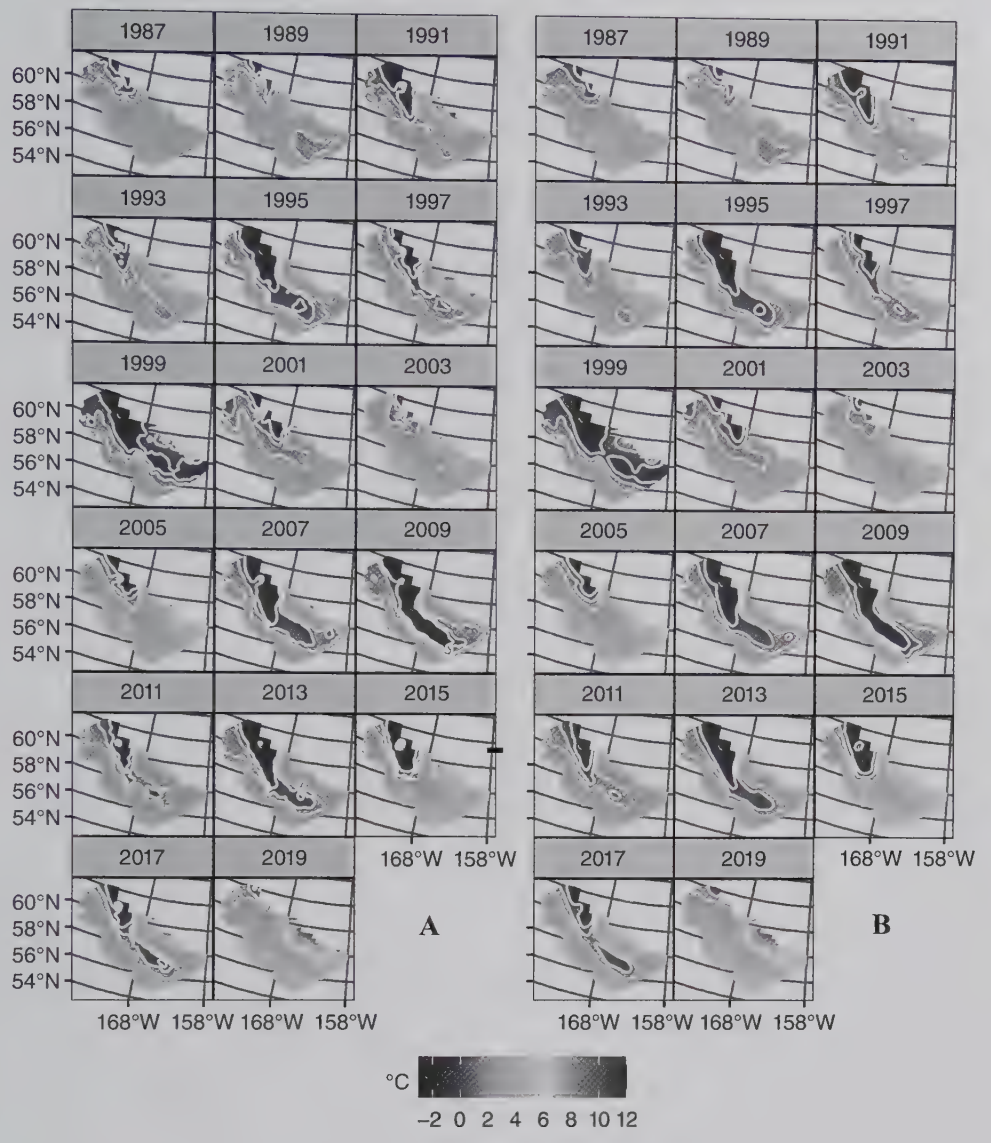

Figure 3

Annual bottom temperature in the eastern Bering Sea for the odd-numbered years from 1987 through 2019: (**A**) rasters of interpolated values based on observations recorded during actual bottom-trawl surveys and (**B**) rasters of simulated values based on the means of 100 replicate rasters produced by simulating random sampling of 230 stations superimposed on the observed temperature raster. The white lines indicate the 0°C, 1°C, and 2°C isotherms.

temperatures were lower than observed temperatures (negative bias). At the lowest effort of 120 stations, random and stratified sampling resulted in errors with greater interannual variability. This variability was more obvious in the bias values, which for some years were of smaller magnitude (less negative) than bias values produced in treatments with higher effort (Fig. 4). The values of RMSE (not shown in a figure) were consistently higher and more variable for treatments with lower effort levels but otherwise had similar patterns across treatments.

Stratum Predicted mean stratum temperatures were higher than observed temperatures (positive bias) in the middle-shelf strata 30, 40, and 82 (for locations of numbered strata, see Figure 1), the principal domain of the cold pool, but lower than observed temperatures in all other strata (Suppl. Fig. 1) (online only). The RMSE values were generally around 0.2°C. They were lowest for outer-shelf stratum 60 and relatively higher and more variable for the inner-shelf strata 10 and 20 and in middle-shelf stratum 82. The RMSE for stratum 50 was anomalously high in 1992 (Suppl. Fig. 2) (online only), a difference that

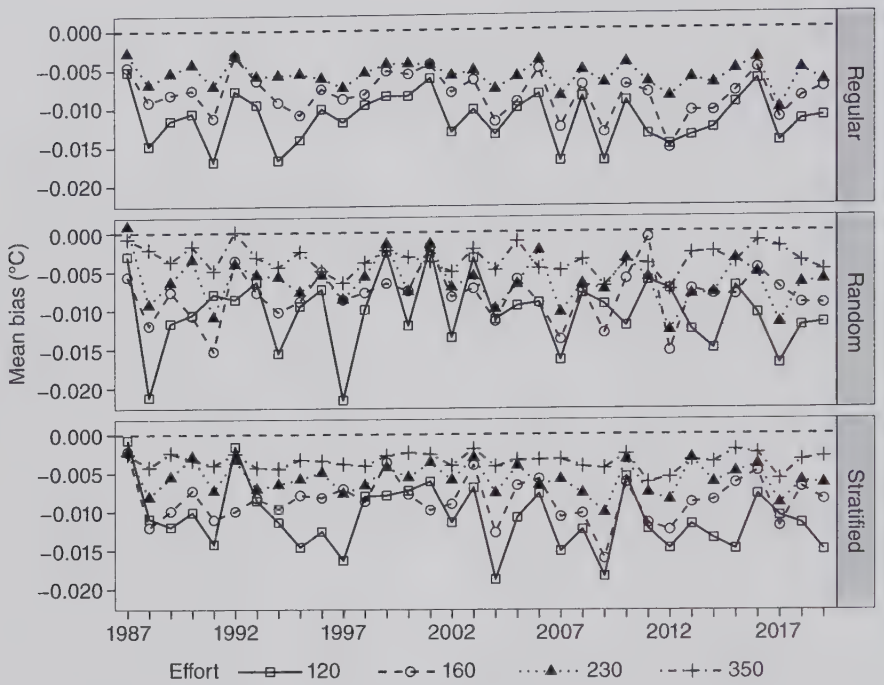

Figure 4

Mean bias in prediction of the mean bottom temperature of the entire continental shelf in the eastern Bering Sea, by sampling design (regular, simple random, or stratified random) and effort level (number of stations) for each survey year from 1987 through 2019.

was likely associated with artifacts of interpolation (fragments of water in stratum 50 with temperatures <2°C in the raster based on observed temperatures that were not replicated in the rasters based on predicted temperatures; Fig. 3). Random sampling resulted in errors that are relatively larger than errors from the use of other designs at the same effort. The difference in level of errors was most noticeable for strata 20 and 82 at the effort of 120 stations.

Cold pool indices

Performance was similar among sampling designs, in predicting total cold pool area, the offshore and southern extents of the cold pool, and the depth at the offshore extent. Regular sampling generally resulted in slightly smaller errors than random and stratified sampling. Differences were in the magnitude of tenths of a unit.

Area Prediction bias in the cold pool area as a percentage of the observed cold pool area was small for CP2, except in the simulation for 2018 (Fig. 5), when bottom water colder than 2°C occupied only 1.2% of the survey area along the northern boundary and water colder than 1°C was not observed (Figs. 3A and 6). The RMSE as a percentage of the observed cold pool area had very similar patterns to the bias percentage. The bias and RMSE percentages were highly correlated, with coefficient of correlations (r) ranging from −0.8, for both CP1 and CP2, to approximately 1 for CP0 (P<0.001, N=352). Excluding the percentage for 2018, the bias percentages across all treatments were larger and more variable for the colder boundaries of the cold pool (0°C and 1°C) and skewed more toward the underestimation of the area: the range for CP2 was −10–4%, the range for CP1 was −30–12%, and the range for CP0 was −97–1%. The bias percentages were moderately correlated with observed cold pool areas (CP2: r=0.37; CP1: r=0.26; CP0: r=0.44; P<0.001, N=11 treatments×33 years×100 replicates of simulated cold pool areas=36,300). In all instances, large negative biases were associated with small cold pool areas.

Extent and depth Bias and RMSE patterns for indices of cold pool location were largely similar. For any combination of sampling design and effort, mean biases in predicting cold pool extent were ≤0.4°N (SD ≤0.3) and ≤±0.2°W (SD ≤0.5); RMSE values were ≤0.6° for both latitude and longitude (for bias plots, see Supplementary Figures 3–5 (online only); plots for RMSE are not provided because the patterns are similar to those for bias). The magnitude of the errors was associated with the cold pool boundary and the survey year (i.e., the thermal environment) and rarely larger than a fraction of a degree in longitude or latitude. The predicted southern extent was farther north than the

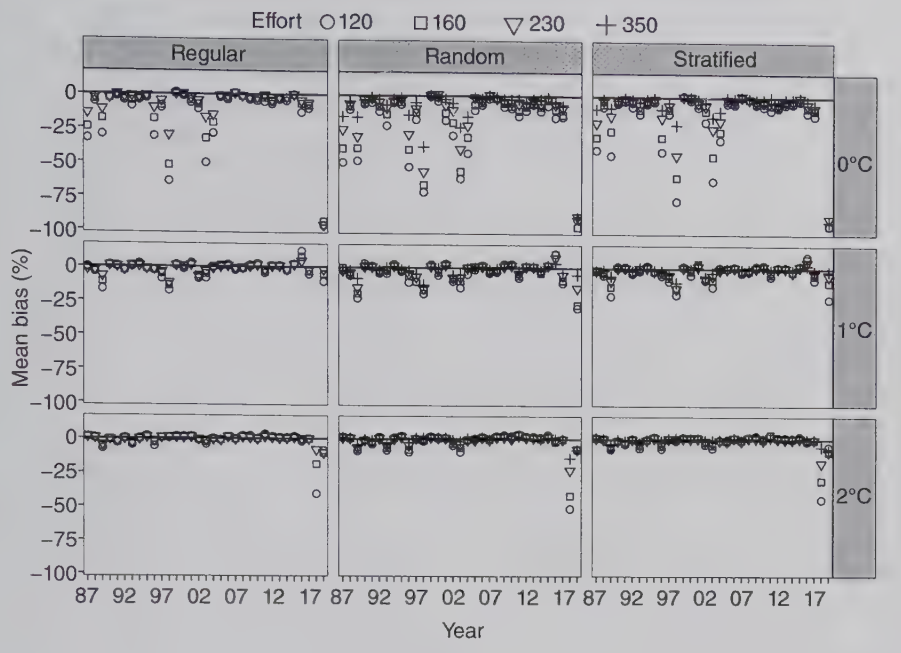

Figure 5

Mean bias in prediction of the cold pool area on the continental shelf in the eastern Bering Sea as a percentage of the observed cold pool area, by sampling design (regular, simple random, or stratified random) and effort level (number of stations) for each survey year from 1987 through 2019. The cold pool is a layer of cold (<0°C, <1°C, or <2°C) bottom water that forms on the shelf below the pycnocline.

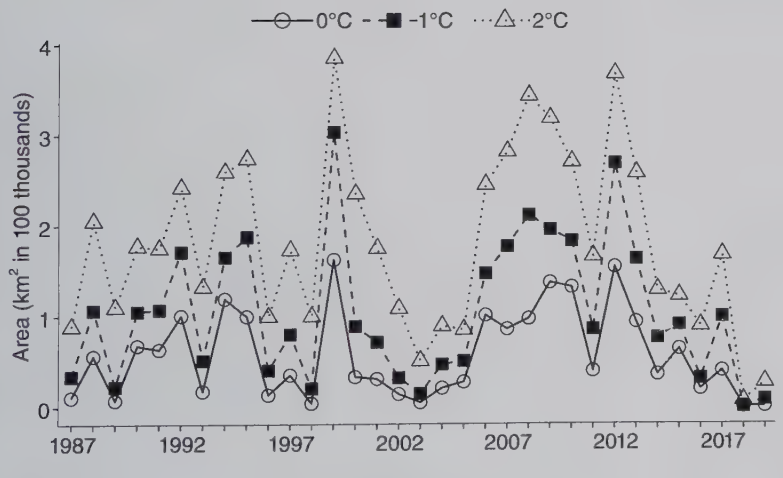

Figure 6

Annual observed area of the cold pool, a layer of cold (<0°C, <1°C, or <2°C) bottom water that forms below the pycnocline, on the continental shelf of the eastern Bering Sea from 1987 through 2019.

observed extent (positive bias) (Suppl. Fig. 3) (online only). The bias in predicting the southern extent of CP2 was largest for 2002 and 2003, for which observed temperature rasters show small, isolated pools of water <2°C farther south that were detached from the main pool, and for 2019, for which the main pool was tiny with an irregular southern boundary (Fig. 3A). The detached pools did not appear in the predicted temperature rasters for the corresponding years (Fig. 3B); hence, the predicted southern extent was farther north than the rasters based on observed temperatures, resulting in relatively large errors. The predicted offshore extent was mostly farther offshore than the observed extent for CP2 and CP1 (negative bias), but the trend was reversed for CP0, for which the biases were mostly positive (Suppl. Fig. 4) (online only).

Biases in predicting the depth at the offshore extent were larger (both mean and SD) for the warmer boundaries of the cold pool (Suppl. Fig. 5) (online only). For CP0 and CP1, the mean bias range was 1–4 m (RMSE: 1–4 m). For CP2, the mean bias ranged from −5 to −9 m (RMSE: 3–4 m) and was more variable annually than for CP0 and CP1. The largest bias of CP2, at about ±100 m, occurred in the simulations for 2002 and 2016 (Suppl. Fig. 5) (online only). The mean predicted offshore depth was shallower than the observed depth for CP0 and CP1 (positive bias) but deeper than the observed depth for CP2 (negative bias).

Discussion

In this study, simulated surveys with regular, simple-random, and stratified-random sampling of the continental shelf of the EBS at the same level of effort have comparable performance in predicting bottom temperatures and temperature-related indices. Regular sampling performed slightly better than the other designs; simple-random sampling performed about the same as stratified-random sampling. Lower effort resulted in larger prediction errors of the indices—on the scale of fractions of a degree for indices of mean temperature and cold pool location (latitude and longitude), thousands of square kilometers for cold pool area, and tens of meters in depth for offshore extent. Whether differences on that scale for an index is significant depends on the application. For example, the performance of ecosystem models and forecasting systems may depend on spatial resolution, coverage, and accuracy of the observational data (Capotondi et al., 2019; Thorson, 2019), whereas current qualitative assessment of ecosystem state and trends may be more tolerant of uncertainties (Zador et al., 2016). Interannual variability was most noticeable at the lowest effort of 120 stations, indicating that this level of effort may be a critical threshold for effort reduction.

The cold pool boundary is most commonly defined as water <2°C (CP2) in the literature. Kotwicki and Lauth (2013) suggested that water <1°C (CP1) better describes the temperature preferences of groundfish and crab species in the EBS. As the benthic environment becomes warmer and the cold pool becomes smaller under climate change, colder boundaries of the cold pool may be increasingly more difficult to delineate with high certainty, especially with reduced effort. It may be necessary to review current temperature-based indices and change them to indices that will more adequately depict thermal variability in the benthic environment in the EBS. In the scenario of an ice-free EBS, thermal variability may have less effect on ecosystem dynamics.

Spatial interpolation is less accurate and generates larger prediction errors generally when the number of data points is small and not uniformly distributed (Achilleos, 2011). These kinds of data insufficiency may have caused the apparent fragmentation of the cold pool in the observed temperature rasters and resulted in relatively large errors in the estimation of the southern extent of the cold pool (e.g., in the simulation for 2003). Higher sampling density in the vicinity where the cold pool generally resides (i.e., the middle shelf and the northern inner shelf) may be necessary to better delineate a small cold pool and estimate cold pool indices.

Prediction errors of the depth at the offshore extent of the cold pool are highly variable, and biases can be as large as ±100 m for CP2 and CP1. The magnitude of errors is small for CP0 because it is located nearshore, usually in depths ≤50 m. The accuracy of the estimated depth at a location is dependent on the resolution and accuracy of the bathymetry raster. The finding of relatively large prediction errors in the index for the depth at the offshore extent of the cold pool indicates that reduced sampling may lead to high uncertainty in the estimation of this index. The current methods of estimation may also be a causal factor. We recommend that this index be used with caution and that the use of other more robust indices may be preferable.

The results of this study indicate that the use of all 3 survey designs can reproduce temperatures and indices of the EBS shelf from the real bottom-trawl survey, for which sampling of 350 stations in a regular grid was done systematically, even with as little as half the effort. Reducing the number of stations that are sampled has definite financial and likely logistical benefits. Total on-station time can be reduced, although the total transit time to cover the survey area cannot necessarily be changed. The current survey requires 2 months to complete with 2 vessels (Conner and Lauth, 2017). Effort reduction may shorten the total survey time and enable the composition of a spatial temperature map that characterizes temperature for a more compressed time frame. It is not apparent that the use of any of the survey designs examined in this study delivers distinctly better performance in the construction of temperature spatial maps and indices or achieves greater economy and efficiency in survey execution. Regular sampling appears to perform slightly better and has been the standard sampling design for the bottom-trawl survey on the EBS shelf for over 30 years. Random sampling may be less effective in capturing a very small cold pool (e.g., the cold pool in 2018).

Changing the spatial extent of the sampling effort will likely also change the survey schedule and the day of the year on which certain stations are sampled. On the basis of Danielson et al. (2011) and Cokelet (2016), the surface mixed layer would warm by an estimate of 3.0°C/d. Analyses indicate that, if stations with depths <50 m in the current grid—which presumably would be fully mixed—are sampled approximately a week or more earlier than their mean sampling day of year, cold pool indices would produce average negative (i.e., cold) biases less than −0.2°C for those stations; conversely, sampling later than their mean sampling day of year would result in a positive (i.e., warm) bias (Rohan et al., 2022). The effect on the temperature indices of the temporal effort shift associated with spatial effort reduction would need to be assessed. Relationships used in stock assessments to correct for variation in density and availability would need to be revisited because they are largely predicated on assumptions of the stationarity of temperature indices.

Conclusions

Long-term ecological studies are imperative to the understanding of climate-scale processes and informing management policy (Sukhotin and Berger, 2013; Hughes et al., 2017; Harvey et al., 2020). The bottom-trawl survey on the EBS shelf provides an invaluable time series of fishery-independent biological data and environmental data essential for stock assessment and fisheries and ecosystem research under climate change (e.g., Holsman et al., 2016; Grüss et al., 2020). The collection of temperature data is

only one of many ancillary tasks of the survey. Evaluation of how changes in sampling design and reduction in effort will affect the accuracy and precision of stock assessment information is ongoing (e.g., Oyafuso et al., 2021).

The future direction of the survey in terms of design and effort will be driven mainly by stock and environmental assessment needs within fiscal constraints. When considering stratification and sample allocations for future surveys, it is important to consider not only species distribution but also the distribution and importance of the temperature indices needed for these assessments. Alternatively, the measurement of temperature during the survey may be independent of the bottom-trawl sampling design if instruments that are not attached to the trawl gear are used. Temperature profiling can be achieved within a reasonably short time at a station or possibly even while the vessel is underway. If measurement of temperature is decoupled from trawl sampling, it may not be necessary to decrease temperature samples by the same amount as trawl samples or restrict temperature sampling only to trawl stations.

Resumen

La temperatura del fondo se mide rutinariamente como parte del estudio de arrastre de fondo realizado cada verano en la plataforma continental del Mar de Bering oriental por el Centro de Ciencias Pesqueras de Alaska de la NOAA. Estos datos se utilizan ampliamente en la evaluación de ecosistemas, evaluación de poblaciones y modelación oceánica. Evaluamos el efecto de diseños de muestreo alternativos y de la reducción del esfuerzo, sobre la calidad de la información de la temperatura del fondo obtenida en la prospección. Se simuló y comparó el muestreo aleatorio simple y el muestreo aleatorio estratificado con el muestreo sistemático de estaciones fijas en una rejilla regular, en relación con el uso de datos de prospección en la estimación de las temperaturas del fondo marino y los índices relacionados. El esfuerzo simulado osciló entre el 34% y el 100% del esfuerzo total. En las prospecciones simuladas, el uso de cada uno de los 3 diseños de muestreo resulto en valores de temperatura del fondo cercanos a los de la prospección real, incluso con tan solo la mitad del esfuerzo. A menor esfuerzo, los errores de predicción de los índices son mayores y más variables. La disminución de los resultados de predicción es más notable en el nivel de esfuerzo del 34%. Los resultados del muestreo sistemático son ligeramente mejores que los del muestreo aleatorio simple y el muestreo aleatorio estratificado. Una de las razones de esta diferencia es que el muestreo aleatorio pudo haber sido menos eficaz que el muestreo estándar a la hora de captar una pequeña onda fría característica del actual estado cálido del océano.

Acknowledgments

We thank all the people who worked on the bottom-trawl surveys in the Bering Sea through the years for the existence of the temperature data time series and the reviewers for helping us to improve this manuscript.

Literature cited

Achilleos, G. A.
2011. The inverse distance weighted interpolation method and error propagation mechanism—creating a DEM from an analogue topographical map. J. Spat. Sci. 56:283–304.

Armistead, C. E., and D. G. Nichol.
1993. 1990 bottom trawl survey of the eastern Bering Sea continental shelf. NOAA Tech. Memo. NMFS-AFSC-7, 190 p.

Bivand, R. S., E. Pebesma, and V. Gómez-Rubio.
2013. Applied spatial data analysis with R, 405 p. Springer, New York.

Brown, J. H., J. F. Gillooly, A. P. Allen, V. M. Savage, and G. B. West.
2004. Toward a metabolic theory of ecology. Ecology 85:1771–1789.

Capotondi, A., M. Jacox, C. Bowler, M. Kavanaugh, P. Lehodey, D. Barrie, S. Brodie, S. Chaffron, W. Cheng, D. F. Dias, et al.
2019. Observational needs supporting marine ecosystems modeling and forecasting: from the global ocean to regional and coastal systems. Front. Mar. Sci. 6:00623.

Coachman, L. K.
1986. Circulation, water masses, and fluxes on the southeastern Bering Sea shelf. Cont. Shelf Res. 5:23–108.

Cokelet, E. D.
2016. 3-D water properties and geostrophic circulation on the eastern Bering Sea shelf. Deep-Sea Res., II 134:65–85.

Conner, J., and R. R. Lauth
2017. Results of the 2016 eastern Bering Sea continental shelf bottom trawl survey of groundfish and invertebrate resources. NOAA Tech. Memo. NMFS-AFSC-352, 159 p.

Cooper, D., L. A. Rogers, and T. Wilderbuer.
2020. Environmentally driven forecasts of northern rock sole (*Lepidopsetta polyxystra*) recruitment in the eastern Bering Sea. Fish. Oceanogr. 29:111–121.

Danielson, S., L. Eisner, T. Weingartner, and K. Aagaard.
2011. Thermal and haline variability over the central Bering Sea shelf: seasonal and interannual perspectives. Cont. Shelf Res. 31:539–554.

Del Vecchio, S., E. Fantinato, G. Silan, and G. Buffa.
2019. Trade-offs between sampling effort and data quality in habitat monitoring. Biodivers. Conserv. 28:55–73.

Eisner, L. B., Y. I. Zuenko, E. O. Basyuk, L. L. Britt, J. T. Duffy-Anderson, S. Kotwicki, C. Ladd, and W. Cheng.
2020. Environmental impacts on walleye pollock (*Gadus chalcogrammus*) distribution across the Bering Sea shelf. Deep-Sea Res., II 181–182:104881.

Gräler, B., E. Pebesma, and G. Heuvelink.
2016. Spatio-temporal interpolation using gstat. R J. 8(1):204–218.

Grüss, A., J. Gao, J. T. Thorson, C. N. Rooper, G. Thompson, J. L. Boldt, and R. Lauth.
2020. Estimating synchronous changes in condition and density in eastern Bering Sea fishes. Mar. Ecol. Prog. Ser. 635:169–185.

Grüss, A., J. T. Thorson, C. C. Stawitz, J. C. P. Reum, S. K. Rohan, and C. L. Barnes.
2021. Synthesis of interannual variability in spatial demographic processes supports the strong influence of cold-pool extent on eastern Bering Sea walleye pollock (*Gadus chalcogrammus*). Prog. Oceanogr. 194:102569.

Harvey, C. J., J. L. Fisher, J. F. Samhouri, G. D. Williams, T. B. Francis, K. C. Jacobson, Y. L. deReynier, M. E. Hunsicker, and N. Garfield.
2020. The importance of long-term ecological time series for integrated ecosystem assessment and ecosystem-based management. Prog. Oceanogr. 188:102418.

Hijmans, R. J.
2020. Raster: geographic data analysis and modeling. R package, vers. 3.3–13. [Available from website, accessed July 2020.]

Hollowed, A. B., K. K. Holsman, A. C. Haynie, A. J. Hermann, A. E. Punt, K. Aydin, J. N. Ianelli, S. Kasperski, W. Cheng, A. Faig, et al.
2020. Integrated modeling to evaluate climate change impacts on coupled social-ecological systems in Alaska. Front. Mar. Sci. 6:00775.

Holsman, K. K., J. Ianelli, K. Aydin, A. E. Punt, and E. A. Moffitt.
2016. A comparison of fisheries biological reference points estimated from temperature-specific multi-species and single-species climate-enhanced stock assessment models. Deep-Sea Res., II 134:360–378.

Hood, D. W., and J. A. Calder (eds.).
1981. The eastern Bering Sea shelf: oceanography and resources, vol. 1, 625 p. Off. Mar. Pollut. Assess., NOAA, Seattle, WA.

Hughes, B. B., R. Beas-Luna, A. K. Barner, K. Brewitt, D. R. Brumbaugh, E. B. Cerny-Chipman, S. L. Close, K. E. Coblentz, K. L. de Nesnera, S. T. Drobnitch, et al.
2017. Corrigendum: long-term studies contribute disproportionately to ecology and policy. BioScience 67:271–281.

ICES (International Council for the Exploration of the Sea).
2020. ICES workshop on unavoidable survey effort reduction (WKUSER). ICES Sci. Rep. vol. 2, issue 72, 92 p. [Available from website.]

Kearney, K., A. Hermann, W. Cheng, I. Ortiz, and K. Aydin.
2020. A coupled pelagic–benthic–sympagic biogeochemical model for the Bering Sea: documentation and validation of the BESTNPZ model (v2019.08.23) within a high-resolution regional ocean model. Geosci. Model Dev. 13:597–650.

Kinder, T. H., and J. D. Schumacher.
1981. Hydrographic structure over the continental shelf of the southeastern Bering Sea. *In* The eastern Bering Sea shelf: oceanography and resources, vol. 1 (D. W. Hood and J. A. Calder, eds.), p. 31–52. Off. Mar. Pollut. Assess., NOAA, Seattle, WA.

Kooijman, S. A. L. M.
2000. Dynamic energy and mass budgets in biological systems, 424 p. Cambridge Univ. Press, Cambridge, UK.

Kotwicki, S., and R. R. Lauth.
2013. Detecting temporal trends and environmentally-driven [sic] changes in the spatial distribution of bottom fishes and crabs on the eastern Bering Sea shelf. Deep-Sea Res., II 94:231–243.

Liu, Y., Y. Chen, J. Cheng, and J. Lu.
2011. An adaptive sampling method based on optimized sampling design for fishery-independent surveys with comparisons with conventional designs. Fish. Sci. 77:467–478.

Loughlin, T. R., and K. Ohtani (eds.).
1999. Dynamics of the Bering Sea. Alsk. Sea Grant Rep. AK-SG-99-03, 838 p. Univ. Alsk. Sea Grant, Fairbanks, AK.

Mueter, F. J., and M. A. Litzow.
2008. Sea ice retreat alters the biogeography of the Bering Sea continental shelf. Ecol. Appl. 18:309–320.

Nichol, D. G., S. Kotwicki, T. K. Wilderbuer, R. R. Lauth, and J. N. Ianelli.
2019. Availability of yellowfin sole *Limanda aspera* to the eastern Bering Sea trawl survey and its effect on estimates of survey biomass. Fish. Res. 211:319–330.

Overland, J. E., M. Wang, and T. J. Ballinger.
2018. Recent increased warming of the Alaskan marine Arctic due to midlatitude linkages. Adv. Atmos. Sci. 35:75–84.

Oyafuso, Z. S., L. A. K. Barnett, and S. Kotwicki.
2021. Incorporating spatiotemporal variability in multispecies survey design optimization addresses trade-offs in uncertainty. ICES J. Mar. Sci. 78:1288–1300.

Pebesma, E.
2018. Simple features for R: standardized support for spatial vector data. R J. 10(1):439–446.

Pebesma, E. J., and R. S. Bivand.
2005. Classes and methods for spatial data in R. R News 5(2):9–13.

Poloczanska, E. S., M. T. Burrows, C. J. Brown, J. García Molinos, B. S. Halpern, O. Hoegh-Guldberg, C. V. Kappel, P. J. Moore, A. J. Richardson, D. S. Schoeman, et al.
2016. Responses of marine organisms to climate change across oceans. Front. Mar. Sci. 3:00062.

R Core Team.
2020. R: a language and environment for statistical computing. R Foundation for Statistical Computing, Vienna, Austria. [Available from website, accessed February 2020.]

Rohan, S. K., L. A. K. Barnett, and N. Charriere.
2022. Evaluating approaches to estimating mean temperature and cold pool area from Alaska Fisheries Science Center bottom trawl surveys of the eastern Bering Sea. NOAA Tech. Memo. NMFS-AFSC-456, 42 p.

Rooper, C. N., I. Ortiz, A. J. Hermann, N. Laman, W. Cheng, K. Kearney, and K. Aydin.
2021. Predicted shifts of groundfish distribution in the Eastern Bering Sea under climate change, with implications for fish populations and fisheries management. ICES J. Mar. Sci. 78:220–234.

Siddon, E. (ed.).
2021. Ecosystem status report 2021. Eastern Bering Sea, 249 p. North Pac. Fish. Manage. Council, Anchorage. AK. [Available from website.]

Stabeno, P. J., and S. W. Bell.
2019. Extreme conditions in the Bering Sea (2017–2018): record-breaking low sea-ice extent. Geophys. Res. Lett. 46:8952–8959.

Stabeno, P. J., N. B. Kachel, S. E. Moore, J. M. Napp, M. Sigler, A. Yamaguchi, and A. N. Zerbini.
2012. Comparison of warm and cold years on the southeastern Bering Sea shelf and some implications for the ecosystem. Deep-Sea Res., II 65–70:31–45.

Stabeno, P. J., R. L. Thoman, and K. Wood
2019. Recent warming in the Bering Sea and its impact on the ecosystem. *In* Arctic report card 2019 (Richter-Menge, J., M. L. Druckenmiller, and M. Jeffries, eds.), p. 81–87. [Available from website.]

Stein, M. L.
1999. Interpolation of spatial data: Some theory for kriging, 249 p. Springer, New York.

Sukhotin, A., and V. Berger.
2013. Long-term monitoring studies as a powerful tool in marine ecosystem research. Hydrobiologia 706:1–9.

Sullivan, M. E., N. B. Kachel, C. W. Mordy, S. A. Salo, and P. J. Stabeno.
2014. Sea ice and water column structure on the eastern Bering Sea shelf. Deep-Sea Res., II 109:39–56.

Thorson, J. T.
2019. Measuring the impact of oceanographic indices on species distribution shifts: the spatially varying effect of cold-pool extent in the eastern Bering Sea. Limnol. Oceanogr. 64:2632–2645.

Thorson, J. T., J. N. Ianelli, and S. Kotwicki.
2017. The relative influence of temperature and size-structure on fish distribution shifts: a case-study on Walleye pollock in the Bering Sea. Fish Fish. 18:1073–1084.
Uchiyama, T., F. J. Mueter, and G. H. Kruse.
2020. Multispecies biomass dynamics models reveal effects of ocean temperature on predation of juvenile pollock in the eastern Bering Sea. Fish. Oceanogr. 29:10–22.
Wyllie-Echeverria, T., and W. S. Wooster.
1998. Year-to-year variations in Bering Sea ice cover and some consequences for fish distributions. Fish. Oceanogr. 7:159–170.
Zador, S., and E. Siddon (eds.).
2016. Ecosystem considerations 2016. Status of the eastern Bering Sea ecosystem, 205 p. North Pac. Fish. Manage. Council, Anchorage, AK. [Available from website.]
Zador, S. G., K. K. Holsman, K. Y. Aydin, and S. K. Gaichas.
2016. Ecosystem considerations in Alaska: the value of qualitative assessments. ICES J. Mar. Sci. 74:421–430.

National Marine
Fisheries Service
NOAA

Fishery Bulletin
established in 1881

Spencer F. Baird
First U.S. Commissioner
of Fisheries and founder
of *Fishery Bulletin*

Development and use of a large, flexible antenna to detect fish implanted with passive integrated transponder tags

Matthew S. Morris[1]
Richard D. Ledgerwood[2]
Alexander J. Borsky[1]
Gabriel T. Brooks[2]
Paul J. Bentley[2]

Email address for contact author: mattmorris@oceanassoc.com

[1] Ocean Associates Inc.
Oceans and Fisheries Consulting
4007 North Abingdon Street
Arlington, Virginia 22207

[2] Fish Ecology Division
Northwest Fisheries Science Center
National Marine Fisheries Service, NOAA
2725 Montlake Boulevard East
Seattle, Washington 98112-2097

Abstract—A novel antenna design has been developed to detect fish implanted with full-duplex passive integrated transponder (PIT) tags. The antenna is constructed of lightweight flexible hose and measures 2.4 by 6.1 m, providing a substantially larger reading range than other PIT antennas. Herein, we describe its use in a small instream monitoring system to detect migrating smolts of steelhead (*Oncorhynchus mykiss*). During testing, the combined detection efficiency for the 2 arrays of antennas with the new design was 97%, which is comparable to efficiencies of standard antennas made with polyvinyl chloride or high-density polyethylene. The lightweight, flexible design of the new antenna affords relatively easy transportation and deployment compared with that of rigid antennas, and smaller crews and vessels are needed for its maintenance and deployment. The development of the flexible antenna has expanded the utility of PIT technology by increasing the scope of potential sampling applications to a wider range of habitats and environmental conditions.

Manuscript submitted: 28 March 2023.
Manuscript accepted: 14 August 2023.
Fish. Bull. 121:124–128 (2023).
Online publication date: 28 August 2023.
doi: 10.7755/FB.121.3.6

The views and opinions expressed or implied in this article are those of the author (or authors) and do not necessarily reflect the position of the National Marine Fisheries Service, NOAA.

Passive integrated transponder (PIT) technology has been used to study a variety of terrestrial and aquatic organisms since its adaptation from the livestock industry in the mid-1980s (Thomas et al., 1987; Jackson and Bünger, 1993; Mills et al., 1995; Ballard et al., 2001; Bubb et al., 2002). Because of its long life, low cost, and low biological impact, the PIT tag has become an important tool in fisheries research and is used in studies of migration timing, behavior, and survival, as well as in comparisons of return rates of smolts and adults (Prentice et al.[1]; Prentice et al., 1990; McCutcheon et al., 1994; Peterson et al., 1994; Ledgerwood et al., 2004). Numerous detection site configurations and antenna designs have been used for such work, and as the technology improves, new configurations and designs have been developed (Lucas et al., 1999; Hill et al., 2006; Bond et al., 2007; Riley et al., 2010).

Early PIT antennas could sample small areas and were limited largely by transceiver capability. Development of the multiplexing transceiver subsequently decreased the size and increased the capacity of transceivers, which now can power and communicate with multiple antennas; however, general antenna design and construction has changed minimally through the years. Instream PIT antennas are traditionally constructed by using 10.2-cm-diameter pipes of polyvinyl chloride (PVC) or high-density polyethylene. The rigidity of these materials allows easy anchoring to stream beds and shorelines, and the pipe diameter provides a large air gap around antenna wires to reduce electrical resistance in submersed applications;

[1] Prentice, E. F., C. W. Sims, and D. L. Park. 1985. A study to determine the biological feasibility of a new fish tagging system. Annual report 1984–1985. U.S. Dep. Energy, Bonneville Power Admin., BPA Rep. DOE/BP-11982-1, 39 p. [Available from website.]

however, these features also present challenges, including bulk, weight, reduced mobility, and cost.

Many challenges associated with rigid antennas can be mitigated by decreasing the overall antenna size. It is common for rigid rectangular antennas to be built with dimensions no larger than 1.2 by 2.4 m, a size that compromises sample area out of necessity. Most research would benefit from larger antennas and detection ranges that maximize both sample area and efficiency associated with antenna construction and use.

In 2012, we modified the rigid antenna design to use a new PIT transceiver and system (IS1001 reader and IS1001 Multiplexing Transceiver System[2], Biomark Inc., Boise, ID) more fully, with improved functionality and performance, for use in experimental stationary and towed applications, similar to the sampling method described by Ledgerwood et al. (2004). The resulting prototype antenna, described herein, was made with small-diameter flexible hose instead of rigid construction materials and increased antenna size to an area of 2.4 by 6.1 m.

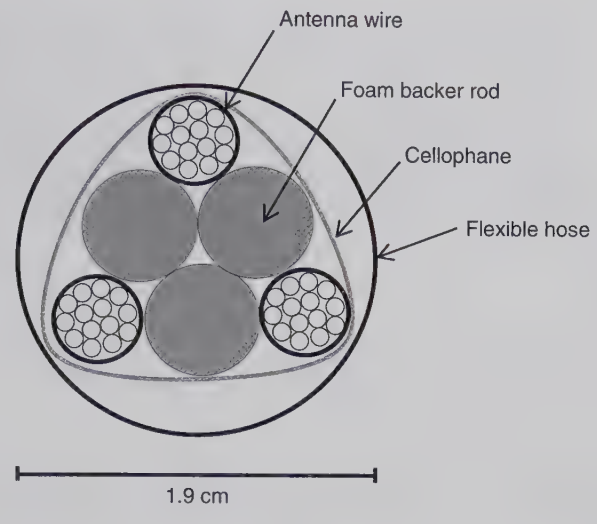

Figure 1

Cross-sectional view of the wire gallery of the flexible antenna developed to detect fish implanted with passive integrated transponder tags. Antenna wires (10 American Wire Gauge Litz wire) are placed between 3 foam backer rods (diameter: 6.5 mm) and wrapped in cellophane to hold the wires in position. The antenna is housed in a 1.9-cm-diameter, flexible PVC hose to create a waterproof barrier and to protect the wires from physical damage. This configuration was used in the antennas deployed for testing of their detection efficiency as part of a system to track migrating steelhead (*Oncorhynchus mykiss*) in Abernathy Creek, of Washington, in 2015.

Materials and methods

Antenna description

The IS1001 Multiplexing Transceiver System was used to power and communicate with the antennas. This system required a dedicated IS1001 reader for each antenna. To operate multiple antennas as an array, we used the multiplexing function of the IS1001 Master Controller (Biomark Inc.). According to the manufacturer, exciter circuitry on the transceiver system was designed to operate antennas as large as 1.2 by 6.1 m (Biomark Inc.[3]). However, after testing various components and configurations, we were able to construct an electronically stable 2.4-by-6.1-m antenna with the capability to detect all sizes of full-duplex PIT tags commonly used in the Columbia River Basin. To produce a detection field this large, we connected the IS1001 reader directly to the antenna windings to maximize current output.

The antenna was constructed by using 3 turns of 10-gauge Litz wire (American Wire Gauge type 5 × 5 × 44/40) with an inductance of 185 µH. To assemble the antenna, we first cut three 18-m sections of wire. Each wire was separated by a minimum of 6.5 mm by using three 6.5-mm-diameter foam backer rods glued together to form a triangle (Fig. 1). Antenna wires were placed in the indentations between backer rods, creating a triangular wire gallery. Cellophane was then wrapped around the wire gallery to maintain wire position.

Once wrapped, the wire gallery was threaded through a 1.9-cm-diameter, flexible PVC hose, which formed the antenna housing. Each end of the hose was then inserted into the reader enclosure (described later), where the turns were soldered together. Two 8200-pF capacitors were soldered in parallel to one of the terminal wires. Finally, both terminal ends of the windings of antenna wires were connected to the reader, along with bus cables for the power and communication of the controller area network (CAN). The enclosure was sealed for deployment, and waterproof connectors and CAN-bus cable were used to connect the reader to another IS1001 antenna in series or to the IS1001 Master Controller.

IS1001 reader enclosure

Underwater deployment required the design and fabrication of a watertight enclosure to house the IS1001 reader near the antenna wires. We designed an enclosure to be hydrodynamically stable and durable in a variety of deployment strategies. The enclosure was constructed in 3 sections for ease of assembly and to allow access to the reader (Fig. 2). Primary components of the enclosure were schedule-40 PVC, with the exception of the schedule-80 PVC end cap, which was drilled and tapped for 2 nylon, submersible, single-cord grips (P/N 69915K53, McMaster-Carr Supply Co., Elmhurst, IL). Wet-pluggable connectors (P/N MCIL-8-FS MP, Teledyne Technologies Inc.,

[2] Mention of trade names or commercial companies is for identification purposes only and does not imply endorsement by the National Marine Fisheries Service, NOAA.

[3] Biomark Inc. 2020. IS1001 reader standalone operation. User manual, rev. 11, 62 p. [Available from website.]

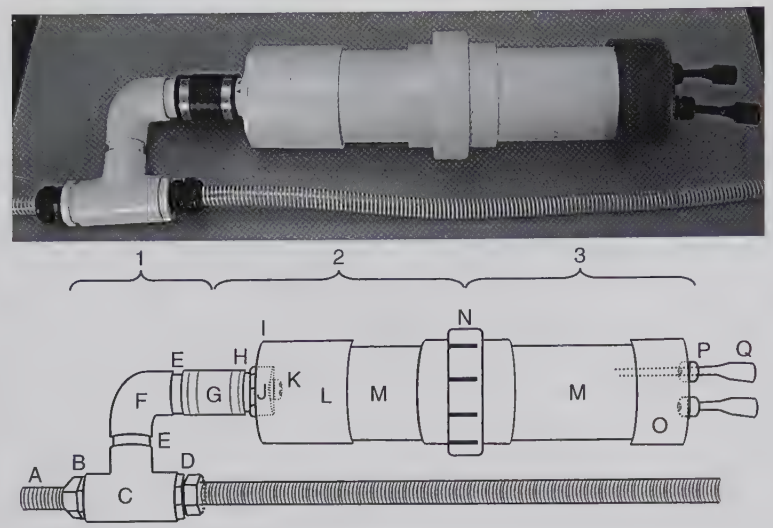

A 1.9-cm flex hose	G 5.1-cm rubber coupler	M 10.2-cm pipe
B 2.5-cm cable gland	H 5.1-by-3.8-cm reducer bushing	N 10.2-cm union
C 3.8-cm tee	I 10.2-by-5.1-cm reducer bushing	O 10.2-cm end cap
D 3.8-by-2.5-cm reducer bushing	J 3.8-by-1.3-cm reducer bushing	P 1.3-cm nylon single-cord grip
E 3.8-cm pipe	K 1.3-cm nylon double-cord grip	Q Waterproof connector
F 3.8-cm elbow	L 10.2-cm coupler	

Figure 2

Photograph and schematic of the enclosure used to house the IS1001 reader, capacitors, and terminal ends of the antenna wires. Components are schedule-40 PVC, except the end cap (O), which was schedule-80 PVC, and cord grips (B, K, and P). Sections 1–3 indicate the 3 removable sections of the capsule, with access points at a coupler (G) and union (N). Waterproof connectors (Q) provide power to the antenna reader and enable multiplexing and communication between antennas and the IS1001 Master Controller through the bus cable for the controller area network. This configuration was used in the antennas deployed for testing of their detection efficiency as part of a system to track migrating steelhead (*Oncorhynchus mykiss*) in Abernathy Creek, of Washington, in 2015.

Thousand Oaks, CA) were threaded through these cord grips and used to connect IS1001 readers and antennas to each other and to the IS1001 Master Controller. All power and communication to and from the reader and master controller traveled through CAN-bus cable.

The previously soldered antenna wire ends entered the lower section of the enclosure through nylon submersible cord grips (P/N 69915K71, McMaster-Carr Supply Co.) threaded into 2 sides of a PVC tee (Fig. 2, section 1). The tee covered these connections and allowed the 2 ends of the antenna loop to be threaded up through the top of the tee and into the main compartment of the enclosure, where it was connected to the reader (Fig. 2, section 2).

An internal multi-cord grip (P/N 7807K33, McMaster-Carr Supply Co.) was used to seal the entry point of antenna wires into the enclosure. This cord grip safeguarded against water intrusion and ensured compartmentalization in case of a water breach, minimizing potential damage to the reader. The second half of the main compartment allowed CAN-bus cables to enter the enclosure and connect to the reader (Fig. 2, section 3).

Once the antenna was constructed, frames of high tensile strength, made with rope of a small diameter that does not stretch, were used in all applications to relieve strain on antennas during deployment. The antenna was secured to the rope frame with cable ties placed at 0.3-m intervals, and plastic thimbles were spliced into the corners of the rope frame to connect multiple antennas to each other or to deployment structures.

Efficiency testing

Antenna efficiency was tested by deploying 3 flexible antennas (2.4 by 6.1 m) in Abernathy Creek, in Washington, prior to a release of hatchery-raised steelhead (*Oncorhynchus mykiss*) on 14 April 2015. Juvenile steelhead were reared and tagged with standard 12-mm PIT tags at the Abernathy Fish Technology Center, a hatchery of the U.S. Fish and Wildlife Service located 5 km from the mouth of the creek. All antennas were deployed in a single pool about 400 m downstream from the hatchery release site, where water velocity was approximately 0.6 m/s throughout.

One antenna was placed at the head of the pool and spanned the entire stream width (array 1). Two flexible antennas were required to span the pool at a second detection site (array 2), which was located 10 m downstream from array 1 and at the maximum water depth of the pool (1.8 m). None of the antennas were fully submerged for this test. Antennas were installed in a pass-through orientation by tying the top and bottom corners to trees and by using weights tied to short lanyards to anchor the bottom of the antennas to the stream bed. We used a Power Puller with a capacity of 2 metric tons (P/N 5541, Tekton Inc., Grand Rapids, MI) to increase tension on the top corners. Arrays were deployed for 45 h post release. In situ antenna efficiency and *combined efficiency* were then calculated as described by Zydlewki et al., (2006):

$$\text{In situ array 1: } E = (d_{\text{common to arrays 1+2}}) \times (d_{\text{unique to array 2}} + d_{\text{common to arrays 1 + 2}})^{-1};$$

$$\text{In situ array 2: } E = (d_{\text{common to arrays 1+2}}) \times (d_{\text{unique to array 1}} + d_{\text{common to arrays 1+2}})^{-1}; \text{ and}$$

$$\text{Combined: } E = 1 - [(1 - E_{\text{in situ array 1}}) \times (1 - E_{\text{in situ Array 2}})],$$

where E = efficiency, and
d = the number of tags decoded.

Results

A total of 300 steelhead implanted with PIT tags were released from Abernathy Fish Technology Center on 14 April 2015. Of these steelhead, 265 fish were detected with antennas located at the hatchery exit, and 85 fish were detected with the 3 flexible antennas deployed downstream. Our upstream antenna (array 1) detected 57 fish, and the 2 downstream antennas (array 2) detected 52 of those 57 fish over the 45-h test period, giving array 2 an efficiency of 91%. Array 2 detected 75 fish, and 52 of those 75 fish were previously detected on array 1, giving array 1 an efficiency of 69%. The combined efficiency of both arrays was 97%. Of the 265 fish detected on antennas at the hatchery exit, 187 fish were later detected at the creek mouth on an array operated by the U.S. Fish and Wildlife Service. The median travel time, from the hatchery exit to the mouth of the creek, of these fish was 21.2 d, and their median travel speed was 0.24 km/d.

Discussion

Our flexible antenna has become a versatile tool used to detect PIT-tagged fish in traditional instream environments. Its adaptability makes it useful in both traditional and innovative approaches to PIT interrogation, such as those in which antennas have been attached to pile dikes (Magie et al.[4]) and towed behind 2 vessels (Morris et al.[5]). In arriving at a final shape and size of a rectangular antenna with dimensions of 2.4 by 6.1 m, we tested different shapes—including circles, squares, trapezoids, and rectangles—and sizes up to 3.0 by 18.3 m. All testing was done in air at our sample station near Jones Beach, Oregon.

The results of testing with circles indicate that a circle is the least efficient shape. Circular antennas quickly lost current and, therefore, detection area as their diameter increased. Results for squares were similar as their length and width increased. The results of testing with rectangles indicate that a rectangle is the most efficient shape, with a narrow width helping to maintain the antenna field and a strong detection area even as their length increased. At some point, the length of rectangles became too great, and the detection area started to weaken. Trapezoids worked as long as the reader could continue to tune the antenna. However, again, a trapezoid was not the most efficient design, and results for this shape compare more closely to those from testing with circles. The shape and size of antenna at which we arrived, on the basis of our testing, produced a substantial detection area, much greater than that of the standard rigid antennas that have been used in the past, and the electronic field was strong enough to handle the depletion of antenna current when deployed in water. It also allowed the antenna to transform in shape by about 1 m in any direction and maintain its functionality.

In creating such a large antenna, our 2 biggest concerns were higher susceptibility to electromagnetic interference and frequency of tag-code collisions due to large numbers of tagged fish entering the antenna field at the same time. As testing progressed, we found that electromagnetic interference was not a deterrent for any of our installations, but given the individual array efficiencies, tag collision was likely present.

Array efficiencies of 69% and 91% at Abernathy Creek indicate that tag collisions might have occurred during periods of high tag density. It is also possible that poor tag orientation contributed to missed detections as the fish moved through the detection field. These are the likely explanations for the lower efficiency of array 1 compared with that of array 2. Array 1 was a single antenna, whereas array 2 was composed of 2 antennas and therefore had more area for fish to pass through without causing tag collisions. River width and associated flow dynamics also may have contributed to suboptimal tag orientation as fish approached array 1. Further, our efficiency estimates may have been biased low, given the long travel times of fish exiting Abernathy Creek. It is also possible that 4 of the 5 fish detected on array 1 and missed on array 2 passed the first antenna and remained at the head of the pool, never reaching the second array during the test period. Of these 4 missed fish, 3 steelhead had travel times to the mouth of the creek that were well above the release group median (27, 28, and 35 d), and 2 fish were detected on the morning of system removal. Regardless of these unknowns, our estimated efficiency is comparable to that estimated for other PIT antennas that detect fish migrating downstream (Aymes and Rives, 2009; Zydlewski et al., 2006). Additionally, the combined array efficiency of 97% indicates the importance of redundancy for instream installations.

The results of the efficiency test also indicate the versatility of the antenna in a traditional instream application. Installing the system took only 3 h, and the weights used to maintain antenna orientation on the substrate remained stable during testing. Although this deployment was for only 2 d, the ability of the flexible antenna to conform to the streambed, as well as its relatively small diameter,

[4] Magie, R. J., M. S. Morris, J. P. Bender, B. F. Jonasson, B. P. Sandford, and R. D. Ledgerwood. 2015. Development of a passive integrated transponder (PIT) tag detection system for adult salmonids in the lower Columbia River, 2013, 33 p. Fish Ecol. Div., Northwest Fish. Sci. Cent., Natl. Mar. Fish. Serv., Seattle, WA. [Available at website.]

[5] Morris, M. S., A. J. Borsky, P. J. Bentley, L. N. Webb, and B. P. Sandford. 2017. Detection of PIT-tagged juvenile salmonids migrating in the Columbia River estuary, 2016, 45 p. Contract report to the Bonneville Power Administration, U.S. Department of Energy (contract no. 46273 RL58; project no. 1993-029-00). Fish Ecol. Div., Northwest Fish. Sci. Cent., Natl. Mar. Fish. Serv., Seattle, WA. [Available at website.]

resulted in less drag and buoyancy in the water than we have observed in similar stream deployments of rigid antennas. Although the flexible antenna was less likely to become disoriented in strong currents, larger weights and more permanent anchors should be used for long-term installations and at sites where water levels and velocities change throughout the year. Pass-over configurations in which flexible antennas are used are also a feasible option.

We tested various components and materials to address the challenges associated with rigid antennas, mainly bulk, weight, reduced mobility, and cost. The resulting antenna design covered a large detection area, and its lightweight construction and flexibility increased utility. Elements of this design are now available commercially, in part because the antenna is adaptable to a wide range of geographic locations, environmental conditions, and freshwater habitats. Installations of flexible antenna arrays for detection of PIT-tagged fish offer considerable potential to advance our understanding of stock-specific differences in behavior, migration timing, and survival, as well as to improve evaluations of restoration and recovery efforts for threatened and endangered species.

Resumen

Se ha desarrollado un novedoso diseño de antena para detectar peces implantados con etiquetas "full duplex" de transmisor pasivo integrado (PIT). La antena está fabricada con manguera flexible ligera y mide 2.4 por 6.1 m, lo que proporciona un alcance de lectura sustancialmente mayor que el de otras antenas PIT. En este artículo se describe su uso en un pequeño sistema de monitoreo para detectar la migración de la trucha arcoiris (*Oncorhynchus mykiss*). Durante las pruebas, la eficacia de detección combinada de los dos conjuntos de antenas con el nuevo diseño fue del 97%, comparable a las antenas estándar fabricadas con cloruro de polivinilo o polietileno de alta densidad. El diseño ligero y flexible de la nueva antena permite transportarla y desplegarla con relativa facilidad en comparación con las antenas rígidas, y para su mantenimiento y despliegue se necesitan tripulaciones y embarcaciones más reducidas. El desarrollo de la antena flexible ha ampliado la utilidad de la tecnología PIT al aumentar el alcance de las posibles aplicaciones de muestreo a una gama más amplia de hábitats y condiciones ambientales.

Acknowledgments

We would like to thank all the vessel operators and deckhands for their tireless support of our work, Biomark Inc. for their technical support, the staff of the U.S. Fish and Wildlife Service Abernathy Fish Technology Center for assisting with the efficiency tests, B. Jonasson for sharing his electronics expertise, and the National Marine Fisheries Service West Coast Region, Bonneville Power Administration, and U.S. Army Corps of Engineers for funding various elements of the development of the antenna.

Literature cited

Aymes, J. C., and J. Rives.
2009. Detection efficiency of multiplexed passive integrated transponder antennas is influenced by environmental conditions and fish swimming behavior. Ecol. Freshw. Fish 18:507–513.

Ballard, G., D. G. Ainley, C. A. Ribic, and K. R. Barton.
2001. Effect of instrument attachment and other factors on foraging trip duration and nesting success of Adélie Penguins. Condor 103:481–490.

Bond, M. H., C. V. Hanson, R. Baertsch, S. A. Hayes, and R. B. MacFarlane.
2007. A new low-cost instream antenna system for tracking passive integrated transponder (PIT)-tagged fish in small streams. Trans. Am. Fish. Soc. 136:562–566.

Bubb, D. H., M. C. Lucas, T. J. Thom, and P. Rycroft.
2002. The potential use of PIT telemetry for identifying and tracking crayfish in their natural environment. Hydrobiologia 483:225–230.

Hill, M. S., G. B. Zydlewski, J. D. Zydlewski, and J. M. Gasvoda.
2006. Development and evaluation of portable PIT tag detection units: PITpacks. Fish. Res. 77:102–109.

Jackson, D. H., and W. H. Bünger.
1993. Evaluation of passive integrated transponders as a marking technique for turkey poults. J. Iowa Acad. Sci. 100:60–61.

Ledgerwood, R. D., B. A. Ryan, E. M. Dawley, E. P. Nunnallee, and J. W. Ferguson.
2004. A surface trawl to detect migrating juvenile salmonids tagged with passive integrated transponder tags. North Am. J. Fish. Manag. 24:440–451.

Lucas, M. C., T. Mercer, J. D. Armstrong, S. McGinty, and P. Rycroft.
1999. Use of a flat-bed passive integrated transponder antenna array to study the migration and behavior of lowland river fishes at a fish pass. Fish. Res. 44:183–191.

McCutcheon, C. S., E. F. Prentice, and D. L. Park.
1994. Passive monitoring of migrating adult steelhead with PIT tags. North Am. J. Fish. Manag. 14:220–223.

Mills, M. S., C. J. Hudson, and H. J. Berna.
1995. Spatial ecology and movements of the brown water snake (*Nerodia taxispilota*). Herpetologica 51:412–423.

Peterson, N. P., E. F. Prentice, and T. P. Quinn.
1994. Comparison of sequential coded wire and passive integrated transponder tags for assessing overwinter growth and survival of juvenile coho salmon. North Am. J. Fish. Manag. 14:870–873.

Prentice, E. F., T. A. Flagg, and C. S. McCutcheon.
1990. Feasibility of using implantable passive integrated transponder (PIT) tags in salmonids. Am. Fish. Soc. Symp. 7:317–322.

Riley, W. D., A. T. Ibbotson, W. R. C. Beaumont, P. Rycroft, and A. C. Cook.
2010. A portable, cost effective, pass-through system to detect downstream migrating salmonids marked with 12 mm passive integrated transponder tags. Fish. Res. 101:203–206.

Thomas, J. A., L. H. Cornell, B. E. Joseph, T. D. Williams, and S. Dreischman.
1987. An implanted transponder chip used as a tag for sea otters (*Enhydra lutris*). Mar. Mamm. Sci. 3:271–274.

Zydlewski, G. B., G. Horton, T. Dubreuil, B. Letcher, S. Casey, and J. Zydlewski.
2006. Remote monitoring of fish in small streams: a unified approach using PIT tags. Fisheries 31:492–502.

National Marine Fisheries Service
NOAA

Fishery Bulletin
established in 1881

Spencer F. Baird
First U.S. Commissioner of Fisheries and founder of *Fishery Bulletin*

Recruitment of juvenile Atlantic sturgeon (*Acipenser oxyrinchus oxyrinchus*) in the Savannah, Ogeechee, and Satilla Rivers in Georgia

Adam G. Fox (contact author)[1]
Michael A. Baker[1]
Alexander J. Cummins[1,2]
Hudman S. Evans Jr.[1,3]
Katherine L. Cummins[1,4]
Nathaniel Q. Hancock[1,5]
David L. Higginbotham[1]

Email address for contact author: agfox@uga.edu

[1] Warnell School of Forestry and Natural Resources
University of Georgia
180 East Green Street
Athens, Georgia 30602-2152

[2] Wildlife Resources Division
Georgia Department of Natural Resources
130 Hatchery Drive
Richmond Hill, Georgia 31324

[3] Wildlife Management Division
Arizona Game and Fish Department
1970 North Page Springs Road
Cornville, Arizona 86325

[4] Technical Regional Execution Center
South Atlantic Division
U.S. Army Corps of Engineers
100 West Oglethorpe Avenue
Savannah, Georgia 31401

[5] North Carolina Division of Marine Fisheries
100 Kitty Hawk Lane
Elizabeth City, North Carolina 27909

Abstract—The Atlantic sturgeon (*Acipenser oxyrinchus oxyrinchus*) is a anadromous fish found along the east coast of North America and is listed under the Endangered Species Act of the United States. Decades of overfishing and habitat degradation have caused range-wide population declines, and the population status of this species in many rivers is unclear. Quantifying annual recruitment is one way to assess the status of sturgeon populations, but such assessments are few. The objective of this study was to quantify recruitment of juvenile Atlantic sturgeon in the Savannah, Ogeechee, and Satilla Rivers in Georgia. Because we used identical methods in 3 rivers simultaneously, we were able to directly compare recruitment among these populations with that of other populations observed in contemporaneous studies in other rivers. We conducted mark-recapture sampling during 2014–2017 and used Huggins closed population models to estimate annual recruitment. Because there are no historical data for comparison, we evaluated the 3 populations in terms of recruit abundance, variation, and consistency. The Savannah River annually had relatively large numbers of recruits (639–937 individuals). Fewer recruits were produced in the Ogeechee (27–57 individuals) and Satilla (51–134 individuals) Rivers; recruitment occurred in only some years in those rivers. Populations that produce few recruits or do not have regular recruitment may be experiencing bottlenecks preventing recovery.

Manuscript submitted 20 September 2022.
Manuscript accepted 24 August 2023.
Fish. Bull. 121:129–140 (2023).
Online publication date: 1 September 2023.
doi: 10.7755/FB.121.3.7

The views and opinions expressed or implied in this article are those of the author (or authors) and do not necessarily reflect the position of the National Marine Fisheries Service, NOAA.

The Atlantic sturgeon (*Acipenser oxyrinchus oxyrinchus*) inhabits the rivers and coastal waters of eastern North America from the St. Lawrence River in Canada to the St. Johns River in Florida. Five distinct population segments (DPSs) of this species have been listed as threatened or endangered under the Endangered Species Act of the United States since 2012 (Federal Register, 2012), and in the United States, these DPSs, based on geographic, genetic, and ecological factors, are independently managed (ASSRT, 2007). For each DPS, genetically distinct spawning populations have been found in one or more rivers (Wirgin et al., 2000; Grunwald et al., 2008). Although this species has now been protected from harvest for over 2 decades, no information indicates that any populations of this species are recovering. The species continues to face other threats, including restriction of spawning habitat due to impoundments in some rivers (ASSRT, 2007), bycatch (Collins et al., 1996), ship strikes (Brown and Murphy, 2010), and dredging (Smith and Clugston, 1997; Winger et al., 2000). Spawning populations of Atlantic sturgeon are currently present in fewer than 30 rivers (Hilton et al., 2016).

Atlantic sturgeon are anadromous: adults generally inhabit marine waters but return to their natal rivers to spawn (Vladykov and Greeley, 1963; Scott and Crossman, 1973). Upon hatching, larvae begin a gradual downstream migration, eventually settling in the upper estuary as river-resident juveniles (RRJs). During their first ~2 years of life, RRJs remain in the freshwater and brackish habitat below the head of tide in their natal river (Bain, 1997). Between the ages of 2 and 4, individuals begin to migrate to

coastal marine habitats and enter the life stage of marine-migratory juveniles (Bain, 1997; Fox and Peterson, 2019). Marine-migratory juveniles reside in nearshore waters until they mature, although they may return to natal or non-natal estuarine or riverine habitats for prolonged periods during this life stage (Dovel and Berggren, 1983; Bain, 1997).

The highly migratory life history of the Atlantic sturgeon makes it difficult to quantify abundance. Adults and marine-migratory juveniles are highly dispersed in marine waters, and not all adults in a population return to their natal river to spawn every year. River-resident juveniles, however, remain in their natal river until at least age 2 (Fox and Peterson, 2019), and their abundance can be estimated by using mark-recapture methods. In several recent studies, such as those in the Delaware River (Hale et al., 2016), the Savannah River (Bahr and Peterson, 2016), and the Altamaha River, also located in Georgia (Schueller and Peterson, 2010; Baker et al., 2023), abundance of the age-1 cohort has been estimated to quantify annual recruitment in those systems. Although the National Marine Fisheries Service has identified recruitment estimates as a key research need to aid species recovery (ASSRT, 2007), assessments are currently lacking for many other populations in other rivers.

The South Atlantic DPS extends from South Carolina to Florida and comprises populations in 8 rivers at the southern part of the range of this species (ASSRT, 2007). The population in the Altamaha River has been identified as one of the most robust in both the South Atlantic DPS and the entire range (ASSRT, 2007; Schueller and Peterson, 2010). Baker et al. (2023) estimated that the Altamaha River had up to 3839 age-1 recruits per year during 2008–2020 and reported that recruitment was highly variable in this river. The Savannah River appears to host a smaller but still robust population—Bahr and Peterson (2016) reported annual recruitment estimates of up to 597 fish for the period 2013–2015. Recruitment of populations of Atlantic sturgeon in the nearby Ogeechee and Satilla Rivers has not been assessed since the species was listed. The objective of this study was to quantify the contemporaneous annual recruitment of juvenile Atlantic sturgeon in the Savannah, Ogeechee, and Satilla Rivers. The expectation was that these concurrent quantitative data would close a data gap identified by the National Marine Fisheries Service and allow direct comparison of the annual recruitment of Atlantic sturgeon throughout the state of Georgia and among the populations that make up much of the South Atlantic DPS.

Materials and methods

Study sites

This study was conducted in the estuaries of 3 coastal rivers in Georgia (Fig. 1). The Savannah River delineates the border between Georgia and South Carolina and is one of the most anthropogenically altered rivers within the range of the Atlantic sturgeon (Pearlstine et al.[1]). It originates in the southeastern Appalachian Mountains and is impounded by 3 dams as it flows 484 km to the Atlantic Ocean. The Ogeechee River flows unimpounded for 390 km from the Piedmont province of Georgia to the Atlantic Ocean; its mouth lies approximately 28 km south of the mouth of the Savannah River. Because of its tannic, nutrient-poor water, the Ogeechee River is classified as a blackwater river, although its pH is closer to neutral than other blackwater systems (Meyer et al., 1997). During the summer months, low flows and hypoxic conditions are common throughout the Ogeechee River estuary (ASSRT, 2007; Farrae et al., 2014). The blackwater Satilla River lies approximately 100 km south of the Ogeechee River and is situated entirely within the coastal plain of Georgia. This 320-km river is unimpounded, but hypoxic conditions have been widespread in the tidally influenced areas of the river during summer months (Fritts, 2011).

Sampling of Atlantic sturgeon

Sampling was conducted below the head of tide in each river system. Data collection in the Savannah River occurred in 2016 and 2017, and sampling in the Ogeechee and Satilla Rivers took place during 2014–2017. In all rivers, netting was conducted on weekdays (weather and tides permitting) between May and August. Atlantic sturgeon were captured with anchored monofilament gill and trammel nets designed to capture juveniles; all nets were 91.4 m long and 3.1 m deep. Gill nets comprised 3 randomly ordered panels of equal length and made of 7.6-, 10.2-, and 15.3-cm (stretch measure) mesh. Trammel nets comprised a 7.6-cm mesh inner panel enclosed by two 30.5-cm mesh outer panels. Nets were deployed within the main channels of the rivers for periods of 30–90 min around slack tides; a typical sample included the catch of 2 gill nets and 1 trammel net. Some of the sampling locations were sites used in previous studies (e.g., Schueller and Peterson, 2010; Farrae et al., 2014; Bahr and Peterson, 2016), and other locations were new sites with similar characteristics (e.g., deeper areas with limited woody debris).

Each captured Atlantic sturgeon was measured to the nearest millimeter in total length (TL) and fork length (FL) and inspected for tags. If no tag was present, a passive integrated transponder tag was injected under the fourth dorsal scute. For a subset of juveniles, we also collected a section (~0.5–1 cm) of the left pectoral-fin spine from near the base of the spine by using a scalpel, wire cutter, or small hacksaw. For fish caught in the Savannah and Ogeechee Rivers, spine samples were collected from the

[1] Pearlstine, L. R., R. Bartleson, W. Kitchens, and P. Latham. 1989. Lower Savannah River hydrological characterization. Univ. Fla., Fla. Coop. Fish Wildl. Res. Unit, Tech. Rep. 35, 139 p. [Available from Fla. Coop. Fish Wildl. Res. Unit, Dep. Wildl. Ecol. Conserv., Univ. Fla., Bldg. 106, 2295 Mowry Rd., P.O. Box 110485, Gainesville, FL 32611-0485.]

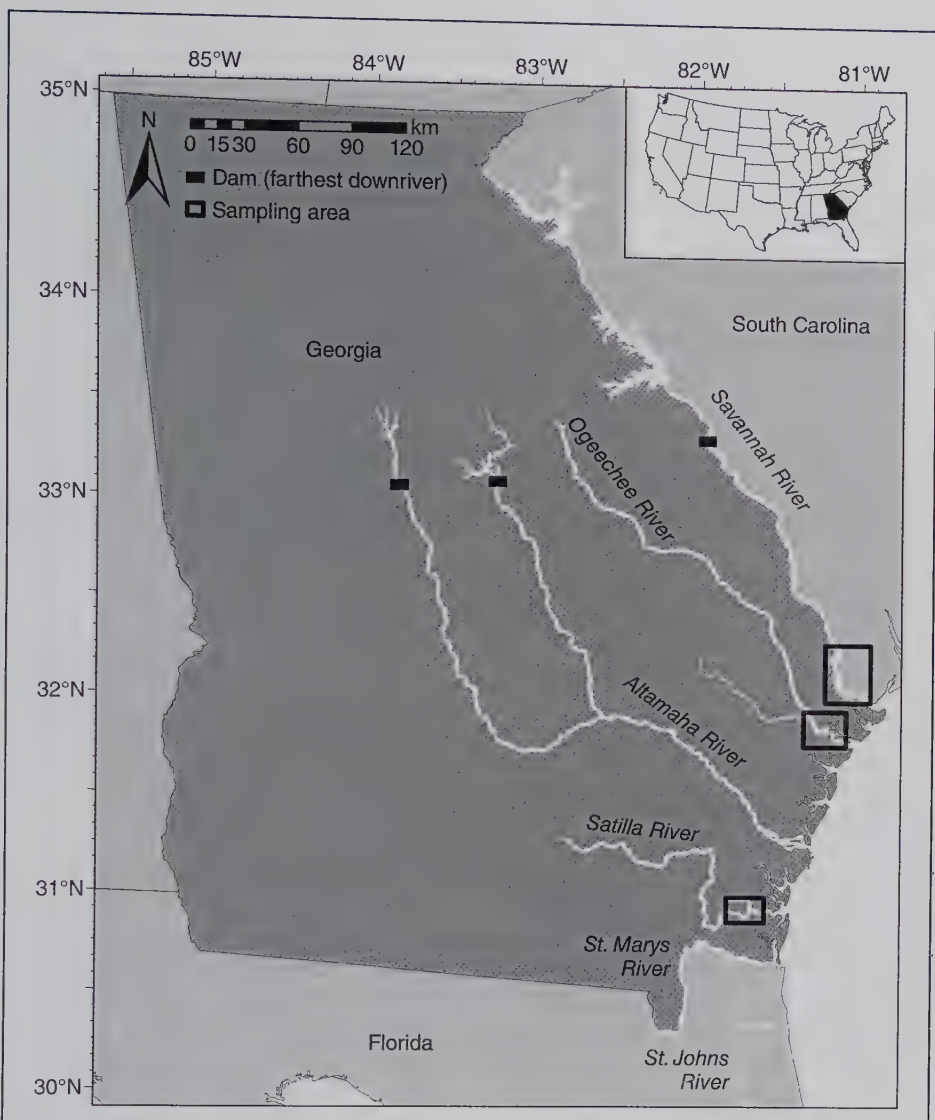

Figure 1

Map showing the locations of areas where Atlantic sturgeon (*Acipenser oxyrinchus oxyrinchus*) were sampled in rivers of Georgia between May and August during 2014–2017. Sampling with gill and trammel nets occurred in the estuaries of the Savannah, Ogeechee, and Satilla Rivers.

first 5 fish captured in each preselected size bin: <299 mm TL, 50-mm intervals from 300 to 700 mm TL, and 100-mm intervals from 700 to 1000 mm TL.

Age determination

We constructed a length–frequency histogram of the entire catch for each sampling year in each river. The modal distribution of juveniles depicted in each length–frequency histogram was used to assign ages to fish on the basis of length (Schueller and Peterson, 2010; Bahr and Peterson, 2016). We examined pectoral-fin spines and counted alternating light and dark rings (Baremore and Rosati, 2014) to validate the age assignments of a subset of individuals caught in the Savannah and Ogeechee Rivers; we did not use fin spines to evaluate age assignments for fish from the Satilla River in this study. Samples of pectoral-fin spines were air dried for at least 2 months and then sectioned with a low-speed saw. The sections were mounted to glass microscope slides and photographed at 1.6× magnification with a digital camera attached to a dissecting microscope. Three (and occasionally 4) independent readers aged each fin-spine section by counting annuli. Readers were trained by someone with numerous years of experience in aging hard structures in fish. Disagreements were settled by group consensus. If readers could not agree, that sample was removed from the analysis.

Recruitment estimation

For each river and year, we divided the sampling period into weekly sampling occasions and constructed capture histories for each individual fish. We then used Huggins models that estimate capture probabilities for closed populations (Huggins, 1989) in the package RMark (vers. 2.2.7; Laake[2]) in statistical software R (vers. 4.2.1; R Core Team, 2022) to estimate the abundance of age-1 juveniles in each year of the study for each river (Schueller and Peterson, 2010; Bahr and Peterson, 2016). The assumptions for our models were that 1) the population was closed to births, deaths, emigration, and immigration during the sampling period, 2) the probability of recapture did not change after initial capture, 3) individuals could randomly disperse in between capture events, 4) individuals were correctly identified, and 5) no tag loss occurred during the sampling period (Conroy and Carroll, 2009). Results from a concurrent telemetry study in the Ogeechee, Altamaha, and Satilla Rivers (Fox and Peterson, 2019) indicate that age-1 individuals typically remained within the study sites and did not leave their natal rivers during the summer sampling periods, supporting the assumption of closure. Additionally, occasional sampling upriver and downriver from the study sites did not result in the capture of any Atlantic sturgeon. Within each year, the weekly sampling periods presumably allowed adequate time for random mixing of marked and unmarked fish between each successive week of sampling.

We developed a suite of candidate models to obtain estimates of juvenile abundance. In the most basic model, a constant capture probability is assumed, and in other models variable capture probability is assumed, by age (as assigned by length–frequency analysis), by weekly sampling occasion, and by additive and interactive combinations of these covariates. The relative likelihood of each model was then assessed by using Akaike information criterion (AIC) (Akaike, 1973; Hurvich and Tsai, 1989) with an adjustment for small sample size (AICc) (Burnham and Anderson, 2002). The most plausible model from the candidate set was selected for estimating abundance in each study year.

To compare populations, we calculated the percentage of study years in each river for which we were able to estimate recruitment and the percentage of years in which we observed age-1 sturgeon. We calculated the mean annual recruitment in each population, as well as the standard deviation (SD) and coefficient of variation (CV) of recruitment, for all years of the study period. In these calculations, recruitment was considered to be zero if an estimate could not be obtained because of no observations of age-1 sturgeon. In cases where recruitment could not be estimated because of a lack of recaptured age-1 fish, recruitment was considered *not available* and the population in that river and year was omitted from calculations of mean annual recruitment and the associated SD and CV.

This study was conducted under National Marine Fisheries Service permits 16482 and 17861 and approved by the University of Georgia Institutional Animal Care and Use Committee.

Results

Sampling of Atlantic sturgeon

During this study, we set 1972 nets, for a total of 1366 h of sampling effort (Table 1). We captured 1336 Atlantic sturgeon with FLs of 182–1945 mm (Fig. 2). Across all rivers and all years, 280 fish were recaptured. In the Savannah River, annual catch varied from 350 to 497 individuals (mean: 423.2 individuals [SD 104.9]), and we marked 847 fish. In the Ogeechee River, we marked 270 Atlantic sturgeon, and annual catch varied from 18 to 105 fish (mean: 71.5 individuals [SD 38.7]). In the Satilla River, we marked

[2] Laake, J. 2013. RMark: an R interface for analysis of capture-recapture data with MARK. Alaska Fish. Sci. Cent., AFSC Processed Rep. 2013-01, 25 p. [Available from website.]

Table 1

Effort and catch during sampling of Atlantic sturgeon (*Acipenser oxyrinchus oxyrinchus*) in 3 coastal rivers of Georgia, the Savannah, Ogeechee, and Satilla Rivers, from May through August in 2014–2017. Effort is given as hours of net soak time; identical nets were used across all 3 rivers. Catch is given as the number of unique Atlantic sturgeon (ATS) and unique age-1 river-resident juveniles (RRJs) that were captured. NA=not applicable because sampling was conducted by Bahr and Peterson (2016).

	Savannah River			Ogeechee River			Satilla River		
Year	Effort (h)	ATS catch	RRJ catch	Effort (h)	ATS catch	RRJ catch	Effort (h)	ATS catch	RRJ catch
2014	NA	NA	NA	137	69	0	93	34	1
2015	NA	NA	NA	175	105	38	153	69	43
2016	253	497	310	156	94	21	168	84	8
2017	188	350	160	14	18	15	29	16	0

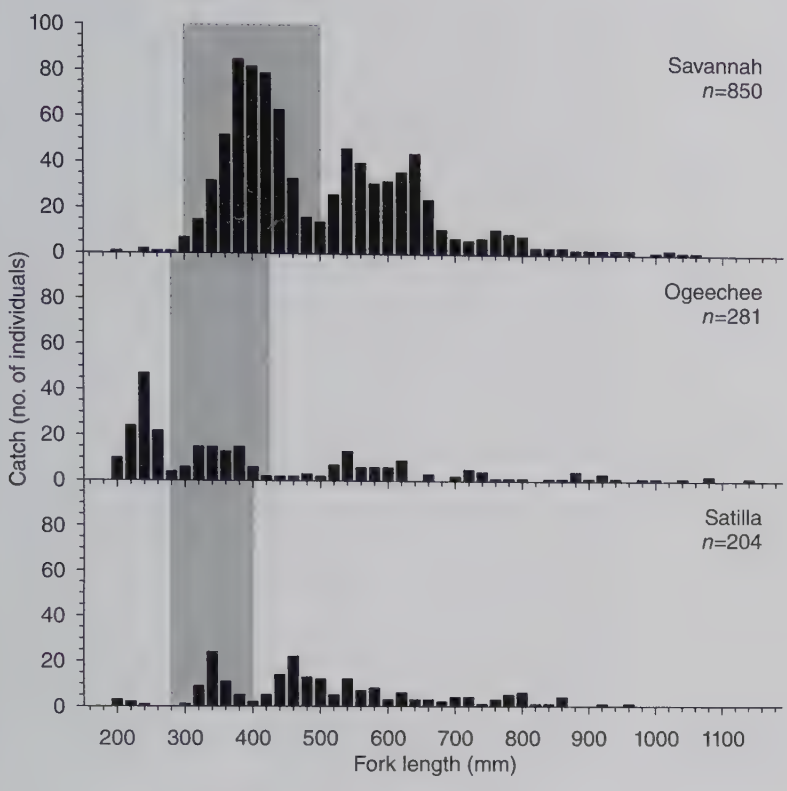

Figure 2

Length–frequency histograms for catch of juvenile Atlantic sturgeon (*Acipenser oxyrinchus oxyrinchus*) in the Savannah, Ogeechee, and Satilla Rivers in Georgia. Data are from sampling in the Savannah River from May through August in 2016 and 2017 and in the Ogeechee and Satilla Rivers from May through August in 2014–2017. Data include only the initial capture of each individual (number of samples [*n*] is provided on the graph for each river). Histograms are truncated to remove individuals over 1200 mm in fork length. The gray-shaded areas indicate the size ranges for age-1 Atlantic sturgeon.

196 individuals, and annual catch was 16–84 individuals (mean: 50.8 individuals [SD 31.2]).

Age determination

Across all rivers, we classified 596 fish as age-1 (Table 1). In the Savannah River, age-1 RRJs were 300–500 mm FL. In the Ogeechee and Satilla Rivers, age-1 RRJs were 280–420 mm FL and 280–400 mm FL, respectively. In the Savannah River, we captured age-1 fish in both 2016 and 2017. In the Ogeechee River, we captured at least 1 age-1 fish in each year during 2015–2017, but none were caught in 2014. In the Satilla River, we captured at least 1 age-1 fish in each year during 2014–2016, but none were caught in 2017. We evaluated the ages of 99 juveniles (<725 mm FL) captured from the Savannah and Ogeechee Rivers in 2015 and 2016. In all cases, initial reader-assigned ages were within 1 year of each other. Overall, readers reached a consensus on the ages of 94% of specimens, and the remaining 6% were removed from additional analysis. Our assigned ages (Fig. 3) largely aligned with the results of the length–frequency analysis. For instance, fin spines were collected from 15 fish captured in the Ogeechee River, and all 15 fish were classified as age 1 on the basis of both our length–frequency analysis and fin-spine analysis.

Recruitment estimation

Results from comparisons of AICc values indicate that the best Huggins closed capture model for estimating recruitment varied among rivers and years of this study (Suppl. Table) (online only). The *time* covariate was featured in the best model for 6 of the 7 combinations of year and river for which an estimate could be calculated. The *age* covariate was also featured in several of the best models as part of either an additive or interactive effect. We successfully estimated recruitment for most years in all 3 rivers (Table 2). Estimates of annual recruitment of age-1 Atlantic sturgeon in the Savannah River varied from a low of 639 individuals in 2017 to a high of 973 individuals in 2016 (Table 2). In the Ogeechee River, estimates of annual recruitment varied from a low of 27 individuals in 2016 to a high of 57 individuals in 2017; recruitment could not be estimated for 2014. In the Satilla River, estimates of annual recruitment varied from a low of 51 individuals in 2016 to a high of 134 individuals in 2015; recruitment could not be estimated for 2014 or 2017.

Discussion

The results of this study provide recruitment estimates for 3 populations of Atlantic sturgeon in the southernmost DPS within the range of this species. The best Huggins closed capture models we used to estimate recruit abundance in each year were similar to the best models used in other studies. For example, the best models used by Bahr and Peterson (2016) for estimating recruitment in all years featured *time* or a combination of *time* and *age* as covariates. We were able to compare our results to estimates from some prior studies conducted in each river.

For the Savannah River, Bahr and Peterson (2016) used Huggins closed capture models to estimate that the abundance of age-1 recruits in 2013–2015 was 528–597 fish per year. Our estimates for the 2 subsequent years indicate greater numbers of age-1 Atlantic sturgeon (973 fish in 2016 and 639 fish in 2017). Abundance of age-1 recruits may be increasing in the Savannah River, but more data are needed to confirm this trend. For the Ogeechee River,

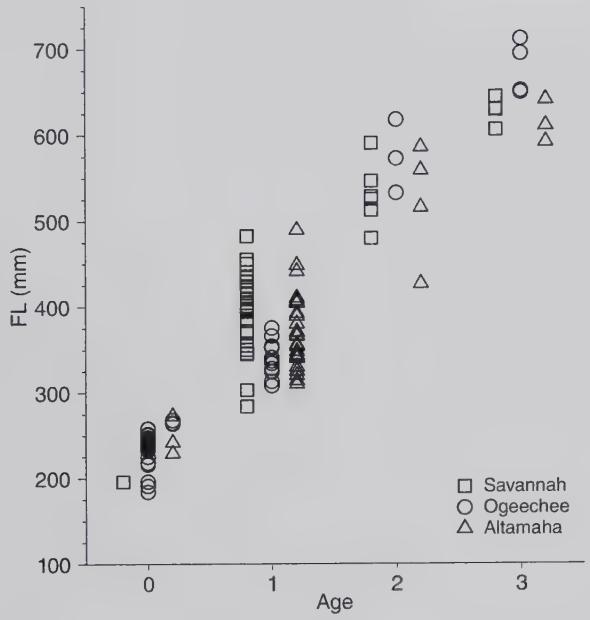

Figure 3

Lengths at age for juvenile Atlantic sturgeon (*Acipenser oxyrinchus oxyrinchus*) caught in 3 rivers of Georgia from 2015 through 2016. Fork lengths (FLs) and ages are from analysis of pectoral-fin spines of fish caught in the Savannah and Ogeechee Rivers for this study. Data for fish caught in the Altamaha River, based on spines collected and analyzed concurrently to those in this study by using identical methods, are included for comparison. From fish sampled in the Savannah River, we collected 20 spines in both 2015 and 2016 and successfully aged 38 spines (95%). We collected 26 spines in 2015 and 33 spines in 2016 from fish captured in the Ogeechee River; 55 spines (95%) were successfully aged.

Farrae et al. (2009) used Huggins closed capture models to estimate that 450 juvenile (age-1–3) Atlantic sturgeon were present during the summer of 2007. By multiplying Farrae et al.'s (2009) total juvenile abundance estimate by their reported percentage of age-1 fish (24%), we calculated that there were 142 age-1 fish present in the Ogeechee River in 2007. This value is almost triple the number of recruits that we estimated more than a decade later. In the Satilla River in 2008–2010, Fritts et al. (2016) captured only a handful of age-0–1 Atlantic sturgeon, and they were unable to estimate age-1 abundances. Similarly, we could estimate recruitment in the Satilla River for only 2 of the 4 years of this study.

We observed substantial variation among rivers in the lengths of age-1 Atlantic sturgeon. Little is known about the growth of juvenile sturgeon, especially in southern river systems, and future studies are needed to address these differences in lengths. The Ogeechee and Satilla Rivers are both blackwater systems with low dissolved oxygen (Zheng et al., 2004; Farrae et al., 2014), a condition that may explain why age-1 fish in these rivers were more similar in length than they were to age-1 fish in the Savannah or Altamaha Rivers (Fig. 3; senior author, unpubl. data; Baker et al., 2023). Our results highlight the need for river-specific information on length at age, especially when classifying age-1 juveniles for estimation of recruitment.

In some rivers, Atlantic sturgeon have been reported to spawn in both the spring and the fall (e.g., the James River; Balazik and Musick, 2015). The Savannah River may (Vine et al., 2019) or may not (White et al., 2021) feature such dual spawning. In this study, our recruitment estimates represent total annual recruitment of age-1 fish and do not distinguish between RRJs that potentially spawned in the spring or fall. The presence of juveniles produced in 2 chronologically distinct

Table 2

Estimates of the abundance (recruitment) of the age-1 cohorts of Atlantic sturgeon (*Acipenser oxyrinchus oxyrinchus*) in the Savannah, Ogeechee, and Satilla Rivers in Georgia during the summers of 2014–2017. Estimates and 95% confidence intervals (CIs) were derived from Huggins models that estimate capture probabilities for closed populations in RMark. An asterisk (*) indicates a result from Bahr and Peterson (2016). NA=not available because no or too few age-1 recruits were captured or recaptured.

	Savannah River		Ogeechee River		Satilla River	
Year	No. of individuals	95% CI	No. of individuals	95% CI	No. of individuals	95% CI
2014	589*	478–742	NA	NA	NA	NA
2015	597*	437–852	55	45–78	134	81–265
2016	973	786–1233	27	23–39	51	23–133
2017	639	449–953	57	25–193	NA	NA

spawning runs is one possible explanation for why, through length–frequency analysis, we found a larger upper size limit for age-1 fish in the Savannah River than for such fish in the other rivers in this study (i.e., the fall and spring modes in Figure 2 could have blurred together). However, the shape of the length–frequency distribution and upper size limit for age-1 Atlantic sturgeon in the Savannah River is the same as those for such fish in the Altamaha River (Baker et al., 2023), where spawning occurs in only the fall. Therefore, the larger size of some age-1 juveniles in the Savannah River, compared with the size of juveniles in the Ogeechee and Satilla Rivers, could instead be attributed to river conditions that enable faster growth.

Overlapping fall and spring cohorts, or simply variation in growth rates among individuals, may explain why results from our analysis of pectoral-fin spines did not align completely with results from our length–frequency analysis, particularly for fish over 500 mm FL. Results from genetic analysis in other studies indicate that dual spawning also occurs in the Ogeechee River (White et al., 2021; Wirgin et al. 2023). In that system, we observed a mode of juveniles with lengths below our age-1 size bracket (Fig. 2). We classified fish in that smaller size bracket as age 0—they were not part of the same annual cohort as the age-1 fish we quantified. Instead, these smaller fish may have been from a spring spawning run that occurred after the fall run.

Within a population, increased abundance of recruits over time could be an indicator of recovery. However, the number of recruits alone may not provide enough information to assess population growth. For instance, the abundance of recruits might be limited by the carrying capacity of the nursery habitat. Additionally, fecundity of female Atlantic sturgeon varies from 0.4 million to 2 million eggs (Van Eenennaam et al., 1996). Recruit abundance does not necessarily reflect the number of spawning adults. Therefore, without the context of historical recruitment data, we cannot state that the population in the Satilla River is any further from recovery than the population in the Savannah River simply because it produces fewer fish each year. A small, coastal plain river like the Satilla River may have never hosted as large a population of Atlantic sturgeon, or as many age-1 recruits per year, as the much larger Savannah River.

When it comes to assessing recruitment in a population of sturgeon (in the absence of historical data), we suggest that there are 3 important recruitment metrics that should be considered: 1) the abundance of age-1 fish (i.e., annual recruitment), 2) the variation in annual recruitment, and 3) the consistency of successful recruitment across multiple years. Because we assessed populations in the Savannah, Ogeechee, and Satilla Rivers concurrently and used the same methods, we can directly compare values for these metrics among these rivers. We can also compare recruitment in these river systems to that of other populations in the southernmost portion of the range of this species, thanks to concurrent studies in which identical methods were used in all other rivers of Georgia and Florida in which Atlantic sturgeon occur (Fig. 1).

Abundance of recruits

As a population recovers, an increase in the number of juveniles surviving to maturity should cause an increase in the number of recruits each year in that population. Atlantic sturgeon are intermittent spawners, returning to their natal rivers to spawn every 1–2 years (Hagar et al., 2020; Breece et al., 2021). Comparing recruitment year to year would not necessarily be informative because not every adult spawns every year. However, over a period of ~5 years, every mature adult in a population should have the chance to spawn, and the maximum cumulative effective population size (N_e) (Waldman et al., 2019) occurred in <5 years of sampling in the Savannah, Ogeechee, and Altamaha Rivers during our study. Because sturgeon spawn intermittently, a single annual calculation of N_e likely underestimates the total number of breeding adults. Waldman et al. (2019) calculated the cumulative N_e for several sequential years, with the juvenile input data for each year consisting of that year's recruits plus all recruits from all previous years. When these results were plotted, the resulting curve had a peak or asymptote, which Waldman et al. (2019) called the *maximum* N_e—an estimate of N_e for the whole population that includes adults that spawn only intermittently. In a recovering population of Atlantic sturgeon, the general trend should be an increase in annual recruitment over time, reflecting the increased number of spawners. Increased recruitment, in turn, should result in faster population recovery, as has been reported, for example, for modeled populations of white sturgeon (*Acipenser transmontanus*) in Idaho (Paragamian and Hansen, 2008).

The Altamaha River likely hosts the most robust population of Atlantic sturgeon within the South Atlantic DPS (ASSRT, 2007), and in 2014–2017, the river had more age-1 recruits per year than any other river in Georgia. For the period 2004–2020, annual recruitment in the Altamaha River varied from 163 to 3839 age-1 recruits per year (Fig. 4; Schueller and Peterson, 2010; Baker et al., 2023). During just the 3 years of 2014–2017 (the period of this study), the mean estimate of recruitment from Baker et al. (2023) was 1173.8 individuals, far greater than the mean number of recruits we observed in any river in this study (Table 3). The St. Marys River, in Georgia, and the St. Johns River also host populations of the South Atlantic DPS; they are located south of the rivers we examined in this study. During 2014–2017, Fox et al. (2018a) were unable to capture enough age-1 fish in the St. Marys River to calculate any recruitment estimates. In 2014–2015, Fox et al. (2018b) observed no age-1 Atlantic sturgeon in the St. Johns River.

Variation in recruitment

In the Altamaha River, Baker et al. (2023) observed annual recruitment that varied from a few hundred to several

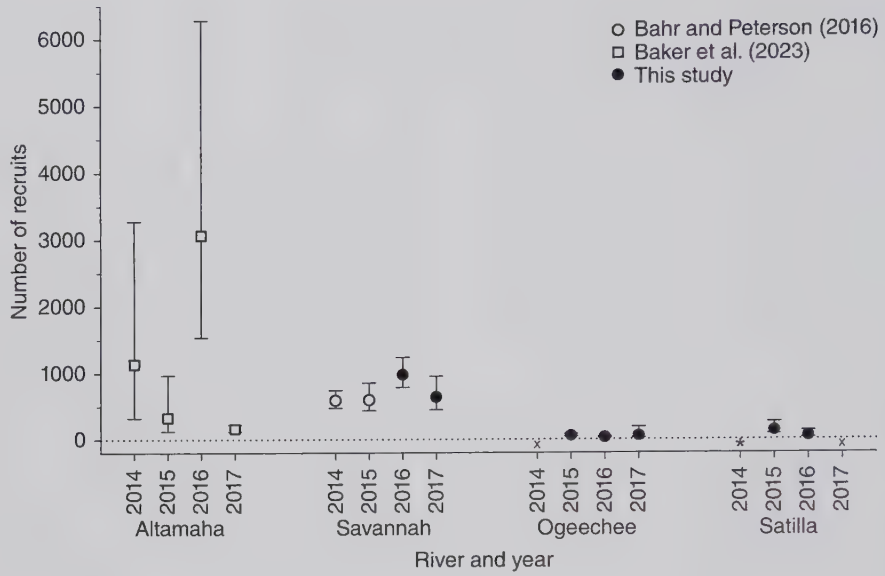

Figure 4

Estimates of recruitment of Atlantic sturgeon (*Acipenser oxyrinchus oxyrinchus*) to age 1 for 4 rivers in Georgia. Estimates provided for comparison are from this study and from previously published works, Bahr and Peterson (2016) and Baker et al. (2023). Error bars indicate 95% confidence intervals. The horizonal dotted line indicates the *y*-axis value of 0. An asterisk (*) indicates that too few age-1 recruits were captured or recaptured to calculate an estimate. A letter × indicates that no age-1 recruits were captured; therefore, no estimate could be calculated.

Table 3

Comparison of the recruitment of Atlantic sturgeon (*Acipenser oxyrinchus oxyrinchus*) in rivers of Georgia and Florida. Values for recruitment metrics were synthesized for each river by using data only from 2014 through 2017, including results from previously published literature. The metrics presented are the number of years during 2014–2017 in which sampling for juvenile Atlantic sturgeon occurred, the mean of all existing estimates of age-1 juvenile abundance (if available), the standard deviation (SD) and coefficient of variation (CV) of all available recruitment estimates, the percentage of sampled years in which age-1 fish were observed, and the percentage of sampled years for which a recruitment estimate could be calculated. NA=not available because of a lack of recaptured age-1 fish.

		Age-1 cohort size (no. of individuals)			Percentage of years sampled		
River	No. of years sampled	Mean	SD	CV	with age-1 fish detected	with recruitment estimate	Source
Savannah	4	699.5	183.6	0.26	100	100	This study; Bahr and Peterson (2016)
Ogeechee	4	34.8	26.9	0.77	75	75	This study
Altamaha	4	1173.8	1328.1	1.13	100	100	Baker et al. (2023)
Satilla	4	61.7	67.6	1.10	75	50	This study
St. Marys	4	NA	NA	NA	25	0	Fox et al. (2018a)
St. Johns	2	0.0	0.0	0.00	0	0	Fox et al. (2018b)

thousand age-1 fish per year (Fig. 4); for 2014–2017, the SD of mean annual recruitment from that study was 1328.1, and the CV was 1.13 (Table 3). During the same time period in the Savannah River in our study, the SD of the mean annual recruitment was 183.6, and the CV was 0.26. In our study, the Ogeechee River had an SD of mean annual recruitment of 26.9 and a CV of 0.77, and the Satilla River had an SD of mean annual recruitment of 67.6 and a CV of 1.10.

Atlantic sturgeon are periodic spawning strategists. As such, variations in recruitment among years are expected—recruitment should be high under appropriate environmental conditions and low otherwise (Winemiller, 2005). Therefore, multiple consecutive years of estimates of the recruitment of Atlantic sturgeon should be considered, to ensure that the estimate for any given year is not an outlier. Interestingly, for the period 2014–2017, the greatest number of recruits was estimated for 2016 in both the Altamaha and Savannah Rivers, indicating that the environmental conditions of both rivers were particularly suitable when that cohort was spawned. The Altamaha River features a single spawning run in the fall (Ingram and Peterson, 2016), meaning that the age-1 RRJs in 2016 would have spawned in the fall of 2014. Because there may be dual spawning in the Savannah River, the age-1 RRJs that we quantified in 2016 could have been produced either in the fall of 2014 or in the spring of 2015. A lower abundance of adult spawners also results in decreased variability in recruitment (DeAngelis et al., 1990), which may explain why, in our study, the (presumably) smaller populations in the Ogeechee and Satilla Rivers did not have a similar increase in recruits in 2016.

Unlike the Altamaha River, the Savannah River is dammed below the fall line, although sturgeon can still access 92% of their historic habitat (ASSRT, 2007). Dams change natural flow regimes in rivers by increasing minimum flows and decreasing maximum flows (Magilligan and Nislow, 2005). For Gulf sturgeon (*Acipenser oxyrinchus desotoi*), decreased river discharge resulted in decreased availability of spawning habitat (Flowers et al., 2009), which could result in decreased recruitment. Although spawning habitat can be extensive in many rivers (e.g., the Altamaha River; Ingram and Peterson, 2016; senior author, unpubl. data), the amount and extent of spawning habitat has not yet been identified in the Ogeechee River or Satilla River. These relatively small rivers are largely or wholly confined to the coastal plain and may not have substantial reaches of hard-bottom habitat.

In the Savannah River, spawning occurs only below the lowest impoundment, in just a fraction of the historic spawning habitat. In systems with limited spawning habitat, discharge-related fluctuations in availability could have relatively large effects on recruitment. Because the dams of the Savannah River reduce variability in flow, and because the habitat has been heavily channelized, sturgeon there may no longer experience the occasional optimal environmental conditions that would allow the production of a much larger juvenile cohort in some years. Although relatively high recruitment occurred in 2016 in the Savannah River, anthropogenic alterations to the habitat in that river may have prevented recruitment from being even better that year, with levels more comparable with that in the Altamaha River.

Both the Ogeechee and Satilla Rivers had relatively high CVs of recruitment compared with that in the Savannah River; however, these systems had far fewer recruits on average each year. Comparing populations solely on the basis of variation in recruitment is not a useful exercise. When the number of annual recruits is very low, annual increases or decreases of just a few fish result in large changes to the CV of recruitment, and this metric may be less useful for comparing systems. For example, recruitment in the Ogeechee River more than doubled from 2016 to 2017, but the actual increase in number of recruits was just 30 individuals. However, with such a limited data set, we cannot determine which of those years featured "normal" recruitment in that river. By looking at both the mean number of recruits and how the number of recruits varies, it may be possible to gain insight into relative population health and the environmental constraints a population may be experiencing.

Consistency of recruitment

Although recruitment in a population of Atlantic sturgeon may be variable, a healthy or recovering fish population should produce measurable recruitment every year. The catch of no age-1 recruits in some years could be attributed to environmental conditions that prevented a spawn or inhibited survival of young juveniles, to a lack of adult spawners that year, or to other bottlenecks.

Age-1 fish were observed every year during 2004–2020 in the Altamaha River (Schueller and Peterson, 2010; Baker et al., 2023). In the Savannah River during 2014–2017, age-1 recruits were also observed every year (Table 3; Bahr and Peterson, 2016). In the Ogeechee River, we observed recruitment in 75% of study years, although estimates of the abundance of age-1 fish were in the tens of individuals, compared with the hundreds of recruits in the Savannah River or the thousands of recruits in the Altamaha River. The fact that recruitment is so consistent in the Ogeechee River could indicate that the population there has recovered to this river's (naturally small) carrying capacity, but such a recovery is unlikely given that 2 separate spawning runs are producing so few juveniles. The lack of recruitment in 25% of study years indicates that an intermittent impediment to successful spawning could be slowing or preventing recovery. In the future, relative contributions of the fall and spring spawning runs to total annual recruitment may provide additional information about the conditions that promote successful recruitment in the Ogeechee River.

The Satilla, St. Marys, and St. Johns Rivers are the southernmost rivers in the historic range of the Atlantic sturgeon, and we have observed inconsistent—or no—annual recruitment of the populations in all 3 rivers, despite our multiyear monitoring. The Satilla River had

age-1 cohorts similar in size to or larger than those in the Ogeechee River, but age-1 fish were observed in only 2 years of the 4-year study period. Again, this low level or lack of recruitment indicates a bottleneck, although further research is needed to determine whether this issue can be attributed to a lack of spawners, to environmental conditions, or to other factors. In the St. Marys River, surveys for juvenile sturgeon occurred in 2008–2010 (Fritts, 2011), in 2013–2019 (Fox et al., 2018a; senior author, unpubl. data), and in 2021–2022 (senior author, unpubl. data), but age-1 fish have been observed in only 2 years, in 2014 and 2019.

Conclusions

Annual recruitment of age-1 Atlantic Sturgeon varied substantially among populations in 3 rivers of Georgia, the Savannah, Ogeechee, and Satilla Rivers. Because we lack historical data on recruitment, we compared characteristics of recruitment in the populations examined in our study to the characteristics of the robust population in the Altamaha River. In addition to producing larger numbers of recruits, healthier populations appear to have had consistent recruitment every year, even if the number of annual recruits was variable. Our results indicate that the population in the Savannah River is relatively healthy in comparison to the other populations that make up the South Atlantic DPS, but the populations in other rivers, especially those populations in the southernmost rivers, had only low numbers of age-1 fish per year, and they may not have had successful recruitment every year.

Resumen

El esturión del Atlántico (*Acipenser oxyrinchus oxyrinchus*) es un pez anádromo que se encuentra a lo largo de la costa este de Norteamérica y está incluido en la Ley de Especies Amenazadas de Estados Unidos. Décadas de sobrepesca y degradación del hábitat han provocado descensos de la población en toda su área de distribución, y el estado de la población de esta especie en muchos ríos no está claro. Cuantificar el reclutamiento anual es una forma de evaluar el estado de las poblaciones de esturión, pero dichas evaluaciones son escasas. El objetivo de este estudio fue cuantificar el reclutamiento de juveniles del esturión del Atlántico en los ríos Savannah, Ogeechee y Satilla en Georgia. Dado que utilizamos métodos idénticos en 3 ríos simultáneamente, pudimos comparar directamente el reclutamiento entre estas poblaciones con el observado en otras poblaciones en estudios contemporáneos en otros ríos. Realizamos muestreos de marcado y recaptura durante 2014–2017 y utilizamos modelos de población cerrada de Huggins para estimar el reclutamiento anual. Dado que no existen datos históricos para comparar, evaluamos las 3 poblaciones en términos de abundancia de reclutas, variación y consistencia. El río Savannah tuvo anualmente un número relativamente grande de reclutas (639–937 individuos). Se produjeron menos reclutas en los ríos Ogeechee (27–57 individuos) y Satilla (51–134 individuos); el reclutamiento sólo se produjo en algunos años en esos ríos. Las poblaciones que producen pocos reclutas o no tienen un reclutamiento regular, pueden estar experimentando cuellos de botella que impiden su recuperación.

Acknowledgments

This work was funded by the National Marine Fisheries Service, the Georgia Department of Natural Resources, and the Warnell School of Forestry and Natural Resources at the University of Georgia. Thanks to D. Peterson and to all the technicians who helped collect the data used in this study.

Literature cited

Akaike, H.
1973. Information theory and an extension of the maximum likelihood principle. *In* Second International Symposium on Information Theory; Tsaghkadzor, 2–8 September 1971 (B. N. Petrov and F. Csaki, eds.), p. 267–281. Akademiai Kiado, Budapest, Hungary.

ASSRT (Atlantic Sturgeon Status Review Team).
2007. Status review of Atlantic sturgeon (*Acipenser oxyrinchus oxyrinchus*), 174 p. Report to Northeast Reg. Off., Natl. Mar. Fish. Serv., Gloucester, MA. [Available from website.]

Bahr, D. L., and D. L. Peterson.
2016. Recruitment of juvenile Atlantic sturgeon in the Savannah River, Georgia. Trans. Am. Fish. Soc. 145:1171–1178.

Bain, M. B.
1997. Atlantic and shortnose sturgeons of the Hudson River: common and divergent life history attributes. Environ. Biol. Fishes 48:347–358.

Baker, M. A., E. C. Ingram, D. L. Higginbotham, B. J. Irwin, and A. G. Fox.
2023. Refining capture-recapture recruitment estimation methods for Atlantic sturgeon. Endanger. Species Res. 51:203–214.

Balazik, M. T., and J. A. Musick.
2015. Dual annual spawning races in Atlantic sturgeon. PLoS ONE 10:e0128234.

Baremore, I. E., and J. D. Rosati.
2014. A validated, minimally deleterious method for aging sturgeon. Fish. Bull. 112:274–282.

Breece, M. W., A. L. Higgs, and D. A. Fox.
2021. Spawning intervals, timing, and riverine habitat use of adult Atlantic Sturgeon in the Hudson River. Trans. Am. Fish. Soc. 150:528–537.

Brown, J. J., and G. W. Murphy.
2010. Atlantic sturgeon vessel-strike mortalities in the Delaware Estuary. Fisheries 35:72–83.

Burnham, K. P., and D. R. Anderson.
2002. Model selection and multimodel inference: a practical information theoretic approach, 2nd ed., 488 p. Springer-Verlag, New York.

Collins, M. R., S. G. Rogers, and T. I. J. Smith.
1996. Bycatch of sturgeons along the Southern Atlantic Coast of the USA. North Am. J. Fish. Manag. 16:24–29.

Conroy, M. J., and J. P. Carroll.
2009. Quantitative conservation of vertebrates, 352 p. Wiley-Blackwell, Oxford, UK.

DeAngelis, D. L., L. W. Barnthouse, W. Van Winkle, and R. G. Otto.
1990. A critical appraisal of population approaches in assessing fish community health. J. Great Lakes Res. 16:576–590.

Dovel, W. L., and J. T. Berggren.
1983. Atlantic sturgeon of the Hudson estuary, New York. New York Fish Game J. 30:140–172.

Farrae, D. J., P. M. Schueller, and D. L. Peterson.
2009. Abundance of juvenile Atlantic sturgeon in the Ogeechee River, Georgia. Proc. Annu. Conf. SEAFWA 63:172–176.

Farrae, D. J., S. E. Albeke, K. Pacifici, N. P. Nibbelink, and D. L. Peterson.
2014. Assessing the influence of habitat quality on movements of the endangered shortnose sturgeon. Environ. Biol. Fishes 97:691–699.

Federal Register.
2012. Endangered and threatened wildlife and plants; final listing determinations for two distinct population segments of Atlantic sturgeon (*Acipenser oxyrinchus oxyrinchus*) in the Southeast. Fed. Regist. 77:5914–5982. [Available from website.]

Flowers, H. J, W. E. Pine III, A. C. Dutterer, K. G. Johnson, J. W. Ziewitz, M. S. Allen, and F. M. Parauka.
2009. Spawning site selection and potential implications of modified flow regimes on viability of Gulf sturgeon populations. Trans. Am. Fish. Soc. 138:1266–1284.

Fox, A. G., and D. L. Peterson.
2019. Movement and out-migration of juvenile Atlantic sturgeon in Georgia, USA. Trans. Am. Fish. Soc. 148:952–962.

Fox, A. G., I. I. Wirgin, and D. L. Peterson.
2018a. Occurrence of Atlantic sturgeon in the St. Marys River, Georgia. Mar. Coast. Fish. 10:606–618.

Fox, A. G., E. S. Stowe, K. J. Dunton, and D. L. Peterson.
2018b. Seasonal occurrence of Atlantic sturgeon (*Acipenser oxyrinchus oxyrinchus*) in the St. Johns River, Florida. Fish. Bull. 116:219–227.

Fritts, M. W., II.
2011. Status of imperiled sturgeon species in the Satilla and Saint Marys Rivers, Georgia. M.S. thesis, 40 p. Univ. Georgia, Athens, Georgia. [Available from website.]

Fritts, M. W., C. Grunwald, I. Wirgin, T. L. King, and D. L. Peterson.
2016. Status and genetic character of Atlantic sturgeon in the Satilla River, Georgia. Trans. Am. Fish. Soc. 145:69–82.

Grunwald, C. J., L. Maceda, J. Waldman, J. Stabile, and I. Wirgin.
2008. Conservation of Atlantic sturgeon *Acipenser oxyrinchus oxyrinchus*: delineation of stock structure and distinct population segments. Conserv. Genet. 9:1111–1124.

Hagar, C. H., J. C. Watterson, and J. E. Kahn.
2020. Spawning drivers and frequency of endangered Atlantic sturgeon in the York River system. Trans. Am. Fish. Soc. 149:474–485.

Hale, E. A., I. A. Park, M. T. Fisher, R. A. Wong, M. J. Stangl, and J. H. Clark.
2016. Abundance estimate for and habitat use by early juvenile Atlantic sturgeon within the Delaware River estuary. Trans. Am. Fish. Soc. 145:1193–1201.

Hilton, E. J., B. Kynard, M. T. Balazik, A. Z. Horodysky, and C. B. Dillman.
2016. Review of the biology, fisheries, and conservation status of the Atlantic sturgeon, *Acipenser oxyrinchus oxyrinchus* Mitchill, 1815. J. Appl. Ichthyol 32(Suppl. 1): 1–137.

Huggins, R. M.
1989. On the statistical analysis of capture experiments. Biometrika 76:133–140.

Hurvich, C. M., and C. Tsai.
1989. Regression and time series selection in small samples. Biometrika 76:297–307.

Ingram, E. C., and D. L. Peterson.
2016. Annual spawning migrations of adult Atlantic sturgeon in the Altamaha River, Georgia. Mar. Coast. Fish. 8:595–606.

Magilligan, F. J., and K. H. Nislow.
2005. Changes in hydrologic regime by dams. Geomorphology 71:61–78.

Meyer, J. L., A. C. Benke, R. T. Edwards, and J. B. Wallace.
1997. Organic matter dynamics in the Ogeechee River, a blackwater river in Georgia, USA. J. North Am. Benthol. Soc. 16:82–87.

Paragamian, V. L., and M. J. Hansen.
2008. Evaluation of recovery goals for endangered white sturgeon in the Kootenai River, Idaho. North Am. J. Fish. Manag. 28:463–470.

R Core Team.
2022. R: a language and environment for statistical computing. R Foundation for Statistical Computing, Vienna, Austria. [Available from website, accessed June 2022.]

Schueller, P., and D. L. Peterson.
2010. Abundance and recruitment of juvenile Atlantic sturgeon in the Altamaha River, Georgia. Trans. Am. Fish. Soc. 139:1526–1535.

Scott, W. B., and E. J. Crossman.
1973. Freshwater fishes of Canada. Fish. Res. Board Can., Bull. 184, 966 p. [Available from website.]

Smith, T. I. J., and J. P. Clugston.
1997. Status and management of Atlantic sturgeon, *Acipenser oxyrinchus*, in North America. Environ. Biol. Fishes 48:335–346.

Van Eenennaam, J. P., S. I. Doroshov, G. P. Moberg, J. G. Watson, D. S. Moore, and J. Linares.
1996. Reproductive conditions of the Atlantic Sturgeon (*Acipenser oxyrinchus*) in the Hudson River. Estuaries 19:769–777.

Vine, J. R., S. C. Holbrook, W. C. Post, and B. K. Peoples.
2019. Identifying environmental cues for Atlantic sturgeon and shortnose sturgeon spawning migrations in the Savannah River. Trans. Am. Fish. Soc. 148:671–681.

Vladykov, V. D., and J. R. Greeley.
1963. Order Acipenseroidei. *In* Fishes of the western North Atlantic. Part 3: soft-rayed bony fishes (Y. H. Olsen, ed.), p. 24–60. Sears Found. Mar. Res., Yale Univ., New Haven, CT.

Waldman, J., S. E. Alter, D. Peterson, L. Maceda, N. Roy, and I. Wirgin.
2019. Contemporary and historical effective population sizes of Atlantic sturgeon *Acipenser oxyrinchus oxyrinchus*. Conserv. Genet. 20:167–184.

White, S. L., D. C. Kazyak, T. L. Darden, D. J. Farrae, B. A. Lubinski, R. L. Johnson, M. S. Eackles, M. T. Balazik, H. M. Brundage III, A. G. Fox, et al.
2021. Establishing a microsatellite genetic baseline for North American Atlantic sturgeon (*Acipenser o. oxyrinchus*) and range-wide analysis of population genetics. Conserv. Genet. 22:977–992.

Winemiller, K.
2005. Life history strategies, population regulation, and implications for fisheries management. Can. J. Fish. Aquat. Sci. 62:872–885.

Winger, P. V., P. J. Lasier, D. H. White, and J. T. Seginak.
2000. Effects of contaminants in dredge material from the lower Savannah River. Arch. Environ. Contam. Toxic. 38:128-136.

Wirgin, I., J. R. Waldman, J. Rosko, R. Gross, M. R. Collins, S. G. Rogers, and J. Stabile.
2000. Genetic structure of Atlantic sturgeon populations based on mitochondrial DNA control region sequences. Trans. Am. Fish. Soc. 129:476–486.

Wirgin, I., A. G. Fox, L. Maceda, and J. Waldman.
2023. Two distinct life history strategies of Atlantic sturgeon in the Ogeechee River, Georgia. Diversity 15, article 325.

Zheng, L., C. Chen, and F. Y. Zhang.
2004. Development of water quality model in the Satilla River Estuary, Georgia. Ecol. Model. 178:457–482.

Fishery Bulletin

Guidelines for authors

Contributions published in *Fishery Bulletin* describe original research in marine fishery science, fishery engineering and economics, and marine environmental and ecological sciences (including modeling). Preference will be given to manuscripts that examine processes and underlying patterns. Descriptive reports, surveys, and observational papers may occasionally be published but should appeal to an audience outside the locale in which the study was conducted.

Although all contributions are subject to peer review, responsibility for the contents of papers rests upon the authors and not on the editor or publisher. *Submission of an article implies that the article is original and is not being considered for publication elsewhere.*

All submissions are subject to a double-blind review to remove the identity of author and reviewer during the review process.

Plagiarism and double publication are considered serious breaches of publication ethics. To verify the originality of the research in papers and to identify possible previous publication, manuscripts may be screened with plagiarism-detection software.

Manuscripts must be written in English; authors whose native language is not English are strongly advised to have their manuscripts checked by English-speaking colleagues before submission.

Artificial intelligence (AI), machine learning, or similar algorithmic tools should not be used to write or generate scientific content, including text, tables, and figures, for manuscripts submitted to *Fishery Bulletin*. Although some authors may use such tools to improve the readability or syntax of their manuscript, it must be done with extreme caution, and authors must review and edit the result. If such a tool is used, authors must declare the name of the tool, where it was used, and the purpose for which it was used in an "Artificial intelligence declaration" section after the "Acknowledgments" section. Authors remain accountable for all elements of their manuscript and should state that they take full responsibility for the content of their manuscript in the AI declaration.

Once a paper has been accepted for publication, online publication takes approximately 2 weeks.

There is no cost for publication in *Fishery Bulletin*.

Types of manuscripts accepted by the journal

Articles generally range from 20 to 30 double-spaced typed pages (12-point font) and describe an original contribution to fisheries science, engineering, or economics. Tables and figures are not included in this page count, but the number of figures should not exceed 1 figure for every 4 pages of text. Articles contain the following divisions: abstract, introduction, methods, results, discussion, and conclusions.

Notes are generally less than 10 double-spaced typed pages (12-point font), including the Literature cited section. Like articles, notes describe an original contribution to fisheries science. They follow a format similar to that for articles: abstract, introduction, methods, results, and discussion, but the results and discussion sections may be combined and a conclusions section should not be included. They should include no more than 2 figures or tables (2 of each would be too many). They are distinguished from full articles in that they report a noteworthy new observation or discovery—such as the first report of a new species, a unique finding, condition, or event that expands our knowledge of fisheries science, engineering, or economics—and do not require a lengthy discussion. Manuscripts on range extensions will not be considered.

Companion articles should be submitted together and are published together as a scientific contribution. Both articles should address a closely related topic and may be articles that result from a workshop or conference.

Review articles of exceptional quality may be considered occasionally for publication on a case-by-case basis. They address a timely topic that is relevant to aspects of fisheries science. They should include an abstract, but the format of the article, per se, will be up to the author. Please contact the scientific editor to discuss your ideas regarding a potential review article before embarking on such a project.

Perspective essays generally are less than 5 double-spaced typed pages (12-point font) and provide clarification of misused terms or misunderstood topics in fisheries science. Essays are accepted at the discretion of the scientific editor. Opinion pieces on policy will not be considered. They should include an abstract and a list of the literature cited, but no other sections should divide the article. Please contact the scientific editor to discuss your idea before making a submission.

Preparation of manuscript

Title page should include authors' full names, affiliations, mailing addresses, and the senior author's email address.

Abstract should be limited to 200 words (one-half typed page), state the main scope of the research, and emphasize the authors' conclusions and relevant findings. Do not review the methods of the study or list the contents of the paper. Because abstracts are circulated by abstracting agencies, it is important that they represent the research clearly and concisely.

General text must be typed in 12-point Times New Roman font throughout. A brief introduction should convey the

broad significance of the paper; the remainder of the paper should be divided into the following sections: Materials and methods, Results, Discussion, Conclusions, and Acknowledgments. Headings within each section must be short, reflect a logical sequence, and follow the rules of subdivision (i.e., there can be no subdivision without at least 2 subheadings). The entire text should be intelligible to interdisciplinary readers; therefore, all acronyms, abbreviations, and technical terms should be written out in full and defined the first time they are mentioned. Abbreviations should be used sparingly because they are not carried over to indexing databases and slow readability for those readers outside a discipline. They should never be used for the main subject (e.g., species or method) of a paper.

For general style, follow the U.S. Government Publishing Office *Style Manual* (2016, available at website) and *Scientific Style and Format: the CSE Manual for Authors, Editors, and Publishers* (2014, 8th ed.) published by the Council of Science Editors. For scientific nomenclature, use the current edition of the American Fisheries Society's (AFS) *Common and Scientific Names of Fishes from the United States, Canada, and Mexico* and its companion volumes (*Crustaceans, Mollusks, Cnidaria and Ctenophora*, and *World Fishes Important to North Americans*). For species not found in the previously mentioned AFS publications and for more recent changes in nomenclature, use the Integrated Taxonomic Information System (ITIS, available at website), or, secondarily, the California Academy of Sciences *Catalog of Fishes* (available at website) for species names not included in ITIS. Common (vernacular) names of species should be lowercase. Citations must be given for the identification of specimens. For example, "Fish species were identified according to Collette and Klein-MacPhee (2002); sponges were identified according to Stone et al. (2011)."

Dates should be written as follows: 11 November 2018. Measurements should be expressed in metric units, for example, "58 metric tons (t);" if other units of measurement are used, please make this fact explicit to the reader. Use numerals, not words, to express whole and decimal numbers in the general text, tables, and figure captions (except at the beginning of a sentence). For example, "We considered 3 hypotheses. We collected 7 samples in this location." Use American spelling. Refrain from using the shorthand slash (/), an ambiguous symbol, in the general text.

Cite all software, special equipment, and chemical solutions used in the study within parentheses in the general text, including the version number, company name, and the city and state (or nation) of the company headquarters, for example, "SAS, vers. 9.4 (SAS Institute Inc., Cary, NC)."

Word usage and grammar that may be useful are the following:

- *Aging*
  For our journal, the word *aging* is used to mean both age determination and the aging process (senescence). Authors should make clear which meaning is intended where ambiguity may arise.

- *Fish and fishes*
  The plural of the word fish (a collective noun that implies individuals without regard to species) is *fish*.
  Example: The *fish* were collected by trawl net.
  Example: The numbers of *fish* collected that season were less than the numbers from previous years.

  The plural for *fish species* is *fishes* (a contrived plural used by taxonomists to mean several or more *fish species*) or one can use *fish species* (which is preferred in this journal for clarity across disciplines).
  Example: The *fishes* of Puget Sound [biodiversity is implied] or
  Example: The *fish species* of Puget Sound [preferred plural for clarity across disciplines].

- *Crab and crabs, squid and squids, etc.*
  The plural of the word *crab* (i.e., many individuals without regard to species) is *crab*.
  Example: The crab were sorted by weight.
  Example: Many red king *crab* were dying [Many individuals of one species of crab.]

  The plural of *crab species* is *crabs* (a word used by taxonomists) or *crab species* (the latter is preferred in this journal for clarity).
  Example: These *crabs* were selected for treatment. [Different crab species are implied.]
  Example: These *crab species* were selected for treatment. [Preferred word choice for clarity.]
  Example: Snow *crabs* are found throughout the North Pacific Ocean and Bering Sea. [There are 2 species of snow crab; therefore the word *crabs* can be used here.]
  Example: *Two species* of snow *crab* are found throughout the North Pacific Ocean and Bering Sea. [Preferred usage for clarity.]
  Example: Three crabs were selected for treatment. [3 species of crab are implied.]
  Example: Three crab species were selected for treatment. [Preferred word choice for clarity.]

- We use *fisherman* and *fishermen*, not *fisher* and *fishers*, in this journal. One can always use crew member, vessel operator, and angler (the latter for recreational fishing).

- *The definite article with common names of species*
  When the singular common name of a species represents the entire class or group to which it belongs, use the definite article.
  Example: Only one species of the genus *Salmo* is found in the Atlantic Ocean—*the* Atlantic salmon (*Salmo salar*).
  Example: The sonic emissions of *the* bottlenose dolphin are complex.

  For plural common names, this rule does not apply.
  Example: Chinook salmon are found throughout the Pacific Ocean.
  Example: Bottlenose dolphins are found in temperate and tropical waters.

- *Sex*
  For the meaning of male and female, use the word *sex*, not *gender*. Do not write, "fish were sexed." Write, "sex was determined."

- *Participles*
  As adjectives, participles must modify a specific noun or pronoun.
  Example: Using mark-recapture methods, these scientists determined the size of the population. [Correct. The participle *using* modifies the word *scientists*.]
  Example: These scientists, based on the collected data, concluded that the mortality rate of these fish had increased. [Incorrect. The scientists were not based on the collected data.]
  Example: These scientists concluded, on the basis of collected data, that the mortality rate of these fish had increased. [Correct. The offending participle has been eliminated and an adverbial phrase modifies the verb *concluded*.]

Equations and mathematical symbols should be set from a standard mathematical program (MathType or Equation Editor). Equations formatted in LaTex are not acceptable. For mathematical symbols in the general text (α, χ^2, π, $\pm$, etc.), use the symbols provided by the MS Word program and italicize all variables, except those variables represented by Greek letters and the superscript and subscript parts of variables and expressions. Do not use photo mode when creating these symbols in the general text, and do not cut and paste equations, letters, or symbols from a different software program.

Number equations (if there are more than one) for future reference by scientists; place the number within parentheses at the end of the first line of the equation.

Literature cited section comprises published works and those accepted for publication (in press) in peer-reviewed journals. Follow the name and year system for citation format in this section (i.e., citations should be listed alphabetically by the authors' last names, and then by year if there is more than one citation by the same author. A list of abbreviations for citing journal titles can be found on our website.

Authors are responsible for the accuracy and completeness of all citations. Avoid the use of multiple citations when a single citation sufficiently supports a statement; cite the work that first reported the information that supports a statement, not all of the subsequent works. Literature citation format: Authors (last name, followed by initials for first name and, if given, middle name of first author; then list names of additional authors with initials before last names). Year. Title of article. Abbreviated title of the journal in which it was published. Always include either the range of page numbers (for a journal article) or a total number of pages (for a book or other type of publication). List a sequence of citations in the general text chronologically, for example, "(Smith, 1932; Green, 1998; Smith and Jones, 2015)."

Acknowledgments should be no more than 6 lines of text. Only those who have contributed in an outstanding way should be acknowledged by name. For recognition of other persons or groups, use a general term, such as *crew*, *observers*, or *research coordinators*, and do not include names with these terms.

Digital object identifier (doi) code ensures that a publication has a permanent location online. A doi link (which may include a doi code) should be included at the end of citations of published literature. Authors are responsible for submitting accurate doi links. Faulty links will be deleted at the page-proof stage.

Footnotes are used for all documents that have not been formally peer reviewed and for observations and personal communications, but these types of references should be cited sparingly in manuscripts submitted to the journal.

All reference documents, administrative reports, internal reports, progress reports, project reports, contract reports, personal observations, personal communications, unpublished data, manuscripts in review, and council meeting notes are footnoted in 10-point font and placed at the bottom of the page on which they are first cited. Footnote format is the same as that for formal literature citations. A link to the online source (e.g., [Available from http://www..., accessed July 2017.]), or the mailing address of the agency or department holding the document, should be provided so that readers may obtain a copy of the document.

Tables are often overused in scientific papers; it is seldom necessary to present all the data associated with a study. Tables should not be excessive in size and must be cited in numerical order in the text. Headings should be short but ample enough to allow the table to be intelligible on its own.

All abbreviations and unusual symbols must be explained in the table legend. Other incidental comments may be footnoted with numeral footnote markers. Use asterisks only to indicate significance in statistical data. Do not put a table legend on a page separate from the table; place the legend above the table. *Do not submit tables in photo mode.*

- Note probability with a capital, italic *P*.
- Provide a zero before all decimal points for values less than one (e.g., 0.07).
- Round all values to 2 decimal points.
- Use a comma in numbers of 5 digits or more (e.g., 13,000 but 3000).

Figures must be cited in numerical order in the text. Graphics should aid in the comprehension of the text, but they should be limited to presenting patterns rather than raw data. The number of figures should not exceed 1 figure for every 4 pages of text.

Figure legends should explain all symbols and abbreviations seen in the figure and should be double spaced on a separate page at the end of the manuscript.

Line art and halftone figures should be saved at resolutions >600 dots per inch (dpi) and >300 dpi, respectively. Color is allowed in figures to show morphological differences among species (for species identification), to show stain reactions, to show gradations (such as those of temperature and salinity within maps), and to distinguish between numerous lines and symbols in graphs. Figures approved for color should be saved in CMYK format.

All figures must be submitted as PDF, TIFF, or EPS files.

- Capitalize only the first letter of the first word and proper nouns in all labels within figures.
- Do not use overly large font sizes for labels in maps and for axis labels in graphs.
- Use the same point size for all labels, except for panel labels (e.g., **A**), which should be slightly larger than other labels (e.g., 11 point versus 8 point).
- Use a sans serif font for all labels. Panel labels (e.g., **A**), however, should be in Times New Roman font.
- Do not use bold fonts or bold lines in figures. Do not use italic fonts. Exceptions include use of italic fonts for labels of bodies of water in maps and a bold font for panel labels (e.g., **A**).
- Do not place outline rules around graphs.
- Do not include vertical and horizontal lines in the background of graphs. Ticks for values on the x-axis and y-axis will suffice.
- Place a north arrow and label degrees latitude and longitude (e.g., 170°E) in all maps. If scale of map requires more than degrees, use degrees minutes, not decimal degrees.
- Place panel labels (e.g., **A**, **B**, **C**) within the upper-left area of each graph or photo in a multi-panel figure, from left to right, then top to bottom. If the letter is not visible against a dark background, put a white box behind it. Do not use white labels.
- Avoid placing labels vertically or diagonally. Y-axis labels can be vertical. Words in horizontal labels can be stacked vertically to fit.
- Use symbols, shading, or patterns (not clip art) in maps and graphs.
- For scale bars in maps, use kilometers. Use the label *km* or *kilometers* (lowercased).

Supplementary materials that are considered essential, but are too large or impractical for inclusion in a paper (e.g., metadata, figures, tables, videos, and websites), may be provided at the end of an article. These materials are subject to the editorial standards of the journal. A URL to the supplementary material and a brief explanation for including such material should be sent at the time of initial submission of the paper to the journal.

- **Metadata, figures, and tables** should be submitted in standard digital format (MS Word or PDF file) and should be cited in the general text, for example, as ". . . was determined (Suppl. Table 3, Suppl. Fig. 1)."
- **Websites** should be cited with a URL in the general text.
- **Videos** must not be larger than 30 MB to allow a swift technical response for viewing the video. Authors should consider whether a short video uniquely captures what text alone cannot capture for the understanding of a process or behavior under examination in the article. Supply an online link to the location of the video.

Copyright law does not apply to *Fishery Bulletin*, which falls within the public domain. However, if an author reproduces any part of an article from *Fishery Bulletin*, reference to source is considered correct form (e.g., Source: Fish. Bull. 117:105).

Failure to follow these guidelines and failure to correspond with editors in a timely manner will delay publication of a manuscript.

Submission of manuscript

Submit a manuscript online at the ScholarOne Manuscripts website for *Fishery Bulletin*. Commerce Department authors must provide proof of internal clearance of their manuscripts with either a completed and signed NOAA Form 25-700 or a copy of the clearance email from the Research Publication Tracking System. For further details on electronic submission, please contact the associate editor, Cara Mayo, at

cara.mayo@noaa.gov.

When requested, the text and tables should be submitted in MS Word format. Each figure should be sent as a separate PDF, TIFF, or EPS file. Send a copy of a figure in the original software if conversion to any of these formats yields a degraded version of the figure.

Questions? If you have questions regarding these guidelines, please contact the managing editor, Kathryn Dennis, at

kathryn.dennis@noaa.gov.

Questions regarding manuscripts under review should be addressed to Associate Editor Cara Mayo.

Fishery Bulletin

Subscription form

Superintendent of Documents **Publications** Order Form

*5178

☐ YES, please send me the following publications:

____ Subscriptions to *Fishery Bulletin*
for $32.00 per year ($44.80 foreign)

The total cost of my order is $ _____ . Prices include regular domestic postage and handling and are subject to change.

_____
(Company or Personal Name) (Please type or print)

_____
(Additional address/attention line)

_____
(Street address)

_____
(City, State, ZIP Code)

_____
(Daytime phone including area code)

_____
(Purchase Order No.)

Charge your order. IT'S EASY!

Please Choose Method of Payment:

☐ Check payable to the Superintendent of Documents
☐ GPO Deposit Account ☐☐☐☐☐☐☐–☐
☐ VISA or MasterCard Account
☐☐☐☐☐☐☐☐☐☐☐☐☐☐☐☐
☐☐☐☐ (Credit card expiration date)

To fax your orders (202) 512-2104

_____
(Authorizing Signature)

Mail to: Superintendent of Documents
P.O. Box 979050, St. Louis, Missouri 63197
Tel. no. (U.S. callers): 866-512-1800
Tel. no. (International callers): 1-202-512-1800

Thank you for your order!

Also available online at
https://bookstore.gpo.gov/products/fishery-bulletin
email: ContactCenter@gpo.gov